TUDelft

Delft University of Technology

Ultrasonic welding of epoxy- to thermoplastic-based composites

Tsiangou, E.

Important note
To cite this publication, please use the final published version (if applicable).
Please check the document version above.

Ultrasonic welding of epoxy- to thermoplastic-based composites

Tsiangou, E.

DOI
10.4233/uuid:4dd0034d-587e-4b9b-9b97-0a24210af123

Publication date
2021

Important note
To cite this publication, please use the final published version (if applicable).
Please check the document version above.

Ultrasonic Welding of Epoxy- to Thermoplastic-Based Composites

Dissertation

for the purpose of obtaining the degree of doctor
at Delft University of Technology
by the authority of the Rector Magnificus Prof.dr.ir. T.H.J.J. van der Hagen
chair of the Board for Doctorates
to be defended publicly on
Monday 19th April 2021 at 12.30 o'clock

by

Eirini TSIANGOU

Diploma in Mechanical Engineering and Aeronautics
University of Patras, Greece
born in Giannitsa, Greece

This dissertation has been approved by the promotors.

An electronic version of this dissertation is available at

http://repository.tudelft.nl/.

`

"No matter how many weapons you have, no matter how great your technology might be, the world cannot live without love."

-from "Castle in the Sky"

Summary

Welding is a promising alternative to mechanical fastening, as currently used, to join dissimilar (i.e., thermoset- to thermoplastic-based) composite parts in modern aircraft. Thermoset composites can be indirectly welded through a thermoplastic coupling layer co-cured on the surface of the laminate that needs to be welded. One of the main challenges when welding thermoset to thermoplastic composites, is the high welding temperatures that are needed to melt the thermoplastic matrix, especially when high-performance thermoplastic polymers are used such as in aerospace applications. The most efficient way to overcome this challenge is by ensuring very fast and localized heating in order to prevent thermal degradation mechanisms from occurring. Out of the currently most developed welding methods, ultrasonic welding can offer exceptionally short heating times of even less than 500 ms, which makes it an excellent candidate for joining thermoset and thermoplastic composites. However, further understanding of the process as applied to dissimilar composite joints is still lacking in order for it to be utilized in actual applications.

The aim of this PhD thesis is to further the knowledge on ultrasonic welding of thermoset to thermoplastic composites by firstly identifying suitable practices for successfully welding the dissimilar composites and secondly assessing the robustness of the ultrasonic welding process with respect to changes in process parameters.

The first subject that was addressed in this research was whether the thermoplastic coupling layer that is co-cured on the thermoset composite can be used as an integrated energy director. Energy directors are resin-rich features commonly used to concentrate heat generation at the interface during the ultrasonic welding process through preferential frictional and viscoelastic heating. The conclusion was that, apart from the coupling layer, a loose energy director is required at the welding interface in order to help promote heat locally, without risking excessive bulk heating and low weld strength. Additionally, comparison between the welded joints and reference co-cured joints revealed that both processes provide joints with similar lap shear strength.

The second part of the research was an investigation on the effect of the material of the energy director (when welding samples in which different thermoplastic resins are used for the coupling layer (i.e., polyetherimide (PEI) and the matrix of the thermoplastic composite adherend (i.e., polyetheretherketone (PEEK)) and the thickness of the coupling layer on the welding process. The material of the energy director was found to have minimal influence on the strength and failure locus of the welded joints. However, in the case of a thermoplastic matrix with a higher melting point than the softening point of the coupling layer, the thickness of the coupling layer played a major role. A 250 µm thickness was deemed necessary in order to produce welds with both fully welded overlaps and strengths comparable to reference thermoplastic composite welded joints. Critically reducing the thickness of the coupling layer to 60 µm resulted in seemingly thermal degradation of the epoxy resin. However, a very thin coupling layer could be successfully used when the thermoplastic matrix was PEI, due to its lower softening point than the melting temperature of PEEK.

Once suitable practices to ultrasonically weld thermoset to thermoplastic composites were defined, the third step was to assess the robustness of the process. Firstly, the sensitivity of ultrasonic welding of dissimilar composites to the heating time was assessed. A relatively wide processing interval could be obtained, provided that the coupling layer had a sufficient thickness. As expected, the welding process for dissimilar adherends was more sensitive to the vibration time than a reference welding process for thermoplastic composites, due to the sensitivity of the thermoset composite adherend to the high welding temperatures. Decreasing the coupling layer thickness also decreased the flexibility of the hybrid welding process with respect to the vibration time, i.e., the width of the processing interval, due to a decreased efficiency of the coupling layer to shield the thermoset composite adherend from the high temperatures at the welding interface.

The robustness of the ultrasonic welding process was also assessed through a study to its sensitivity to variations in welding force and amplitude of vibrations. In the state of the art, high force/high amplitude combinations are used, since they enable the shortest heating times. It was assumed that such short heating times were necessary in order to minimize the risk of thermal degradation in the thermoset composite adherend. Decreasing either of these parameters did not have a measurable effect on the maximum achievable lap shear strength. Nevertheless, faster degradation of the weld strength for heating times beyond the optimum, i.e., heating time that results in the highest weld strength, was found in all the cases with lower force or amplitude than the reference as a result of higher temperatures between the coupling layer and the thermoset composite adherend.

In conclusion, the present thesis aimed at furthering our knowledge on ultrasonic welding of thermoset to thermoplastic, i.e., dissimilar, composites. Despite the contributions of this PhD Thesis to the topic at hand, further research is still necessary before the process can be used for industrial applications. Main points for future studies are a wider range of suitable thermoset and thermoplastic material combinations and the mechanical performance of dissimilar composite welded joints under different testing and loading conditions.

Samenvatting

Lassen is een veelbelovend alternatief voor mechanische bevestigingen die momenteel worden gebruikt voor het verbinden van ongelijksoortige (d.w.z. thermoharder met thermoplastische) composietonderdelen in moderne vliegtuigen. Thermoharder composieten kunnen indirect worden gelast door middel van een thermoplastische koppelingslaag die op het te lassen oppervlak van het laminaat wordt uitgehard. Een van de belangrijkste uitdagingen bij het lassen van thermohardende tot thermoplastische composieten zijn de hoge lastemperaturen die nodig zijn om de thermoplastische matrix te smelten, met name wanneer hoogwaardige thermoplastische polymeren worden gebruikt voor lucht- en ruimtevaarttoepassingen. De efficiëntste manier om deze uitdaging te overwinnen, is door te zorgen voor een zeer snelle lokale verwarming om thermische degradatiemechanismen te voorkomen. Van de momenteel verst ontwikkelde lasmethoden kan ultrasoon lassen uitzonderlijk korte opwarmtijden bieden van zelfs minder dan 500 ms. Hierdoor is het een uitstekende kandidaat voor het verbinden van thermohardende en thermoplastische composieten. Echter, momenteel ontbreekt het inzicht in het proces toegepast op ongelijksoortige composietverbindingen om het in de praktijk te kunnen toepassen.

Het doel van dit proefschrift is om de kennis over het ultrasoon lassen van thermohardende tot thermoplastische composieten te bevorderen. Ten eerste door geschikte methodes te identificeren voor het succesvol lassen van de ongelijksoortige composieten en ten tweede door de robuustheid van het ultrasoon lasproces te beoordelen met betrekking tot veranderingen in de procesparameters.

Het eerste onderwerp dat in dit onderzoek aan de orde kwam, was de vraag of de thermoplastische koppelingslaag die op het thermohardende composiet samen gehard (co-cured) is, gebruikt kan worden als een geïntegreerde energierichtingsgever. Energierichtingsgevers zijn harsrijke onderdelen die vaak worden gebruikt om de warmteontwikkeling te concentreren op het grensvlak tijdens het ultrasoonlasproces door middel van wrijving en visco-elastische verwarming. De conclusie was dat, afgezien van de koppelingslaag, een losse energierichtingsgever nodig is bij de lasinterface om de warmte lokaal te bevorderen zonder het risico te lopen op overmatige bulkverwarming en een lage lassterkte. Bovendien bleek uit een vergelijking tussen de gelaste verbindingen en de referentie samen-geharde (co-cured) verbindingen met hetzelfde materiaal dat het lasproces in staat is om lassen te leveren met een vergelijkbare afschuifsterkte als de referentie van het samen-geharde (co-cured) proces.

Het tweede deel van het onderzoek was een onderzoek naar het effect van het materiaal van de energierichtingsgever (bij het lassen van proefstukken waarin verschillende thermoplastische harsen worden gebruikt als koppelingslaag en matrix van het thermoplastische composiet) en de dikte van de koppelingslaag in het lasproces. Het materiaal van de energierichtingsgever bleek een minimale invloed te hebben op de sterkte van de lasverbindingen. In het geval van een thermoplastische matrix met een hoger smeltpunt dan het materiaal van de koppelingslaag speelde de dikte van de koppelingslaag echter een grote rol. Een dikte van 250 µm werd noodzakelijk geacht om lassen te produceren met zowel volledig gelaste overlappingen als sterktes die vergelijkbaar zijn met de referentie thermoplastische composiet lasverbindingen. Het nauwkeurig reduceren van

de dikte van de koppelingslaag tot 60 μm resulteerde in ogenschijnlijk thermische degradatie van de epoxyhars. Een zeer dunne koppelingslaag kon echter met succes worden gebruikt wanneer het materiaal ervan overeenkwam met dat van de thermoplastische matrix.

Toen eenmaal geschikte methodes voor het ultrasoon lassen van thermohardende tot thermoplastische composieten waren gedefinieerd, was de derde stap het beoordelen van de robuustheid van het proces. Eerst werd de gevoeligheid van ultrasoon lassen van ongelijksoortige composieten voor de verhittingstijd beoordeeld. Een relatief breed proces interval kon worden verkregen, mits de koppelingslaag een voldoende dik was. Zoals verwacht was het lasproces voor ongelijksoortige composieten gevoeliger voor de vibratietijd dan een referentielasproces voor thermoplastische composieten, vanwege de gevoeligheid van de thermohardende composietmateriaal voor de hoge lastemperaturen. Het verminderen van de dikte van de koppelingslaag verminderde ook de flexibiliteit van het hybride lasproces met betrekking tot de vibratietijd, d.w.z. de breedte van het procesinterval, als gevolg van een verminderde efficiëntie van de koppelingslaag om het thermoharder composietmateriaal af te schermen van de hoge temperaturen bij de lasinterface.

De robuustheid van het ultrasoon lasproces werd ook beoordeeld door middel van een studie naar de gevoeligheid voor variaties in de laskracht en de amplitude van de trillingen. Momenteel worden hoge kracht en hoge amplitude combinaties gebruikt omdat deze de kortste opwarmtijden mogelijk maken. Er werd aangenomen dat dergelijke korte opwarmtijden noodzakelijk zijn om het risico van thermische degradatie in het thermohardende composietmateriaal tot een minimum te beperken. Het verlagen van een van deze parameters had geen meetbaar effect op de maximaal haalbare afschuifsterkte. Desondanks werd in alle gevallen met een lagere kracht of amplitude dan de referentie een snellere vermindering van de lassterkte gevonden voor langere verhittingstijden dan de optimale (verhittingstijd die resulteert in de hoogste lassterkte) als gevolg van hogere temperaturen tussen de koppelingslaag en het thermohardende composietmateriaal.

Tot slot heeft dit proefschrift tot doel onze kennis over het ultrasoon lassen van thermohardende tot thermoplastische, ofwel ongelijksoortige, composieten te bevorderen. Ondanks de bijdragen van dit proefschrift aan het onderwerp in kwestie, is er nog steeds verder onderzoek nodig voordat het proces kan worden gebruikt voor industriële toepassingen. Hoofdpunten voor toekomstige studies zijn een breder scala aan geschikte thermoharder en thermoplastische materiaalcombinaties en de mechanische prestaties van ongelijksoortige composiet-lasverbindingen onder verschillende test- en belastingscondities.

Contents

List of Figures

13

List of Tables

1 Introduction

1.1 Composites in aviation

Aerospace industries are constantly striving to further enhance the performance of commercial, private and military aircraft. The most straightforward way to do so is by greatly decreasing the weight of the aircraft structure for both reduction of fuel consumption, hence operational costs, and lower environmental impact. Due to the appealing weight-to-strength ratio of composite materials, a great number of efforts into utilizing composite structures in primary and secondary aircraft structures have been made. A gradual increase in applications of composite structures was seen around the 1970's, as seen in Figure 1.1. Initially and currently, the focus was placed on thermoset composite structures, such as the rudder of the Airbus A300 and A310 and the elevator of the Airbus A310. However, the high costs linked to the manufacturing of such composite structures, i.e., use of an autoclave and long curing cycles, have motivated research and development by industries and academic institutes alike towards more efficient material usage and manufacturing technologies. For that reason, thermoplastic composites started gaining attention in the late 1980's, since their significantly shorter consolidation cycles than the thermoset curing cycles can lead to significant manufacturing cost reductions, despite the currently higher material cost of the thermoplastic materials. On top of that, thermoplastic composites offer enhanced properties in comparison with thermosets, such as superior impact toughness, excellent environmental and chemical resistance, infinite shelf life etc. [1] Examples of utilization of thermoplastic composites include the press-formed ribs of the Dorniesr 328 [1], the thermoplastic composite clips and brackets in the Airbus A350 and Boeing 787 passenger aircraft [2], the rudder and elevators of the Gulfstream G650 jet, as well as the wing leading edges of the Airbus A340 and A380 [3]. However, given the fact that thermoset composite manufacturing processes are more mature and material properties are more understood than the thermoplastic composite ones and can also be more suitable for the production of complex-shaped structures (via liquid moulding), combined with the lower cost of the thermoset-based composites as compared to thermoplastic-based composites, it is safe to assume that both thermoset and thermoplastic composites will co-exist in the aircraft of the near future. In such aircraft, the joining of these two dissimilar composites is inevitable. It is hence of paramount importance to find efficient ways to join these two materials.

Nowadays, in Airbus A350 and Boeing 787 aircraft, thermoplastic composite clips and brackets are attached to the epoxy-based composite skin via the traditional mechanical fasteners [2]. Mechanical fastening is one of the most efficient ways in terms of joining conventional metallic parts, however it is not a composite friendly joining technology. Drilling holes in composites induces stress concentrations and fibre damage [4]. Additionally, the installation of mechanical fasteners is time and labour-intensive [5]. An alternative joining method is adhesive bonding, which prevents open hole stress concentrations and enables airtight connections. However, manufacturing time and cost can be extensive, which must include surface preparation, and in most cases, long curing cycles [5].

Fast alternatives to the joining technologies mentioned above are welding technologies, which are unique to thermoplastic polymers and composites, since they take advantage of the ability of the thermoplastic resins to be (re-) melted without any significant impact on their original mechanical and physical properties. Welding follows the fusion bonding principle. Firstly, the two parts to be welded are brought into contact using pressure. Local heating at the interface is generated depending on the nature of the chosen welding process,

i.e., thermal, friction or electromagnetic welding. The increasing temperature in combination with the applied pressure enable intimate contact of the surfaces to be welded. Then, the increasing temperature causes movement of the thermoplastic polymer chains which start to flow and diffuse from one part to the other. Once proper degree of inter-diffusion is achieved, i.e. when fully fusion bonded overlaps are achieved, the heating is terminated and the joint starts to cool down and solidify while constant pressure is still applied to achieve proper consolidation [5]. A schematic of the fusion bonding process is depicted in Figure 1.2. The greatest advantages of the welding techniques are the extremely short manufacturing process, from a few seconds to a few of minutes (depending on the dimensions of the parts to be welded), in comparison with high-performance adhesives and the elimination of drilling holes, as well as the potential to be much less labour-intensive when compared to mechanical fastening [4,5].
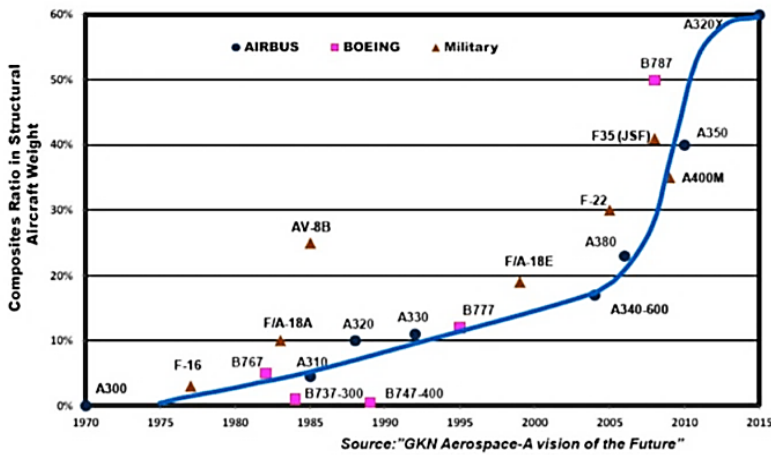
Figure 1.1: Use of composites in commercial and military aircraft in the last decade. Image adapted from [6]
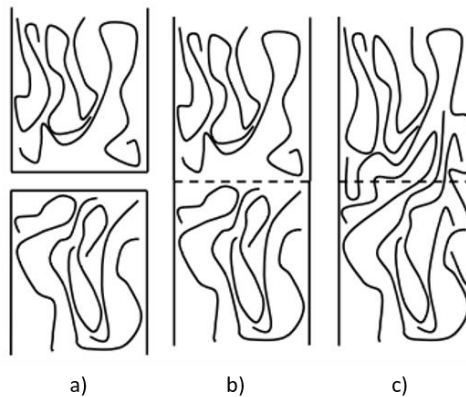
Figure 1.2: Schematic of fusion bonding of a polymer-polymer interface in which a) shows the two distinct interfaces, b) shows intimate contact and c) achievement of interdiffusion. This schematic has been adapted from [5]

1.2 Welding of thermoset composites

During their curing process, thermoset resins cross-link, which means that once they are cured, they cannot be reheated and subsequently reshaped without deteriorating their properties. One way to overcome this issue is by attaching a thermoplastic film, hereafter referred to as coupling layer, to the surface(s) of the thermoset composite part and co-curing them. It should be noted that despite the fact that curing refers to the chemical reaction that occurs in the thermoset resin only, the term "co-curing" is typically used in literature to describe the process of attaching a thermoplastic material on a thermoset composite [2]. A number of studies can be found in open literature that describe ways to achieve such connection between the thermoset composite and the thermoplastic coupling layer. Jacaruso et al [7] proposed the use of a coupling layer that consists of a fabric reinforcement impregnated half way through with a thermoplastic film. The other half is impregnated by the thermoset matrix during curing, thus creating a connection mostly based on mechanical interlocking. Another practice entails treatment of a neat thermoplastic coupling layer, e.g. via ultraviolet-ozone radiation, in order to enhance its adhesion to the thermoset composite [8]. Finally, a coupling layer made out of a thermoplastic resin compatible with the thermoset matrix can be used [2]. In this context, compatibility implies partial solution of the thermoplastic polymer during the curing process and, as a result, diffusion of the thermoset monomer into the thermoplastic polymer and vice versa [9]. This diffusion process followed by phase separation results in an interphase with gradient composition and morphology between the thermoset composite and the thermoplastic coupling layer (see example in Figure 1.3). The existence of such an interphase is regarded as a reliable connection between the thermoplastic coupling layer and the thermoset composite [10].
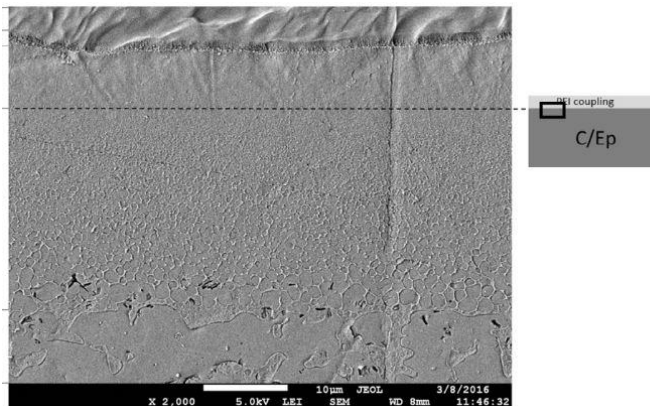
Figure 1.3: Gradient morphology of the interphase formed after co-curing a PEI film (coupling layer) on a CF/epoxy Hexply M18-1 laminate. Figure adapted from [2].

After the coupling layer is attached to the thermoset composite following any of the practices mentioned above, the thermoset composite can be welded through the coupling layer following any welding process. Numerous attempts to utilize fusion bonding and welding techniques to join thermoset composite parts have been reported by several research groups. Hou presented a study [11] in which CF/epoxy specimens were fusion bonded through a

compatible coupling layer that was co cured with the adherends. The nature of the coupling layer or the CF/epoxy system were not stated in that study. The specimens were fusion bonded via co-consolidation in an oven under vacuum pressure or localized heating in a hot press. Single lap shear testing performed under various temperatures and exposure to several chemicals revealed strengths that were equivalent or higher than that of reference CF/epoxy specimens bonded via a Cytec film adhesive FM300K. In a later study, Hou performed co-consolidation of CF/epoxy (Hexcel F593) specimens, through a polysulfone (PSU) layer. PSU was used due to its compatibility with most epoxy systems. Out of several considered co-consolidation temperatures and times, the highest LSS was obtained when selecting the highest values, i.e. 215 °C and 15 mins, respectively, and amounted up to 27 MPa.

Several studies were also performed using resistance welding as the joining technique of thermoset-based composites. Ageorges et al. [12], used this method to weld CF/epoxy (system MTM56/T300C, Advanced Composites) to CF/PEI specimens. The connection between the CF/epoxy adherend and a PEI coupling layer was achieved using a glass fibre (GF) fabric partially impregnated in the PEI layer and partially in the CF/epoxy adherend (after the co-curing process). Specimens that yielded the highest LSS (around 20 MPa) failed within the so-called hybrid interlayer (PEI and GF fabric), which the authors attributed to either thermal degradation of the epoxy resin which impregnated the GF fabric or insufficient impregnation of the interlayer in the CF/epoxy adherend. Don et al. [13] welded bismaleimide (BMI) specimens using two approaches to connect with the thermoplastic layer, i.e. either directly co-curing with a PSU layer or using the hybrid interlayer concept, however for the latter the nature of the thermoplastic layer was not reported. The first approach resulted in LSS around 18 MPa whereas the second approach resulted in LSS between 24 to 27 MPa. The lower strength of the former approach was attributed to limitations of the materials used. McKnight et al. [14] welded CF/epoxy specimens (resin system 3501-6, Hexcel) through either 0.15 mm or 0.3 mm-thick co-cured PSU layers. Absolute LSS values were not reported in the study. However, it was shown that for welding temperatures above 300 °C, degradation in the CF/epoxy adherend occurred which led to low strengths. Specimens welded in optimum conditions (at 300 °C for 10 sec) failed mainly in the composite adherends.

Beiss et al. [15] used vibration joining to join GF/epoxy specimens via polyamide (PA6), which was either used without reinforcement or reinforced with short GFs and/or aluminum oxide (Al2O3). As a first step, the PA6 compound was attached to the CF/epoxy adherend using vibration joining. In this manner, the former material melts due to frictional heating, wets the surface of the CF/epoxy substrate and adhesion between the two is achieved after cooling and consolidation. After that, the other CF/epoxy adherend is joined to the PA6 compound following a similar process. In that study, the adherends were joined in a single lap configuration. The highest strength was achieved when a combination of GFs and Al2O3 was used, attributed to enhanced performance of the hot melt bond.

Schieler and Beier [16] presented a feasibility study on induction welding of CF/epoxy (RTM6 system, Hexcel) to CF/PEI or CF/polyethersulfone (PES), using a PEI or PES co-cured film, respectively. They reported thermal degradation in the CF/epoxy adherend when its temperature exceeded 250 °C. They also showed that a sufficient coupling layer thickness is needed to achieve high LSS, with a suggested minimum thickness being 0.25 mm.

Another method that has been used to join thermoset composites or thermoset- to thermoplastic-based composites is ultrasonic welding. Villegas and Rubio showed in [8] that very fast heating when attempting to weld CF/epoxy (system Hexply 913, Hexcel) to CF/PEEK composites parts through a PEEK co-cured layer (which was subjected to ultraviolet-ozone treatment), has the potential to minimize the risk of thermal degradation of the thermoset matrix. In particular, heating times of less than 500 ms were reported which resulted in absence of noticeable thermal degradation signs. Lionetto et al. presented in [17] a comparative study between CF/epoxy (resin system 3501-6, Hexcel) specimens welded by means of induction welding and CF/epoxy specimens welded through ultrasonic welding. In both cases, a polyvynilbutyral (PVB) coupling layer was used. It was reported that the PVB resin was able to partially penetrate in the first layer of the CF/ epoxy composite due to its low viscosity in the co-curing stage before gelation of the epoxy resin. Single lap shear testing of the specimens revealed that the ultrasonically welded joints yielded a higher strength as compared to the induction welded joints, i.e., a minimum 20% higher lap shear strength in the former than in the latter joints, as well as low porosity, indicating the suitability of the ultrasonic welding process. Finally, Villegas and van Moorleghem presented in [2] an investigation on ultrasonic welding of CF/epoxy (system Hexply M18-1) and CF/ polyetheretherketone composites through a PEI coupling layer. It was confirmed that the compatibility between the PEI coupling layer and the epoxy matrix promoted the formation of a gradient interphase between those two materials, contrarily to when a PEEK coupling layer was used, in which case a clear boundary between it and the epoxy matrix was seen. In fact, a few months after the co-curing of the PEEK layer with the CF/epoxy laminate, the layer could be peeled off manually, indicating poor durability of the connection. Preliminary results after lap shear tests of CF/epoxy to CF/PEEK specimens welded through the PEI coupling layer showed a promising LSS of 28.6 ± 2.3 MPa (average $\pm$ standard deviation).

One challenge posed when attempting to weld thermoset to high-performance thermoplastic composites is the high welding temperatures that are required to soften or melt the thermoplastic matrix, since they typically possess a high glass transition (e.g., PEI with a T_g around 217°C) or melting temperature (e.g. PEEK with a T_m around 343 °C). When thermoset composites are exposed to such high temperatures (generally well above their Tg), their mechanical properties tend to deteriorate and eventually decomposition occurs [18]. In some of the above-mentioned studies, thermal degradation in the CF/epoxy adherend was indeed reported [8,14,16] or suspected [12]. A way to prevent the interface between the coupling layer and the thermoset composite from reaching too high temperatures, thus to limit the risk for thermal degradation mechanisms to occur in the thermoset resin, is by ensuring very fast and localized heating during welding [8]. Among the abovementioned fusion bonding techniques that have been used to join thermoset composites, ultrasonic welding possesses the shortest heating times of less than 500 ms [8], as well as the potential to create high-strength joints [19] making it an excellent candidate for joining thermoset to high-performance thermoplastic composites .

1.3   Ultrasonic welding

In ultrasonic welding heat generation occurs through interfacial and intermolecular friction [20]. It is based on high-frequency (typically between 20 kHz and 70 kHz) and low-

amplitude (10- 250 µm) vibrations. A typical ultrasonic welding setup can be seen in Figure 1.4. The ultrasonic welding process comprises two main phases, the vibration and consolidation phases. During the vibration phase a welding force and amplitude of vibrations are applied on the parts to be welded through the sonotrode. In order to promote heat generation at the welding interface and avoid excessive bulk heating, an artificial surface asperity is placed at the interface, called energy director (ED) [21]. Typically these asperities are matrix resin protrusions on the surfaces to be welded, however research by Villegas revealed that, for welding thermoplastic composites, flat thermoplastic films can be successfully used as EDs, leading to less complex manufacturing [22]. Due to its lower stiffness, the ED undergoes higher cyclic strains than the composite adherends and, in that way, heat generation is concentrated at the welding interface.

Frictional heating is generated at the beginning of the process and it is believed to be the dominant heating mechanism until the Tg of the ED material is reached [20]. After that point, viscoelastic heating becomes the dominant heating mechanism [20]. Once the temperature exceeds its melting temperature (for semi-crystalline resins) or softening point (for amorphous resins), the ED starts flowing due to the applied pressure. At the same time heat is being transferred from the ED to the surface of the adherends in contact with it, which causes melting/softening of the thermoplastic matrix in contact with the ED. Once sufficient heating time is provided, the polymer chains of the molten thermoplastic matrix diffuse into the molten ED and vice-versa, creating chain entanglements [23]. Finally, the vibrations are stopped and the weld is allowed to cool down and solidify while still applying a consolidation force (consolidation phase).
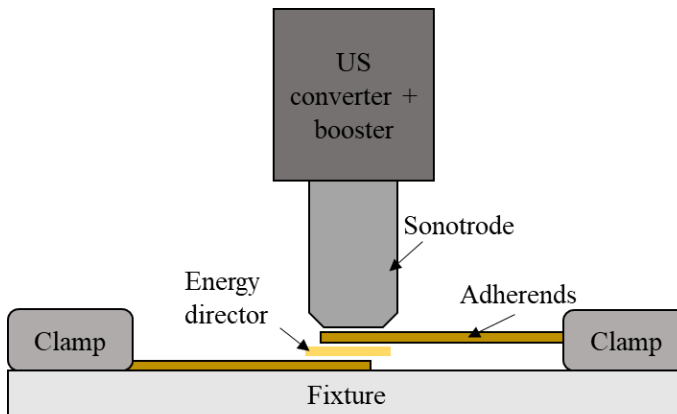
Figure 1.4: Schematic of a typical ultrasonic welding setup. Dimensions are not to scale.

1.4   Objective of this research

A number of studies with respect to the utilization of ultrasonic welding for joining thermoplastic to thermoplastic composite can be found in open literature [5,19]. However, prior to the completion of this thesis, only three studies regarding utilizing ultrasonic welding to join thermoset- to thermoplastic (or thermoset) composites could be found in open literature, as mentioned in section 1.2. The results presented in these preliminary studies

demonstrated the high potential of ultrasonic welding as the joining technique of dissimilar composite parts in the future aircraft. However, further understanding of the process as applied to dissimilar composite joints is still lacking in order for it to be utilized in actual applications.

Therefore, the objective of the current work is to gain further understanding on the ultrasonic welding of thermoset to thermoplastic composites and to identify the potential and limitations of such process. The first part of this research focusses on identifying well-suited techniques for the production of ultrasonically welded epoxy- to PEI- or PEEK-based composites. The main difference between welding of thermoplastic composites and welding of thermoset or dissimilar composites is the existence of the thermoplastic coupling layer. The first logical question that needs to be addressed is whether the coupling layer by itself can be used as an integrated energy director or a loose ED is still needed. The answer to this question influenced the direction of the rest of this thesis. A loose energy director was found to produce welds of better quality as compared to when only the coupling layer was used, therefore this practice, i.e., the use of a loose energy director was adopted for the rest of this thesis. Note that loose, flat EDs were used instead (see schematic in Figure 4) of the traditional triangular ones since they offer simplified processing without a significant negative impact on the mechanical performance [22]. Subsequently, the effect of the material of the energy director (in the cases where PEI was used as the material of the coupling layer and PEEK as the matrix of the thermoplastic composite) and of the thickness of the coupling layer on the weld strength and welding process were investigated. The second part of this research comprises two studies with respect to the robustness of the ultrasonic welding of epoxy- to PEEK-based composites. The first study focusses on the sensitivity of the weld quality to the duration of the vibration phase, whereas the second one targets the sensitivity of the ultrasonic welding process to changes in the process parameters, namely welding force and amplitude of vibrations.

To achieve the abovementioned objectives the following questions based on the knowledge gaps should be answered:

1. How are the ultrasonic welding process and weld mechanical performance affected when welding dissimilar composites solely through the coupling layer i.e., without an energy director?

2. How does the nature of the material of the energy director (i.e., PEI or PEEK) affect the ultrasonic welding process and mechanical performance of the dissimilar composite welds?

3. What are the limitations regarding the thickness of the coupling layer for the production of high-strength dissimilar composite welds?

4. How sensitive is the weld quality to changes in the duration of the vibration phase?

5. How sensitive is the ultrasonic welding process and mechanical performance of the welds to changes in the welding force and amplitude of vibrations?

1.5 Thesis outline

Based on the research questions, the thesis is divided into six chapters. Chapters 2 and 3 focus on assessing different welding stack (i.e., adherends, coupling layer and energy directors) morphologies and their impact on the welding process and mechanical performance, whereas the aim of Chapters 4 and 5 is to determine the robustness of the ultrasonic welding of dissimilar composites with respect to changes in the process parameters. Note that Chapters 2-5 are adaptations of peer-reviewed journal papers or papers currently under peer-review, thus their format has remained the same as the (to-be) published format. Final conclusions and recommendations for future studies can be found in Chapter 6. More specifically, this thesis is divided as follows:

- **Chapter 2: Investigation on energy director-less ultrasonic welding.** The first research question will be addressed in this chapter. Dissimilar composite joints were welded solely through the coupling layer. Two coupling layer thicknesses were evaluated. The welding process and the mechanical performance of the hybrid joints were compared to that of dissimilar composite joints welded through an additional loose energy director. The mechanical performance of all the dissimilar composite joints was then compared to reference co-cured joints.
- **Chapter 3: Investigation on the material of the energy director and the thickness of the coupling layer.** The second and third research questions will be addressed in this chapter. Two different energy director materials and two thicknesses were assessed. The welding process and the mechanical performance of the dissimilar composite welds was compared to that of reference of thermoplastic composite welds.
- **Chapter 4: On the sensitivity of ultrasonic welding on the heating time.** The fourth research question will be addressed in this chapter. Dissimilar composite and reference thermoplastic composite joints were welded at different heating times and their lap shear strength was measured and compared. Processing intervals were defined. In the dissimilar composite configuration three coupling layer thicknesses were assessed, in order to determine their effect on the width of the processing interval.
- **Chapter 5: On the sensitivity of ultrasonic welding on the process parameters.** The fifth research question will be addressed in this chapter. The sensitivity of the ultrasonic welding process and the weld mechanical performance to changes in the welding force and amplitude of vibrations was determined.
- **Chapter 6: Conclusions and recommendations**

1.6 References

[1]   Offringa AR. Thermoplastic composites - Rapid processing applications. Compos Part A Appl Sci Manuf 1996;27:329–36. doi:10.1016/1359-835X(95)00048-7.

[2]   Villegas IF, van Moorleghem R. Ultrasonic welding of carbon/epoxy and carbon/PEEK composites through a PEI thermoplastic coupling layer. Compos Part A Appl Sci Manuf 2018;109:75–83.

[3]   Barile M, Lecce L, Iannone M, Pappadà S, Roberti P. Thermoplastic Composites for Aerospace Applications. In: Pantelakis S, Tserpes K, editors. Revolutionizing Aircr. Mater. Process., Cham: Springer International Publishing; 2020, p. 87–114. doi:10.1007/978-3-030-35346-9_4.

[4]   Yousefpour A, Hojjati M, Immarigeon J-P. Fusion Bonding/Welding of Thermoplastic Composites. J Thermoplast Compos Mater 2004;17:303–41. doi:10.1177/0892705704045187.

[5]   Ageorges C, Ye L, Hou M. Advances in fusion boding techniques for joining thermoplastics materials composites: a review. Compos Part A Appl Sci Manuf 2001;32:839–57.

[6]   Ono K, Gallego A. Research and applications of AE on advanced composites. 30th Eur. Conf. Acoust. Emiss. Test. 7th Int. Conf. Acoust. Emiss., 2012.

[7]   Jacaruso GJ, Davis GC, McIntire AJ. Method of Making Thermoplastic Adhesive Strip for Bonding Thermoset Composite Structures, 1993.

[8]   Villegas IF, Rubio PV. On avoiding thermal degradation during welding of high-performance thermoplastic composites to thermoset composites. Compos Part A Appl Sci Manuf 2015;77:172–80.

[9]   Lestriez B, Chapel J-P, Gérard J-F. Gradient interphase between reactive epoxy and glassy thermoplastic from dissolution process, reaction kinetics, and phase separation thermodynamics. Macromolecules 2001;34:1204–13.

[10]   Deng S, Djukic L, Paton R, Ye L. Thermoplastic-epoxy interactions and their potential applications in joining composite structures - A review. Compos Part A Appl Sci Manuf 2015;68:121–32.

[11]   Hou M. Thermoplastic adhesive for thermosetting composites. Mater Sci Forum 2012;706–709:2968–73.

[12]   Ageorges C, Ye L. Resistance welding of thermosetting composite / thermoplastic composite joints. Adv Mater 2006;32.

[13]   Don RC, McKnight H, Wetzel ED, Gillespie Jr. JW. Application of thermoplastic resistance welding techniques to thermoset composites. Annu Tech Conf Soc Plast 1994:1295–7.

[14]   McKnight SH, Fink BK, Monnard V, Bourban P-E, Manson J-AE, Eckel DA, et al. Processing and characterization of welded bonds between thermoset and thermoplastic composites. Army Res Lab 2001.

[15]   Beiss T, Menacher M, Feulner R, Huelder G, Osswald TA. Vibration joining of fiber-reinforced thermosets. Polym Compos 2010;31:1205–12.

[16]   Schieler O, Beier U. Induction welding of hybrid thermoplastic-thermoset composite parts. Int J Appl Sci Technol 2016;9:27–36.

[17]   Lionetto F, Morillas MN, Pappadà S, Buccoliero G, Villegas IF, Maffezzoli A. A Hybrid welding of carbon-fiber reinforced epoxy based composites. Compos Part A 2018;104:32–40.

[18]   Abouhamzeh M, Sinke J. Effects of fusion bonding on the thermoset composite. Compos Part A Appl Sci Manuf 2019;118:142–9. doi:10.1016/j.compositesa.2018.12.031.

[19]   Villegas IF. Ultrasonic Welding of Thermoplastic Composites. Front Mater 2019;6:1–10. doi:10.3389/fmats.2019.00291.

[20]   Zhang Z, Wang X, Luo Y, Zhang Z, Wang L. Study on heating process of ultrasonic welding for thermoplastics. J Thermoplast Compos Mater 2010;23:647–64.

[21]   Benatar A. Ultrasonic welding of plastics and polymeric composites. Power Ultrason. Appl. High-Intensity Ultrasound, 2014. doi:10.1016/B978-1-78242-028-6.00012-0.

[22]   Villegas IF, Valle Grande B, Bersee HEN, Benedictus R. A comparative evaluation between flat and traditional energy directors for ultrasonic welding of CF/PPS thermoplastic composites. Compos Interfaces 2015;22:717–29. doi:10.1080/09276440.2015.1053753.

[23]   Benatar A, Gutowski TG. Ultrasonic welding of PEEK graphite APC-2 composites. Polym Eng Sci 1989;29:1705–21. doi:10.1002/pen.760292313.

2 Investigation on energy director-less ultrasonic welding of polyetherimide (PEI)- to epoxy-based composites[1]

In ultrasonic welding of thermoplastic composites an energy director (ED) (i.e., neat thermoplastic film), is used between the two adherends to be welded, to promote frictional and viscoelastic heating. For welding of thermoset composites (TSC), a thermoplastic coupling layer is co-cured on the surface to be welded as typical procedure to make the TSC "weldable". This study focuses on investigating whether a polyetherimide (PEI) coupling layer by itself has the potential to promote heat generation during ultrasonic welding of CF/epoxy and CF/PEI samples, without the need for a separate ED, and if so, what thickness should that coupling layer be. The main findings were that welding without a loose ED resulted in overheating of the CF/PEI adherend and/or coupling layer due to the inability of the latter to promote heat generation efficiently. However, welding of CF/epoxy and CF/PEI samples with the use of a loose ED resulted in high-strength welds.

2.1 Introduction

Using dissimilar composite parts is becoming more popular in the aerospace industry. Two examples are the Airbus A350 and Boeing 787 passenger aircraft, in which thousands of thermoplastic composite (TPC) clips are used in the carbon fibre (CF)/epoxy fuselage. The joint between these parts is currently attained with mechanical fasteners, which are not the most suitable for composite structures [1]. An alternative joining method is adhesive bonding. However, extensive surface preparation is necessary to create strong bonds, and in most cases, curing of the thermoset adhesive is time consuming (minimum a couple of hours) [1]. Welding, on the other hand, does not require any surface preparation and is a much faster joining process as compared to the two methods mentioned above (from a few seconds to a couple of minutes) [2,3]. In order for welding to become an alternative to mechanical fastening of dissimilar composite parts, it should be further explored and understood since only a limited number of studies can be found in literature [1,4,5]

One way to make thermoset composites (TSC) weldable is by placing a neat, compatible thermoplastic (TP) layer, hereafter called "coupling layer", on the surface of the uncured laminate, and subsequently subjecting the stack (i.e., the adherend and the coupling layer) to a co-curing process [6]. Even though curing refers to the chemical reaction that occurs in the thermoset resin only, the term "co-curing" is used in literature to describe the process of bonding a thermoplastic film with a TSC [5]. Therefore, the same term will be used in this study for consistency. Compatibility between the coupling layer and the thermoset (TS) adherend allows for interdiffusion of the monomers of the thermoset resin into the polymer and vice versa, during the co-curing process [7]. Interdiffusion and ultimately phase separation between the thermoset and thermoplastic resins results in an interphase with gradient composition and morphology between the two materials, which is a reliable way to bond a TP layer to a TSC [7]. Note that apart from partial solubility, compatibility between the TP and TS materials requires that the TP material has a glass transition temperature (Tg) above the curing temperature of the TS resin. In principle, after the co-curing process is finished, the TSC laminate can be welded through the coupling layer following any welding process.

In this study, ultrasonic welding was used to weld a TSC material to a TPC material, as it is the fastest welding method at the moment, with heating times of less than 1 s [4,8]. As reported in a previous study [3], the short heating times of less than 500 ms, can help prevent the epoxy matrix from thermally degrading during welding, since the time for the heat to be transferred from the weld interface to the TS component as well as for the degradation mechanisms to occur is limited. To ensure very short heating times, a combination of high force and amplitude of the vibrations were used in that study. In the ultrasonic welding process of TPCs, a neat, flat TP resin layer (normally made of the same material as the TP matrix), referred to as energy director (ED), is placed between the two adherends to be welded. The ED is responsible for generating heat locally at the interface through preferential frictional and viscoelastic heating. Frictional heating is responsible for initiating heat generation. Viscoelastic heating becomes the dominant heating mechanism once the temperature of the resin reaches its Tg [8]. However, for welding TSCs a neat TP layer already exists, i.e. the TP coupling layer co-cured on the TSC laminate. It is unknown whether an additional ED is still needed or whether the coupling TP layer itself is sufficient to guarantee a weld with good mechanical performance. Not using an ED could make the assembly process faster by eliminating the step of fixing the ED on the surface of the

adherend and result in the use of less material. On the other hand, removing the ED is expected to affect the heat generation at the interface. The coupling layer and TPC adherend will be more involved in heat generation, as compared to the case when an ED is used. Hence the coupling layer is expected to be unable to act as a thermal barrier for the TS resin and it is possible that more heat will be transferred from the coupling layer to the TSC adherend. This might subsequently result in overheating of the TSC adherend and thus poor weld quality.

The present paper aims at assessing whether it is feasible to ultrasonically weld CF/ Polyetherimide (PEI) to CF/epoxy composites by using only the co-cured PEI coupling layer as an integrated ED. PEI was chosen as the material for the coupling layer as it is known to be compatible with most epoxy systems [7]. Two thicknesses were examined for the coupling layer, namely 60 and 250 µm. The TPC adherend was made out of CF/PEI to match the material of the coupling layer. The main aspects investigated were the effect of the absence of a loose ED (hereafter referred to as ED-less process) on: (i) the welding process (e.g., the power dissipated during the process and the displacement of the sonotrode curves), (ii) the integrity of the welding stack, i.e., the adherends and the coupling layer after welding and (ii) the mechanical performance of the welded joints. The ED-less process was compared to a reference welded case, in which a loose flat PEI ED was used. The mechanical performance of the samples of all welded cases were also compared to reference co-cured samples.

2.2   Experimental Procedure

2.2.1 Materials and manufacturing

In this study, Cetex® CF/PEI powder-coated semi-preg with a 5-harness satin weave fabric, manufactured by TenCate Advanced Composites (The Netherlands) was used as the material to produce the TPC adherends. The CF/PEI laminates had a [0/90]3s stacking sequence and were consolidated in a hot-platen press at 320 °C and 20 bar for 30 min. The thickness of the consolidated laminates was around 2 mm.

As the TSC material, T800S/3911 unidirectional CF/epoxy prepreg from TORAY (Japan) was used. Unidirectional CF/epoxy pre-preg was manually stacked in a [0,90]2s configuration. A neat PEI film was placed on one of the sides of the CF/epoxy laminates, serving as the coupling layer. Two PEI coupling layers with two different thicknesses were used, a 60 µm-thick PEI film provided by SABIC (The Netherlands), and a 250 µm-thick PEI film provided by LITE (Germany). The PEI coupling layer was degreased with isopropanol prior to its application on top of the CF/epoxy prepreg stack. The coupling layer was kept in place because of the tackiness of the uncured epoxy resin. The CF/epoxy laminates with the attached coupling layer were cured in an autoclave at 180°C and 7 bars for 120 min, according to the specifications of the manufacturer. A Wrightlon® 7400 nylon foil provided by MCTechnics was used as the material of the vacuum bag. To ensure flat surfaces on both sides of the CF/epoxy laminate, an aluminium caul plate was used on the side of the vacuum bag and on the opposite side a standard aluminium flat mould. The thickness of the CF/epoxy/PEI cured laminates was 1.9 mm for the 60 µm coupling layer and 2.28 mm for the 250 µm one. Even though extensive work has been published on the

miscibility of epoxy and PEI resins [5,7,9], the combination of the T800S/3911 and PEI materials has not been reported yet in literature. Hence, an investigation on whether an interphase was formed between the two abovementioned materials was conducted and it is presented in the baseline study of the results section. Finally, a loose, flat ED cut out of the same film as the 250 μm-thick PEI coupling layer was used. The ED was cut in dimensions slightly bigger than the overlap and then attached with adhesive tape on the CF/epoxy/PEI adherend.

The CF/PEI and CF/epoxy/PEI adherends with dimensions 25.4 mm x 101.6 mm were cut from the laminates using a water-cooled circular diamond saw. The CF/PEI adherends were cut with their longitudinal direction parallel to the main apparent orientation of the fibres. The CF/epoxy/PEI adherends were cut with their longitudinal direction parallel to the 0° fibres.
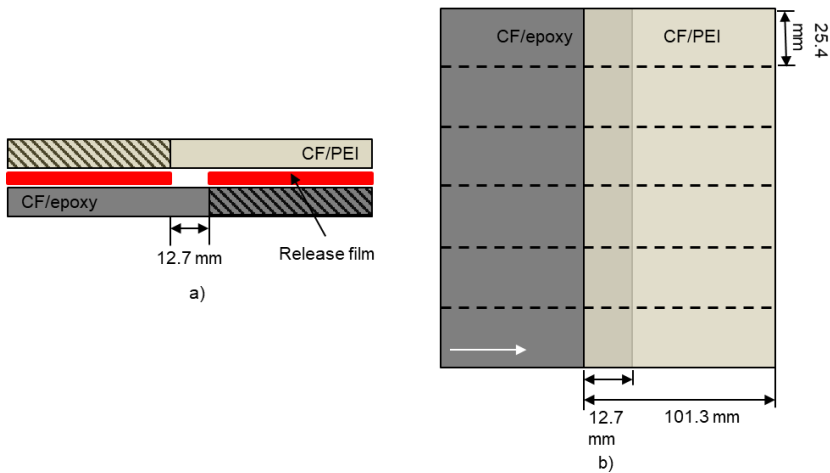
Figure 2.1: Schematic representations of a) the manufacturing of the reference co-cured samples and b) the location of the cuts, represented by the dash lines. The white arrow points at the 0° fibres of the CF/epoxy adherend and the main apparent orientation of the fibres of the CF/PEI adherend. Dimensions are not to scale.

CF/epoxy laminates directly co-cured with CF/PEI laminates were manufactured as co-cured reference specimens. Note that, in this case, a neat PEI film was not used on top of the CF/epoxy laminate, because at 180 °C the PEI resin is still in solid state, hence it cannot adhere to the CF/PEI adherend. Placing a PEI film on top of the CF/PEI laminate and co-consolidating them together was also not performed since it was not easy to ensure that the thickness of the PEI resin at the bond line would be the same as the weld line in the welded joints. Nevertheless, the reference configuration was only used in order to assess how the welded joints perform in comparison to a standard industrial procedure. An uncured CF/epoxy prepreg stack and a consolidated CF/PEI laminate were first cut in 200 mm-length and 200 mm-width and then stacked. In order to produce samples with a single-lap configuration, two release films were placed between the uncured CF/epoxy and the CF/PEI laminates with a gap of 12.7 mm, as seen in Figure 2.1a. Afterwards, the stack was co-cured following the same autoclave cycle mentioned above for the CF/epoxy laminate. The release films allowed for the two materials to be co-cured only at the desired location. Subsequent to the co-curing process, the parts indicated with the diagonal lines in Figure 2.1a were cut

out, in order to produce the single-lap specimens. Finally, the individual specimens were cut in 25.4 mm-width dimension, as seen in Figure 2.1b.

2.2.2 Welding process

Individual samples were welded with a Rinco Dynamic 3000 ultrasonic welder in a single lap configuration, with the overlap being 12.7 mm long and 25.4 mm wide. The custom-made welding jig shown in Figure 2.2 was used. A cylindrical sonotrode with a 40 mm diameter was utilised. To ensure minimum heating times, and hence minimum risk of thermal degradation at an acceptable level of dissipated power, the parameters chosen were 1500 N welding force and 86.2 µm peak-to-peak vibration amplitude. These parameters, which are close to the highest within the limits of the machine, result in very short heating times [3]. Solidification force and time were kept constant at 1500 N and 4 s respectively. The duration of the vibration phase was indirectly controlled through either the downward displacement of the sonotrode or the dissipated energy, as it will be explained in more detail in section 3.2. The variation of the power and displacement of the sonotrode during the vibration phase were provided by the welding machine at the end of the welding process.
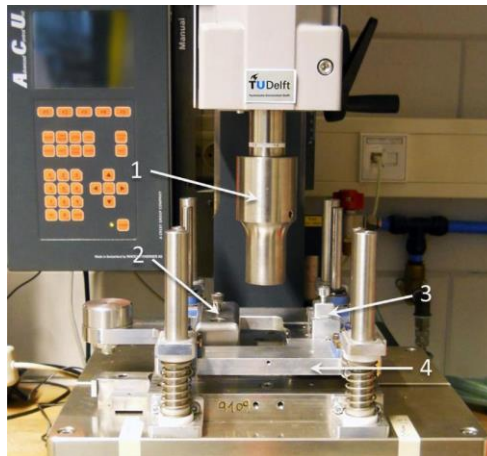
Figure 2.2 Custom made welding setup. 1: sonotrode, 2: clamp for the lower sample, 3: clamp for the upper sample and 4: sliding platform. [9]

Figure 2.3 shows the schematics of the different types of joints that were developed in this study. The schematics correspond to (a) joints welded through a 60 µm-thick coupling layer, hereafter referred to as ED-less-60 case, (b) joints welded through a 250 µm-thick coupling layer, hereafter referred to as ED-less-250 case, (c) reference joints welded with a 250 µm-thick loose ED and a 60 µm-thick coupling layer, hereafter referred to as welded reference ED case and (d) co-cured reference joints. In the reference ED case, the ED was fixed on top of the CF/epoxy adherend with adhesive tape (the size of the ED was slightly bigger than the size of the overlap).
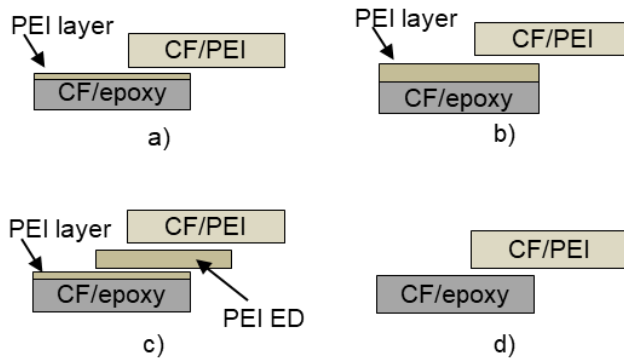
Figure 2.3: Schematic representation of CF/PEI- CF/epoxy/PEI stack for the a) ED-less-60 case, b) ED-less-250 case, c) reference ED case and d) reference co-cured case. Dimensions are not to scale.

2.2.3 Testing

Single-lap shear tests were performed in order to assess the mechanical performance of the joints based on the ASTM D 1002 standard. A Zwick 250 kN universal testing machine operating at 1.3 mm/min cross-head speed and under displacement control was used for these tests. The apparent lap shear strength (LSS) of the joints was calculated as the maximum load divided by the overlap area. Five specimens were tested per welding case to determine the average LSS and corresponding standard deviation. Naked-eye observation and scanning electron microscopy (JEOL JSM-7500F Field Emission Scanning Electron Microscope, SEM) were used for fractographic analysis of tested joints. An optical microscope (Zeiss Axiovert 40) together with the SEM were used for cross-sectional analysis of as-welded specimens. Samples for cross-sectional microscopy were embedded in EpoFix resin and subsequently grinded and polished. To observe the epoxy-PEI interphase, polished samples were etched with 1 ml of N-Methyl-2-pyrrolidone (NMP) and then immediately rinsed with ethanol and distilled water to provide a better contrast [5].

2.3 Results

2.3.1 Baseline study: Interphase between T800s/3911 and PEI materials

This section aims at i) answering whether an interphase was formed between the T800s/3911 prepreg and the PEI coupling layers, and the T800s/3911 prepreg and the CF/PEI adherend in the co-cured reference joints, after the co-curing process and ii) describing the interphase morphology. Figure 2.4a shows the optical micrograph of an etched CF/epoxy sample with the 60 µm thick PEI coupling layer. A darker grey area can be seen in between the epoxy matrix, which is a lighter grey colour, and the PEI, which shows scratches that were exposed by the etching process. Note that the spherical particles present in the epoxy resin, with diameters between a few µm and 10 µm, are thermoplastic toughening particles present in the T800s/3911 prepreg. A closer look to the circled area (b) in Figure 2.4a is presented in the SEM image of Figure 2.4b. In this image is shown that the above-mentioned darker grey

area corresponds to the interphase that was formed between the epoxy and PEI materials during the co-curing process. The interphase consists of epoxy spheres dispersed in a PEI-rich matrix, with diameters decreasing towards the PEI coupling layer. Similar interphase morphologies have been seen in previous works, in which PEI was co-cured with a Hexply M18/1 (Hexcel) prepreg [5] or epoxy resins with different formulations [7], [10]–[12]. As explained in those studies, during the co-curing process, the liquid-reactive epoxy system acts as a solvent of the PEI resin. This results in the epoxy monomers diffusing into the glassy PEI and partially dissolving it. Partial dissolution of the PEI polymer allows at the same time for diffusion of the PEI into the liquid epoxy resin. This interdiffusion process between the epoxy and PEI systems stops once the epoxy resin reaches the gelation point. Because of the limited miscibility between the rubbery epoxy and the PEI resins, phase separation occurs. This results in a gradient concentration of the two polymers, hence a gradient interphase between the two materials, with the morphology seen in Figure 2.4b. The epoxy flow front into the PEI material is also visible in Figure 2.4b. The area between this flow front and the smallest visible epoxy spheres, with an apparently smooth texture corresponds, most likely, to either an area in which the concentration of the epoxy monomers in the PEI resin was very low, resulting in no phase separation of the two resin systems, or an area with epoxy spheres with a size that was not resolved by the microscope. The thickness of the interphase varies and has a maximum value of around 25 μm. The same interphase morphology was observed in the co-cured T800s/3911 prepreg and 250 μm-thick coupling layer.
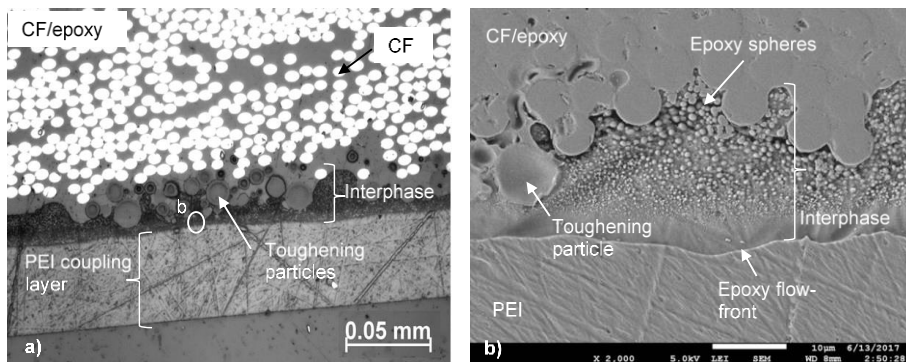
Figure 2.4: Cross-section images of an etched sample cut from the CF/epoxy/PEI laminate obtained via a) optical microscopy, in which the interphase can be seen as a dark grey area between the epoxy and the PEI resin (both with lighter grey colours) and b) SEM, which shows an interphase with a gradient morphology.

Figure 2.5a presents the optical micrograph of an etched reference co-cured sample. As shown in the image, the interphase is not visible with optical microscopy, therefore SEM analysis is necessary to examine whether an interphase was formed. The SEM image in Figure 2.5b shows the existence of an interphase similar to the one formed in the CF/epoxy/PEI laminates, with epoxy spheres dispersed in the PEI-rich matrix resin, indication of inter-diffusion between the epoxy and PEI matrices. However, the two interphases have a different maximum thickness, with the interphase of the co-cured reference sample being almost 40 μm, whereas for the interphase formed with the neat PEI film the thickness is 25 μm. Epoxy spheres can be found deeper into the CF/epoxy laminate, in the interphase of the co-cured reference sample. The density of the epoxy spheres in the PEI resin also seems to be higher for the co-cured reference samples. The reason why the

interphase formed between the CF/epoxy and CF/PEI prepregs shows some differences, might be a different PEI grade between the 60 microns SABIC PEI coupling layer and the Cetex® CF/PEI prepreg of the TPC adherend (reference co-cured case).
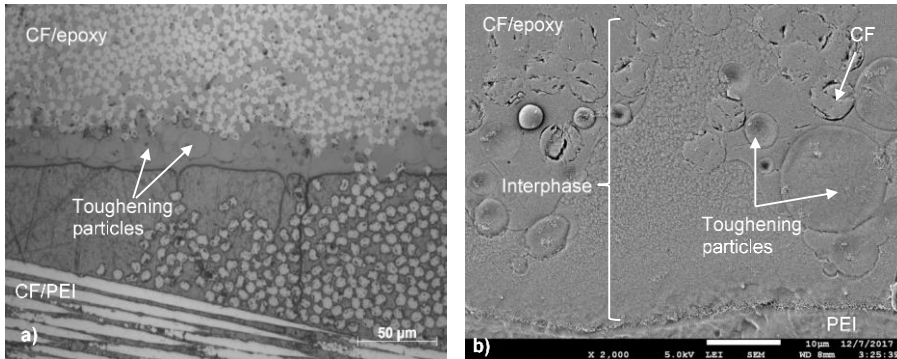
Figure 2.5: Cross-section images of etched co-cured reference sample obtained via a) the optical microscope, in which no signs of a formed interphase can be seen, and b) the SEM, which shows that an interphase is formed with epoxy spheres embedded in the PEI resin.

2.3.2 Effect of the different welding cases on the welding process

Figure 2.6 illustrates the representative power and displacement curves plotted versus time of samples welded according to the three welding cases shown in Figure 2.3, namely the ED-less-60, ED-less-250 and the reference ED cases. The curves correspond to displacement-controlled process in which the downward movement of the sonotrode reached the total thickness of the coupling layer, for the ED-less cases, or the thickness of the ED for the reference ED case. Two power peaks can be found in the power curves of all cases. The displacement stays at around zero during the first power peak. The time during which the displacement is zero, however, differs per case. This stage lasts approximately 250 ms longer for the ED-less cases, as compared to the reference ED case. The displacement starts increasing when the power starts increasing after the first peak. The rate at which the displacement increases is the fastest for the reference ED case and the slowest for the ED-less-60 case.

In welding of TPCs the power and displacement curves are used to determine the optimum duration of the vibration phase [13]. It is shown in [13] that stopping the welding process close to when the second power peak occurs, results in welds with the highest strength. In the reference ED case, samples welded in displacement-control mode with a target displacement of 0.13 mm (which corresponds to the second power peak) featured, upon mechanical testing, no signs of overheating and satisfactory strength values, as it will be shown in section 3.4.2. In the ED-less-60 case, the second power peak corresponded to zero displacement and hence an energy-controlled process had to be used. Through a trial-and-error process, it was found that welding between 500 J (which corresponds to the second increase in power and is indicated with the black "+" point in Figure 2.6) and 700 J (which corresponds to the second power peak, indicated with the grey "x" point), resulted in welds with similar strength. All of them featured unwelded areas and degradation signs of the PEI

resin, as it will be shown in section 3.4.2. Hence, to minimise the thermal effects, 500 J was chosen as the optimum energy. In the ED-less-250 case, samples welded with a target displacement of 0.15 mm (expected optimum displacement, indicated with the grey "x" point in Figure 2.6) featured, upon testing, fibre distortion in the CF/PEI adherend, potentially due to excessive PEI resin flow [14]. A trial-and-error process had to be followed, in order to find more adequate welding conditions. It was found that the welds with the highest mechanical performance and least fibre distortion were achieved for an energy value of 600 J (black "+" point in Figure 6). Note that energy-controlled welding had to be used since the vibration had to be stopped close to the onset of the downward displacement of the sonotrode, therefore at approximately zero displacement, as seen in Figure 2.6.
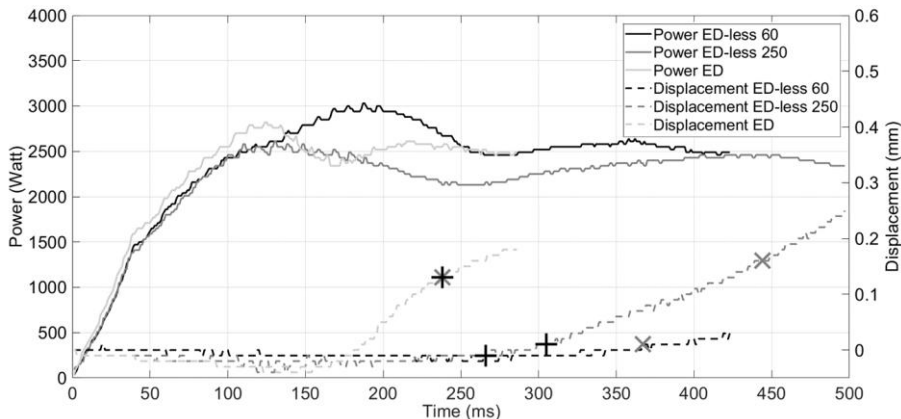
Figure 2.6: Representative power (solid line) and displacement (dotted line) curves of samples welded according to the three different welding cases. The grey "x" points indicate the initial expected optimum displacement values, according to the procedure defined for ultrasonic welding of TPCs with a loose ED [13]. The black "+" points indicate the actual optimum displacement values used for the welding.

2.3.3 Effect of the welding process on the welding stack integrity

2.3.3.1 Optical microscopy

In order to evaluate the effect of the welding process on the integrity of the welding stack, i.e., the adherends, the coupling layer and the interphase, cross-sectional analysis of as-welded samples was performed. The main focus points of this analysis were (i) to determine the thickness of the weld line, since it is an indication of how much neat resin has flowed and it can also have an influence on the mechanical performance of the joints, and (ii) to identify thermal degradation signs in the form of porosity. Note that the weld line is defined in this study as the PEI-rich region between the fibre bundles of the CF/epoxy and CF/PEI adherends. Figure 2.7 shows the optical micrograph of the cross-section of an ED-less-60 sample. Porosity within the weldline and the first ply of the CF/PEI adherend can be observed, as seen in the circled areas in Figure 2.7. The weldline has a thickness of around 70 µm. Figure 2.8 presents the cross-sectional optical micrograph of an ED-less-250 sample. Some porosity can be seen near the edge of the overlap and close to the CF/PEI adherend. The thickness of the weldline is approximately 200 µm.

Figure 2.9 presents an optical micrograph of a reference ED sample. No signs of porosity within the weld line and in the two composite adherends can be found. The thickness of the weld line is approximately 110 µm and it seems to be similar to the ones typically observed in literature for ultrasonically welded TPC joints [15,16]. The thickness of the weld line decreases towards the edges, where squeeze out of resin occurs.
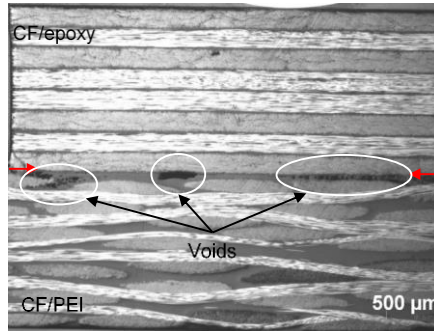
Figure 2.7: Cross-sectional micrograph close to the edge of an ED-less-60 sample welded at 500 J. Porosity can be seen within the weld line. Red arrows indicate the weld line.
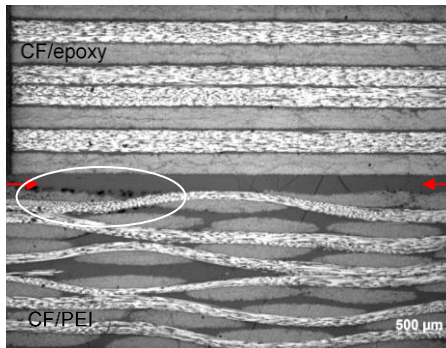
Figure 2.8: Cross-sectional micrograph close to the edge of an ED-less-250 case sample welded at 600 J. A thick weld line and porosity in the weld line can be observed. Red arrows indicate the weld line.
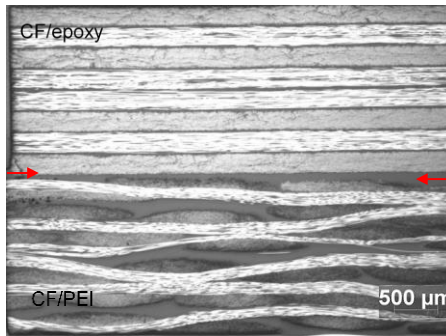
Figure 2.9: Cross-sectional micrograph close to the edge of a reference ED sample welded at 0.13 mm displacement revealing no porosity in the weld line. Red arrows indicate the weld line.

2.3.3.2 Scanning electron microscopy

During the welding process, it is likely that the coupling layer will soften and flow, especially in the ED-less cases, in which the coupling layer is expected to act as an integrated ED. Hence, it could happen that flow of the coupling layer close to the interphase altered the initial interphase morphology between the epoxy matrix and the PEI film. In order to assess whether the welding process affected the interphase, SEM analysis of the cross-sections presented in the previous section was performed. Figure 2.10 depicts the SEM images of as-welded specimens for each welding case. It is observed that for all cases the post-welded interphase has the same morphology as the original one.
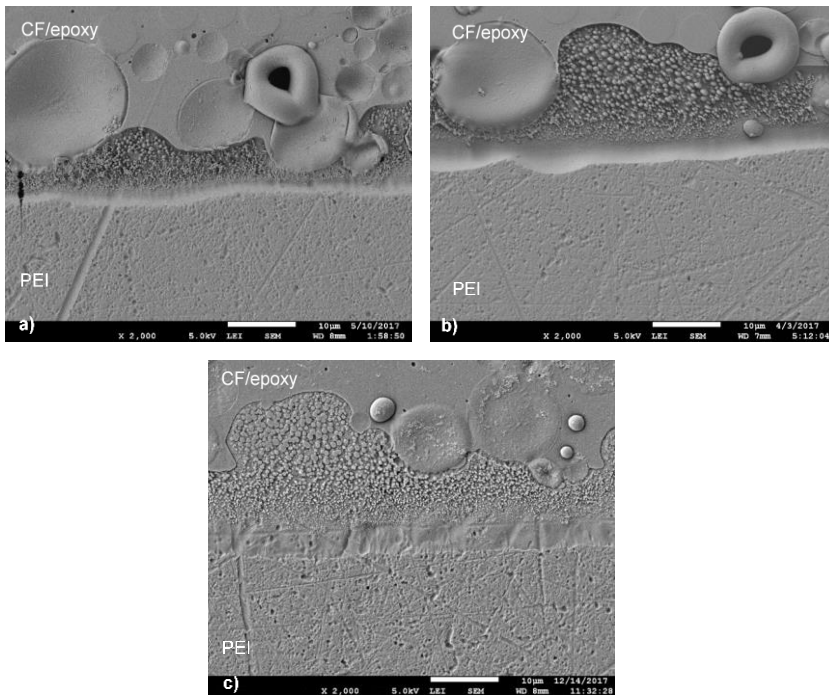
Figure 2.10: SEM images of as-welded specimens for the a) ED-less-60, b) ED-less-250 and c) reference ED cases. The interphase morphology is the same for all welding cases.

2.3.4 Mechanical performance and failure analysis of welded and reference joints

2.3.4.1 Single-lap shear tests

The results of the single-lap shear tests are illustrated in Figure 2.11. The ED-less-60 samples have a LSS of 17.3±4.5 MPa (average ± standard deviation) with a 26% coefficient of variation (cov), while the ED-less-250 case samples have a LSS of 29.3± 3.2 MPa (11% cov). The LSS of the reference ED samples is the highest with the lowest scatter amongst

the welded samples, i.e. 37.7 ± 1.6 MPa (4% cov) . The co-cured samples exhibit a LSS of 34.7 ±1.4 MPa (4% cov).
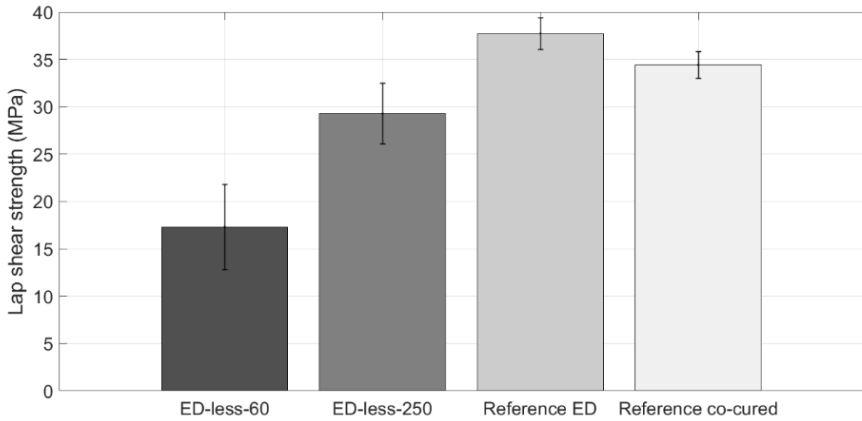
Figure 2.11: LSS values of the reference and welded samples with corresponding standard deviation.

2.3.4.2 Fractography

Fractographic analysis was used in order to further evaluate the mechanical performance of the joints. Figure 2.12 shows three typical fracture surfaces of ED-less-60 samples after testing. Note that they were all welded with the same welding parameter, i.e. 500 J. Unwelded areas covering a significant part of the overlap can be seen in all samples. The amount and location of the unwelded areas are inconsistent per sample and most of the welded areas display discoloured resin that can potentially result from thermal degradation. The lack of exposed fibres indicates that failure occurred entirely in the neat PEI resin, most probably in the coupling layer. The sample exhibiting the highest strength and largest welded areas is chosen for further microscopic analysis (the left most sample in Figure 2.12), the results of which are presented in Figure 2.13a.

Figure 2.12: Fracture surfaces obtained from ED-less-60 samples welded at 500 J. The white lines indicate the unwelded areas.

Figure 2.13b depicts a SEM image of the area circled in Figure 13a. Numerous voids and flakes can be seen in the PEI resin, however it is unclear whether they were coming from the coupling layer or the PEI matrix in the CF/PEI adherend. Such features are mostly linked to thermal degradation of the PEI resin, as presented in the work of Palardy and Villegas [15]. A closer examination of the area (c) indicated in Figure 2.13b, reveals exposed epoxy spheres which are part of the interphase, and toughening particles, which are indications of interphase failure and possibly epoxy matrix failure (Figure 2.13c). Note that the distinction between the PEI and the epoxy resins in these micrographs was made based on the plastic deformations that were found in the former and the embedded toughening particles and remains of the interphase in the latter.
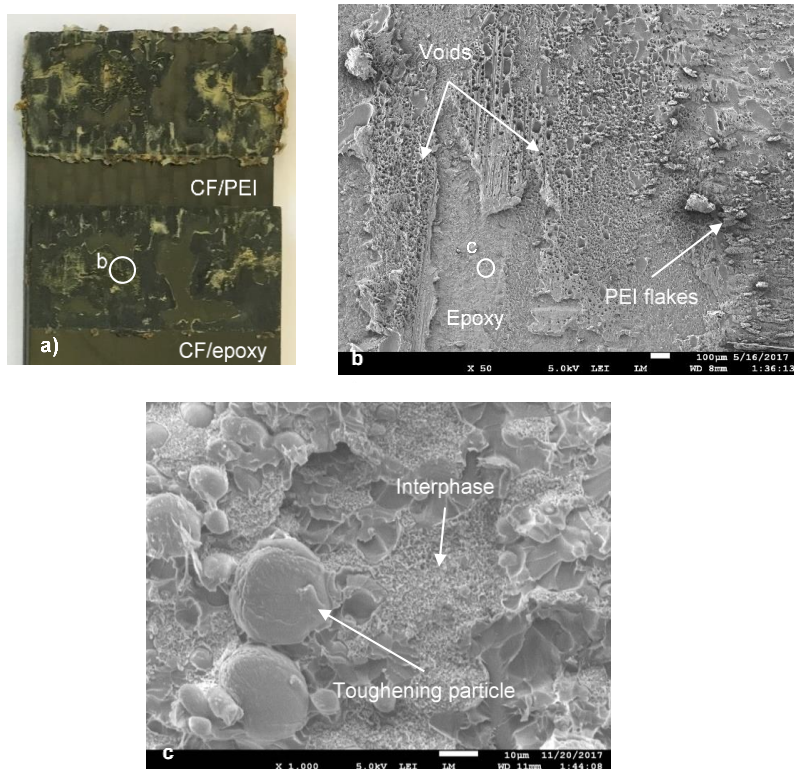
Figure 2.13: a) Representative fracture surfaces of an ED-less-60 case sample showing large unwelded areas and signs of thermal degradation of the PEI resin. b) SEM image corresponding to the circled area in (a), depicting voids in the PEI resin and PEI resin flakes, both features associated with thermal degradation and c) is a detailed SEM image showing failure in the interphase.

Figure 2.14 shows three typical ED-less-250 fracture surfaces of samples welded with the same parameters. The fracture surfaces appear more uniform than in the ED-less-60 case and for most samples no unwelded areas are present. The failure mechanism is characterized by first ply failure in the CF/PEI adherend. In some samples, however, like the first and third samples in Figure 2.14, discoloured PEI resin is seen, similar to what was observed in the ED-less-60 samples. For further analysis the sample exhibiting the highest strength and largest welded area (left most sample in Figure 2.14) iss chosen and is illustrated in Figure 2.15a.

Figure 2.14: Fracture surfaces obtained from ED-less-250 samples welded at 600 J. Unwelded areas are indicated by the white lines. White arrows indicate locations with discoloured PEI resin.
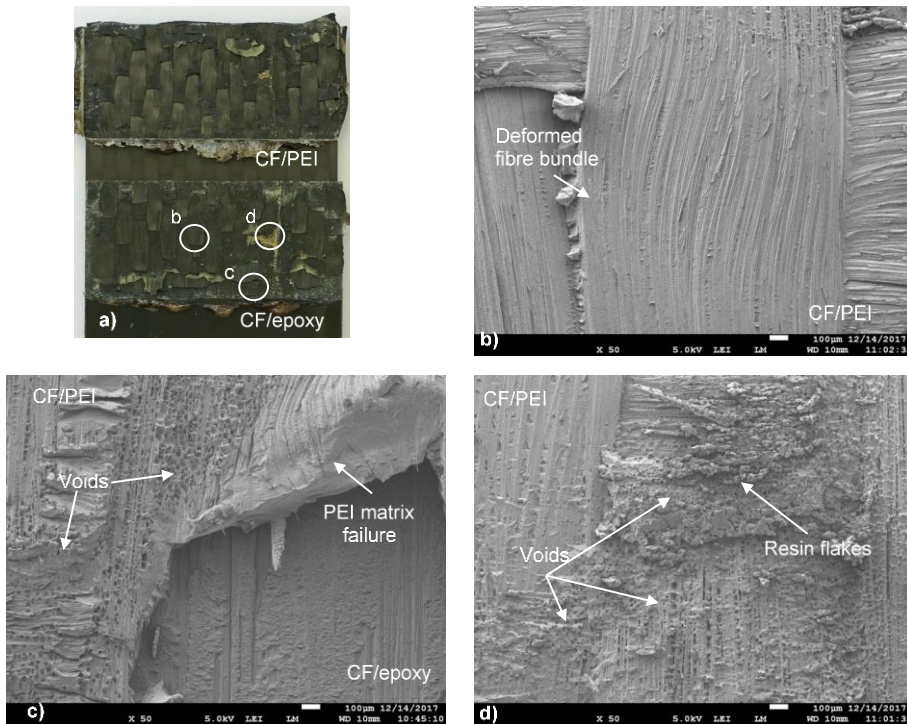
Figure 2.15: a) Representative fracture surfaces of an ED-less-250 sample showing failure mostly in the CF/PEI adherend, with only partial failure in the CF/epoxy adherend and b), c), d) are SEM images corresponding to the circled areas in (a), showing b) deformed fibre bundles c) degradation signs in the form of voids close to the edge of the overlap and d) voids and resin flakes in the middle of the overlap.

Figure 2.15b shows a SEM micrograph of the circled area (b) in Figure 2.16a and displays slightly deformed fibre bundles in the CF/PEI adherend. In Figure 2.15c, failure in the CF/epoxy adherend is also partially seen, characterized by mostly matrix failure and only a few exposed fibres or fibre imprints. This failure however iss not the predominant type of

failure and it iss only found at one of the edges of the overlap on the CF/epoxy adherend, as indicated by the circled area (c) in Figure 2.15a. Numerous voids on the fracture surface of the CF/PEI adherend can be seen at the abovementioned location, indicating thermal degradation of the PEI resin. Degradation signs in the form of voids and resin flakes are also found in an area in the middle of the overlap (region (d) in Figure 2.15a) , depicted in Figure 2.15d.

Figure 2.16a shows the representative fracture surfaces of reference ED samples, exhibiting a fully welded overlap. First-ply failure in the CF/PEI adherend is the dominant failure mechanism, indicated by the broken fibre bundles of the CF/PEI adherend that are found on the CF/epoxy adherend. Failure in the CF/epoxy adherend is limited and only some exposed fibres are seen on the fracture surfaces. Such observations are supported by SEM inspection pertaining to the CF/epoxy adherend, as the micrograph in Figure 2.16b illustrates. The micrograph also shows some epoxy-rich areas. Closer inspection of the epoxy-rich areas reveals failure both in the epoxy resin and the interphase, presented in Figure 2.16c. However, such failure type is found only at a few locations in the overlap. No thermal degradation signs of the PEI resin can be observed throughout the fracture surfaces.
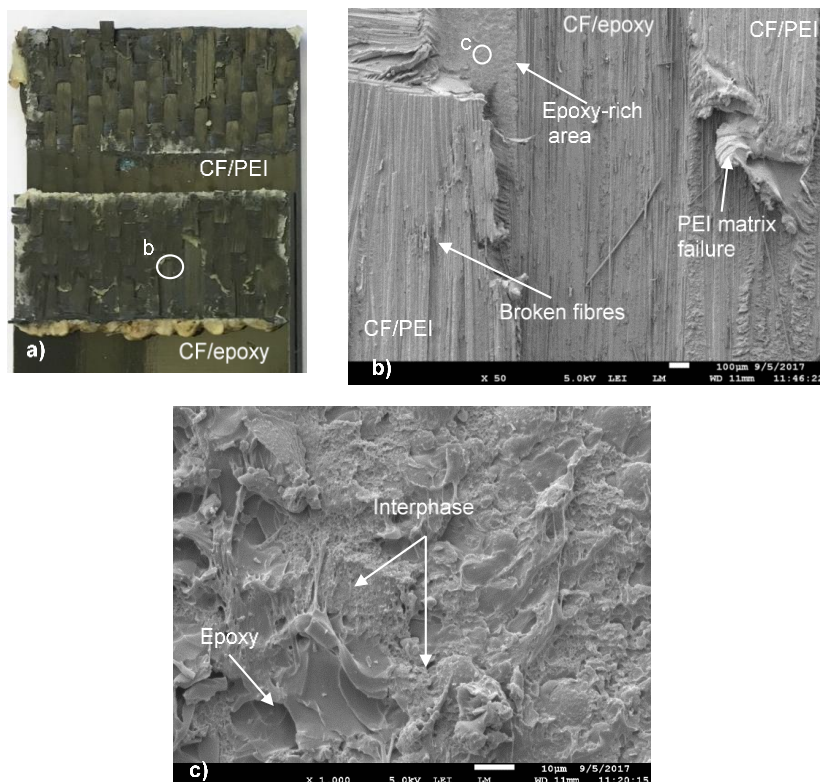
Figure 2.16: a) Representative fracture surfaces of a reference ED sample welded at 0.13 mm displacement, showing failure mostly in the CF/PEI adherend, with only partial failure in the CF/epoxy adherend. b) SEM image corresponding to the circled area in (a), showing broken CF/PEI bundles and exposed fibres in the CF/epoxy adherend, c) SEM image showing failure in the epoxy and interphase.

Figure 2.17a illustrates representative fracture surfaces for the reference co-cured case. Naked-eye inspection reveals first ply failure in both CF/epoxy and CF/PEI adherends. The failure is characterized by exposed fibres and resin rich areas. Closer inspection of the circled area (b) in Figure 2.17a by means of SEM (Figure 2.17b), shows matrix failure in the CF/PEI adherend, exposed fibres from the CF/epoxy adherend, as well as epoxy resin rich areas. Figure 2.17c depicts a closer view of the circled area (c) in Figure 2.17b, in which epoxy resin is fractured, demonstrating matrix failure, and what seem to be epoxy spheres from the interphase are exposed, linked to interphase failure.
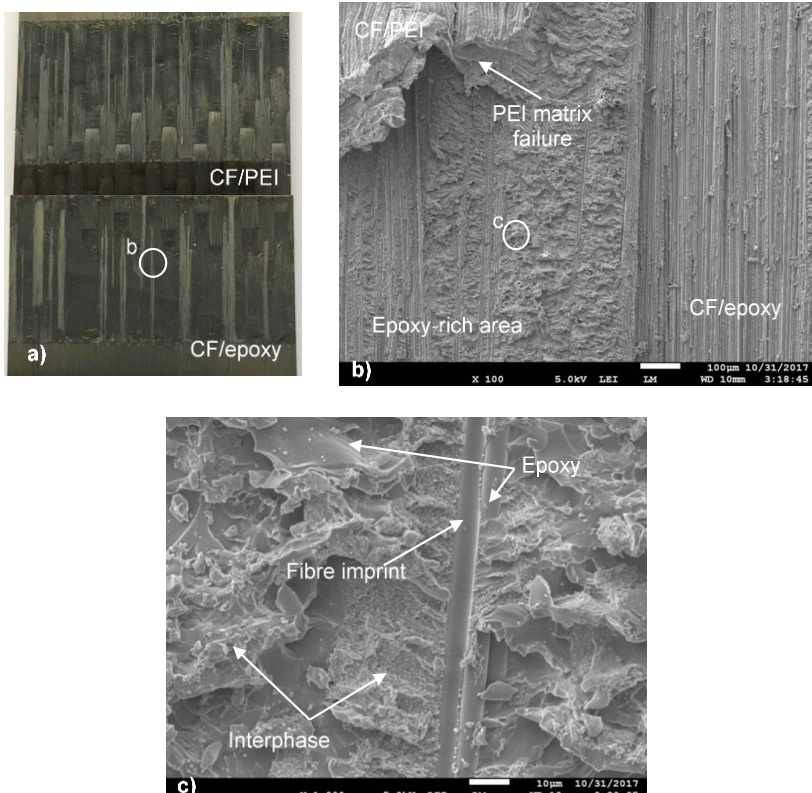
Figure 2.17: a) Representative fracture surfaces of a reference co-cured sample, showing failure in the two composites adherends characterised by exposed fibers and resin failure, b) SEM image corresponding in the circled area in (a), matrix failure in the CF/PEI adherend, exposed fibres in the CF/epoxy adherend and matrix failure, and c) a more detailed SEM image showing failure in the interphase and epoxy matrix.

2.4   Discussion

The findings presented in the Results section show that welding of dissimilar composite materials without a loose ED can have a large effect on the quality of the welds, especially when a thin coupling layer is used. The ED-less-60 samples yielded the lowest strength of 17.3 ± 4.5 MPa. The ED-less-250 samples resulted in a higher LSS (29.3± 3.2 MPa) as compared to the ED-less-60 samples, but still lower than the reference cases. The reference

ED samples yielded the highest LSS, i.e., 37.7 ± 1.6 MPa, and the reference co-cured samples exhibited an average strength of 34.7 ±1.4 MPa.

Comparing the ED-less-60 samples with the reference ED samples, it is obvious that the lower LSS of the former is attributed to the large unwelded areas and the degradation of the PEI resin that were found on all samples. On the contrary, the reference ED samples featured fully welded overlaps and no signs of thermal degradation of the PEI resin. The unwelded areas in the ED-less-60 samples can be attributed to firstly limited contact areas and secondly the lack of resin flow during the welding process, evident by the fact that the final thickness of the weld line was similar to the original thickness of the 60 µm-thick coupling layer. During welding, frictional heating was initiated in areas where the two adherends were in good contact with each other, for the ED-less-60 case, or with the ED, for the reference ED case. The locations at which a good initial contact is established, is normally random per sample since it depends on the surface quality and the thickness variations of the ED and the adherends. It is expected that the initial contact areas are larger in the reference ED case as opposed to the ED-less-60 case. The ED is relatively thin and has the ability to deform and therefore conform to the surface irregularities. On the other hand, the coupling layer is fixed on the much stiffer adherend, hence deformation of the coupling layer is more limited than the ED. Regarding the resin flow, in the reference ED case, once the Tg was reached, the PEI resin in those areas flowed under the pressure applied by the sonotrode. Thus, the downward movement of the sonotrode and the flow of the resin in the initial contact areas, resulted in a good overall contact in the rest of the overlap, ensuring fully welded areas. However, in the ED-less-60 case, the welding process was stopped before any downward movement of the sonotrode occurred. Hence, only the initial contact areas were being heated up. This resulted in the large and non-uniformly distributed unwelded areas. Regarding the degradation signs found in the ED-less-60 samples, they are most likely caused by (i) the lack of resin flow, (ii) limited frictional heating when solely the coupling layer is used, as compared to when the ED is used and (iii) the small thickness of the coupling layer. Firstly, lack of resin flow in the ED-less-60 case caused the resin at the initial contact areas to be continuously heated up and most likely eventually overheated. Secondly, in welding of the reference ED case, friction was generated between two sides of the ED and the adherends in contact, most probably securing that the ED will reach the Tg faster than the adherends. However, in the ED-less-60 case, only one side of the coupling layer was subjected to frictional heating. It is possible that both coupling layer and CF/PEI adherend were heating up at the same rate, exposing them to high temperatures for a longer time in comparison with the reference ED case. Lastly, the small thickness of the coupling layer might also have contributed to overheating of the CF/PEI adherend. As seen in the research by Palardy and Villegas [15], a 60 µm-thick ED was unable to generate preferential heat at the interface, causing overheating of the CF/PEI adherends.

Increasing the thickness of the coupling layer to 250 µm resulted in welds with a higher strength when compared to the ED-less-60 case, probably because of the fully welded overlaps. The final thickness of the weld line of the ED-less-250 samples was 200 µm, indicating that flow of the PEI resin occurred during welding. Note that since the vibration phase was stopped when the displacement of the sonotrode was zero, flow of the PEI resin most likely occurred during the solidification phase. This allowed for the whole overlap to be welded in most samples. However, the limited frictional heating on the coupling layer caused overheating of the coupling layer and CF/PEI adherend, resulting subsequently in a lower strength when compared to the reference ED samples. Moreover, the thicker weld line

of the ED-less-250 samples (i.e., 200 µm) as compared to the reference ED samples (i.e., 110 µm), might have resulted in higher peel stresses due to secondary bending during the SLS test, hence a lower LSS for the ED-less-250 case [16].

As already discussed in the previous paragraphs, there were clear indications of thermally degraded PEI resin after the welding process. However, no visible signs of degraded epoxy resin (in the form of voids) could be found in any of the as-welded samples and, the interphase appeared to be intact after welding. Still, when the 60 µm-thick coupling layer was used, either by itself or with the addition of an ED, failure occurred partially in the epoxy resin and interphase. However, when the 250 µm-thick coupling layer was used failure occurred almost entirely in the CF/PEI adherend. Failure in the epoxy resin and interphase could be a sign of thermal degradation of the epoxy resin, even though no porosity or altered features of the epoxy resin could be seen with the microscopes used in this study. However, this type of failure also occurred in the reference co-cured samples, in which it is certain that no thermal degradation occurred. Therefore, failure in the CF/epoxy adherend might be possibly attributed to the thin weld line or bond line of the ED-less-60 (i.e., 70 µm) and reference co-cured samples (practically zero), which can potentially have an effect on the stresses developed during the SLS test. Nevertheless, further research is needed to determine whether the epoxy resin is degraded during welding.

2.5   Conclusions

In this paper experimental assessment of the feasibility of ED-less ultrasonic welding of CF/epoxy to CF/PEI composites was presented. Two welding cases were considered: welding solely with (i) a 60 µm-thick (ED-less-60 case) and (ii) a 250 µm-thick (ED-less-250 case) co-cured coupling layer. These welding cases were then compared to two reference cases, a) welding with a 250 µm-thick loose ED and a 60 µm-thick coupling layer (reference ED case) and b) co-cured CF/epoxy and CF/PEI samples, without a coupling layer (reference co-cured case). The analysis of the results led to the following conclusions:

- Welding with solely the coupling layer probably caused limited frictional heating, which in return resulted in overheating of the CF/PEI adherend and/or coupling layer. Overheating of the CF/PEI adherend was indicated by PEI resin flakes and voids, features that have been associated in previous research with thermal degradation of the PEI resin.
- For the ED-less-60 case, absence of resin flow during welding resulted in large unwelded areas. The only areas that were heated and welded where the initial contact areas where the coupling layer and the CF/PEI adherend were in intimate contact. On the other hand, flow of the coupling layer during the welding process of the ED-less-250 case resulted in better contact between the coupling layer and the adherends and therefore fully welded overlaps.
- For the reasons mentioned above, the ED-less-60 samples yielded a lower LSS of 17.3 ± 4.5 MPa when compared to the ED-less-250 samples that provided a LSS of 29.3 ± 3.2 MPa. The reference samples yielded higher LSS values, possibly because of the lack of thermal degradation signs of the PEI resin. The reference ED samples and reference co-cured samples exhibited a 37.7 ± 1.6 MPa and 34.7 ±1.4 MPa LSS accordingly.

- Failure in the CF/epoxy for the welded joints in which a 60 m-thick coupling layer was used, might indicate some type of thermal degradation of the epoxy resin not traceable through SEM, as no porosity could be found in the epoxy resin. Further research on whether the epoxy resin is affected by the welding process is needed.

2.6   References

[1]   Ageorges C, Ye L, Hou M. Advances in fusion boding techniques for joining thermoplastics materials composites: a review. Compos Part A Appl Sci Manuf 2001;32:839–57.

[2]   da Costa AP, Botelho EC, Costa ML, Narita NE, Tarpani JR. A review of welding technologies for thermoplastic composites in aerospace applications. J Aerosp Technol Manag 2012;4:255–65.

[3]   Villegas IF, Rubio PV. On avoiding thermal degradation during welding of high-performance thermoplastic composites to thermoset composites. Compos Part A Appl Sci Manuf 2015;77:172–80.

[4]   Schieler O, Beier U. Induction welding of hybrid thermoplastic-thermoset composite parts. Int J Appl Sci Technol 2016;9:27–36.

[5]   Villegas IF, van Moorleghem R. Ultrasonic welding of carbon/epoxy and carbon/PEEK composites through a PEI thermoplastic coupling layer. Compos Part A Appl Sci Manuf 2018;109:75–83.

[6]   Don RC, Gillespie Jr. JW, McKnight SH. Bonding techniques for high performance thermoplastic compositions. US5643390A, 1997.

[7]   Lestriez B, Chapel J-P, Gérard J-F. Gradient interphase between reactive epoxy and glassy thermoplastic from dissolution process, reaction kinetics, and phase separation thermodynamics. Macromolecules 2001;34:1204–13.

[8]   Zhang Z, Wang X, Luo Y, Zhang Z, Wang L. Study on heating process of ultrasonic welding for thermoplastics. J Thermoplast Compos Mater 2010;23:647–64.

[9]   Deng S, Djukic L, Paton R, Ye L. Thermoplastic-epoxy interactions and their potential applications in joining composite structures - A review. Compos Part A Appl Sci Manuf 2015;68:121–32.

[10]   Vandi LJ, Hou M, Veidt M, Truss R, Heitzmann M, Paton R. Interface diffusion and morphology of aerospace grade epoxy co-cured with thermoplastic polymers. 28th Int. Congr. Aeronaut. Sci., 2012, p. 1–9.

[11]   Bonnet A, Pascault JP, Sautereau H, Taha M. Epoxy− diamine thermoset/thermoplastic blends. 1. Rates of reactions before and after phase separation. Macromolecules 1999;32:8517–23.

[12]   Wang M, Yu Y, Wu X, Li S. Polymerization induced phase separation in poly (ether imide)-modified epoxy resin cured with imidazole. Polymer (Guildf) 2004;45:1253–9.

[13]   Villegas IF. Strength development versus process data in ultrasonic welding of thermoplastic composites with flat energy directors and its application to the definition of optimum processing parameters. Compos Part A Appl Sci Manuf 2014;65:27–37.

[14]   Villegas IF. In situ monitoring of ultrasonic welding of thermoplastic composites through power and displacement data. J Thermoplast Compos Mater 2015;28:66–85.

[15]   Palardy G, Villegas IF. On the effect of flat energy directors thickness on heat generation during ultrasonic welding of thermoplastic composites. Compos Interfaces 2016;24:203–14.

[16]   Gleich DM, Tooren MJL Van, Beukers A. Analysis and evaluation of bondline thickness effects on failure load in adhesively bonded structures. J Adhes Sci Technol 2001;15:1091–101.

3 Ultrasonic welding of epoxy-to polyetheretherketone (PEEK)- based composites: investigation on the material of the energy director and the thickness of the coupling layer[2]

For welding CF/ polyetheretherketone (PEEK) to TSC samples, a PEEK film is not preferable as a coupling layer, due to its immiscibility with epoxy resins. On the other hand, polyetherimide (PEI) is an excellent candidate, since it is known to be miscible to most epoxy systems at high temperatures and PEEK polymers. The existence of two different thermoplastic materials at the welding interface raises two main questions, which will be addressed in this chapter. The first question considers the nature of the material of the energy director (ED). In this case, the ED can be either PEI, as in the coupling layer or PEEK material, as in the matrix of the TPC adherend. It was found that both materials can produce welds with similar mechanical performance. The second question concerns the thickness of the coupling layer. Due to the high melting temperature of the PEEK matrix, a 60 µm-thick coupling layer was seemingly too thin to act as a thermal barrier for the epoxy resin for heating times long enough to produce fully welded joints. Such an issue was found to be overcome by increasing the thickness of the coupling layer to 250 µm, which resulted in high-strength welds.

3.1   Introduction

The appealing properties of thermoplastic composites (TPC), such as their easy and fast processing capabilities and infinite shelf life of the raw materials, have led to an increasing interest in their usage in the aerospace industry. One example is the thousands of carbon fibre/ polyetheretherketone (CF/PEEK) clips that already exist in the A350 and Boeing 787 aircraft. The clips are currently joined to the CF/epoxy fuselage skin via mechanical fasteners [1]. However, mechanical fasteners are not the best choice for composites, since drilling holes results in breakage of the reinforcing fibres, and furthermore it is time consuming. Welding on the other hand can produce high-strength joints without damaging the parts and in a rather fast way [2].

Welding of thermoset composites (TSC) is possible by placing a thermoplastic film (namely coupling layer) on the uncured TSC laminate and curing them together. A reliable way of bonding the two materials is with the use of a compatible thermoplastic (TP) film that allows for interdiffusion of one material into the other and vice versa [3]. Out of the thermoplastic materials that are known to be miscible with epoxy [4], PEI is the one with the best mechanical performance and is also compatible with PEEK. Compatibility between these two materials allows for them to be fusion bonded [5].

Ultrasonic welding is the fastest joining technology to assemble TSC and TPC. Its remarkably fast heating times have been found to help prevent the TS matrix from thermally degrading during the welding process [6]. Ultrasonic welding is based on high-frequency and low-amplitude vibrations and relies on frictional and viscoelastic heating. In order to promote heat generation at the welding interface and avoid excessive bulk heating, a flat thermoplastic film is placed at the interface, called energy director (ED) [7]. Due to the lower stiffness of the ED, hence its higher cyclic strains when compared to the reinforced composite adherends, the ED is going to concentrate heat generation at the interface. Frictional heating is generated at the beginning of the process and is the dominant heating mechanism until the Tg of the ED material is reached. After that point viscoelastic heating becomes the dominant mechanism [8]. Figure 3.1 shows the typical 5 stages in the vibration phase (or heat generation phase) of the welding process of thermoplastic composites, as identified by Villegas in [7] in which CF/PEI composites were welded. The stages are the following:

- Stage 1: heating of the ED without physical changes being observed at the interface. The power starts increasing during this stage.
- Stage 2: local melting of the ED due to frictional heating. The power starts decreasing with the displacement remaining constant around 0 mm.
- Stage 3: the entire ED is molten (or softened when an amorphous material is used). The sonotrode starts moving downwards as the ED is being squeezed out. The power and the displacement both increase at this stage.
- Stage 4: the ED is flowing and the matrix of the uppermost layers of the adherends starts melting. The power remains constant whereas the displacement keeps increasing until the end of the vibration phase.
- Stage 5: further melting and occasionally squeeze out of the matrix of the adherends. The power starts decreasing.
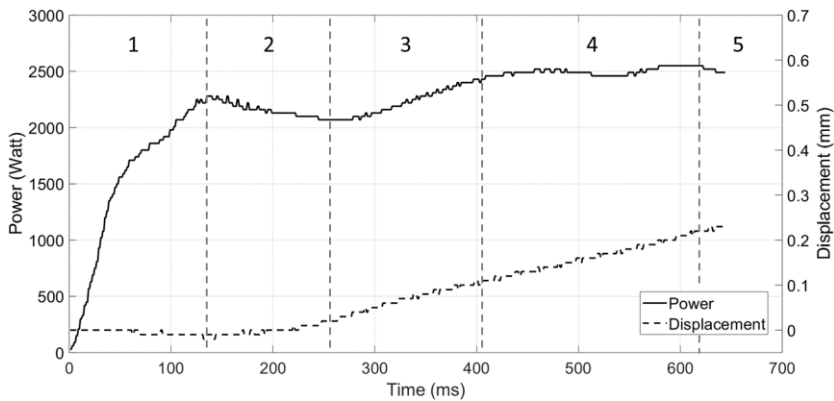
Figure 3.1: Typical power and displacement curves obtained during the vibration phase when welding CF/PEEK and CF/PEEK composites.

In a latter study [9], Villegas correlated these stages to the mechanical performance of samples welded within each stage. She concluded that the optimum weld quality can be achieved within stage 4. It was shown therefore that the power and displacement curves can be a useful tool to determine the desired weld quality. This can ensure a high reproducibility rate.

Despite the increasing knowledge of ultrasonic welding, the process has still not been widely utilized in welding of TSC. The limited studies found in open literature include a study by Lionneto et al [10], in which CF/epoxy samples were welded to each other through a poly-vynil-butyral (PVB) coupling layer and using either induction or ultrasonic welding. Comparison between the two techniques showed that the ultrasonically welded samples yielded higher lap shear strengths (LSS). Previous work from the authors [11] focused on ultrasonic welding of dissimilar composites without a loose ED, solely with the coupling layer. PEI was used as the material of both coupling layer and matrix of the TPC adherend. It was concluded that the use of an ED is necessary in order to avoid excessive bulk heating and to achieve high strengths. The CF/epoxy and CF/PEI welded samples had a LSS of 37.7 ± 1.6 MPa (average ± LSS standard deviation), which was similar to the LSS of CF/epoxy and CF/PEI co-cured joints which had a 34.7 ± 1.4 MPa LSS. In the research by Villegas and van Moorleghem [1], a preliminary study on the ultrasonic welding of CF/epoxy/PEI (i.e. CF/epoxy with a PEI coupling layer) and CF/PEEK with the use of a PEI ED was performed. Unwelded areas were observed in the samples and the LSS of the samples was lower than the reference co-cured samples. No further investigation on the failure mechanisms of the joints was performed.

Considering the current application of CF/PEEK and CF/epoxy composites in the aerospace industry, the focus of this paper is on further understanding ultrasonic welding of CF/epoxy and CF/PEEK composites. Based on previous works [1,6,11], PEI was chosen as the coupling layer. Firstly, it was interesting to evaluate whether the most suitable material for the ED will be PEI (same as the coupling layer) or PEEK (same as the matrix of the TPC adherend). Additionally, it was important to determine the effect of the thickness of the coupling layer on the weld quality. A study on induction welding of CF/epoxy/PEI samples

showed that the thickness of the coupling layer plays an important role in the mechanical performance of the welds [12]. Our hypothesis was that a thin coupling layer might not be able to act as a thermal barrier for the epoxy resin during welding, especially taking into account the high melting temperature of the PEEK resin. Hence, two different coupling layer thicknesses were examined, namely 60 µm and 250 µm. Cross sectional analysis was used to identify the effect of the welding process on the adherends. The mechanical performance of the welds was assessed through single lap shear tests and fractographic analysis.

3.2   Experimental Procedure

3.2.1 Materials and manufacturing

As the TSC material, T800S/3911 unidirectional CF/epoxy prepreg from TORAY (Japan) was used. The prepreg plies were manually stacked in a $[0,90]_{2s}$ configuration. A PEI film was attached on one of the sides of the CF/epoxy laminates, serving as the coupling layer. Two PEI coupling layers with two different thicknesses were used, a 60 µm-thick PEI film provided by SABIC (The Netherlands), and a 250 µm-thick PEI film provided by LITE (Germany). The 60 µm-thick PEI film was chosen due to its usage in prior studies considering ultrasonic welding of thermoset- and thermoplastic-based composites[1,11], and the 250 µm-thick PEI film was chosen due to its availability as an ED in the same studies. Analysis to determine the chemistry of the two different PEI films was not performed. However, comparison between the data sheets of the two PEI films showed similar thermal and physical properties, which are the main points of interest for this study. Moreover, the epoxy-PEI interphase was identical in both cases.

 The CF/epoxy laminates with the attached coupling layer were cured in an autoclave at 180°C and 7 bars for 120 min. An aluminium caul plate was used on the side of the vacuum bag, in order to ensure a flat surface. The thickness of the CF/epoxy/PEI laminate (i.e., the CF/epoxy laminate with the co-cured PEI film on its surface) was approximately 2 mm.

Note that the CF/PEI laminates and PEI films were not dried prior to welding. Single-lap shear tests that were performed on i) untreated CF/PEI-CF/PEI welds and ii) dried CF/PEI-CF/PEI welds revealed identical LSS and failure mechanisms. Thus, not drying the PEI resins should not have had an impact on the mechanical performance of the welds.

In our previous study, we found that during co-curing, an interdiffusion process occurs between the monomers of the T800S/3911 epoxy and the PEI polymer. Due to the limited miscibility between the two materials after the gelation point of the epoxy resin, phase separation occurs, which results in the formation of a gradient interphase [11]. Figure 3.2 shows the morphology of this interphase, which consists of epoxy spheres dispersed in a PEI-rich matrix, with diameters decreasing towards the PEI coupling layer. The interphase has a varying thickness, with a maximum of 25 µm. The existence of the interphase is a strong evidence that a reliable bond is created between the epoxy and PEI resins [4].
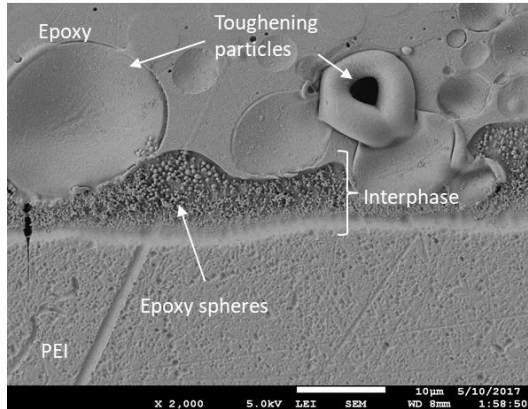
Figure 3.2: Morphology of the interphase formed between the epoxy and PEI materials.

The material of the TPC adherend was CF/PEEK (carbon fibre/polyetheretherketone) powder-coated semi-preg with a 5-harness satin weave fabric, manufactured by TenCate Advanced Composites (The Netherlands). The CF/PEEK laminates with a $[0/90]_{3s}$ stacking sequence were consolidated in a hot-platen press at 385 °C at 20 bar for 30 min. The thickness of the consolidated laminates was approximately 1.9 mm.

Both adherends were cut from the laminates with dimensions 25.4 mm x 106 mm using a water-cooled circular diamond saw. The CF/epoxy/PEI adherends were cut with their longitudinal direction parallel to the 0° fibres. The CF/PEEK adherends were cut with their longitudinal direction parallel to the main apparent orientation of the fibres.

The EDs used in this study were a 250 μm-thick PEI film provided by LITE, Germany, and a 250 μm-thick PEEK film provided by Victrex, UK.

3.2.2 Welding process

Individual samples were welded with a Rinco Dynamic 3000 ultrasonic welder in a single-lap configuration, with the overlap being 12.7 mm long and 25.4 mm wide. The custom-made welding jig shown in Figure 3.3 was used. A cylindrical sonotrode with a 40 mm diameter was utilised. To ensure minimum heating times, and hence minimum risk of thermal degradation at an acceptable level of dissipated power, the parameters chosen were 1500 N welding force and 86.2 μm peak-to-peak vibration amplitude. These parameters are close to the highest within the limits of the machine and hence result in very short heating times, as shown in the study by Villegas and Rubio [6]. Solidification force and time were kept constant at 1500 N and 4 s respectively. The duration of the vibration phase was indirectly controlled through the downward displacement of the sonotrode. The power and displacement of the sonotrode values during the vibration phase, as well as the total duration of the vibration phase were recorded by the welding machine and could be obtained at the end of the welding process.
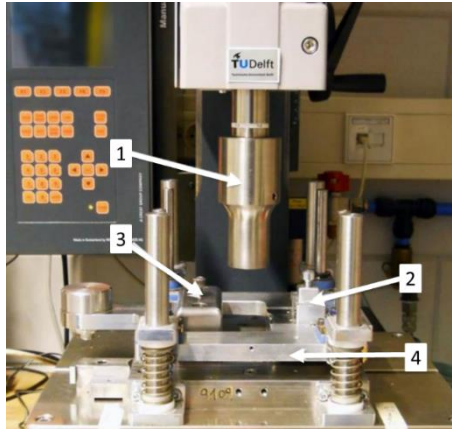
Figure 3.3: Custom made welding setup. Arrows point at the sonotrode (1), the clamp for the top sample (2), the clamp for the bottom sample (3) and the sliding platform (4).
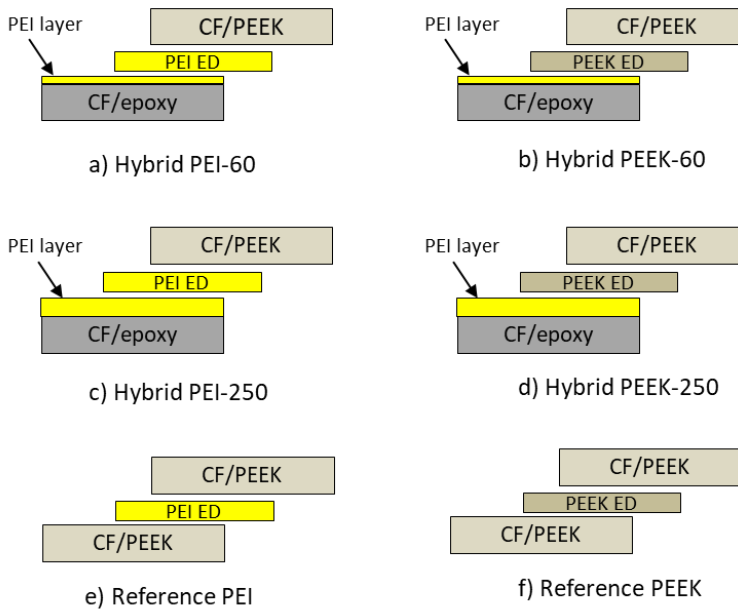
Figure 3.4: Schematic representation of all the welded configurations. ED is an abbreviation for energy director. Dimensions are not to scale.

Figure 3.4 shows the schematics of the different types of joints in this study. The first row of the figure corresponds to joints welded through a 60 µm-thick coupling layer, hereafter referred to as hybrid-60 configurations, in which a) is with a PEI ED (hybrid PEI-60) and b) is with a PEEK ED (hybrid PEEK-60). The second row corresponds to joints welded through a 250 µm-thick coupling layer, hereafter referred to as hybrid-250 configurations, in which c) is with a PEI ED (hybrid PEI-250) and d) is with a PEEK ED (hybrid PEEK-250). The

third row corresponds to reference joints with CF/PEEK adherends, in which e) is with a PEI ED (reference PEI) and f) is with a PEEK ED (reference PEEK).

3.2.3 Testing

3.2.3.1 Single-lap shear

Single-lap shear tests were performed in order to assess the mechanical performance of the joints, following the ASTM D 1002 standard. A Zwick 250 kN universal testing machine operating at 1.3 mm/min cross-head speed and under displacement control was used for these tests. The apparent lap shear strength (LSS) of the joints was calculated as the maximum load divided by the overlap area. Five specimens were tested per welding case to determine the average LSS and corresponding standard deviation.

3.2.3.2 Material characterization

Heating during ultrasonic welding relies on frictional and viscoelastic heating. Frictional heating is not expected to change significantly when using different ED materials. On the other hand, viscoelastic heating depends on the material of the ED among other parameters. Specifically, the rate of viscoelastic heat generation can be described by the following equation [13]:

$$\dot{Q}v = \frac{\omega \cdot \varepsilon_0^2 \cdot E^{"}}{2} \quad (1)$$

where $\dot{Q}v$ is the rate of viscoelastic heat generation, ω is the frequency of the vibrations, ε_0 is the cyclic strain and $E^{"}$ is the loss modulus of each material. Assuming that the frequency and cyclic strains are the same for both ED materials, the loss modulus seems to play the biggest role in viscoelastic heat generation rate, and it is important that it is determined for both materials. The viscoelastic properties were measured with a Dynamic Mechanical Analysis (DMA) apparatus. Tensile DMA tests were carried out in a Pyris Diamond DMA (Perkins Elmer) between room temperature and 300 °C for the PEI resin and 400 °C for the PEEK resin, at 1 Hz frequency. Those temperatures were chosen since they were the threshold above which the PEI and PEEK samples failed and thus the DMA apparatus stopped recording. Samples were cut out of the films that were used for the ED materials in dimensions 8 x 20 mm.

Another parameter that can have an influence in the welding process is the viscosity of the two resins. The viscosity determines how easily a resin flows, thus the material with the lowest viscosity will probably result in faster displacement increase, i.e., shortest duration of stages 3-5. A Thermo Scientific™ HAAKE™ MARS™ rheometer was used to measure the viscosity of the PEI and PEEK resins under plate-plate test conditions. For that, samples were punched out of the films that were used for the EDs in 8 mm diameter. The viscosity was measured at 1 Hz frequency and for a temperature range between 220 °C and 400 °C for the PEI resin and 290 °C and 420 °C for the PEEK resin.

3.2.4 Process characterization

Schematics of the two types of temperature measurements that were performed can be seen in Figure 3.5. In the first type of measurement, the temperature at the welding interface was measured in order to determine whether temperature evolution depended on the material of the ED. For that, the thermocouple was placed between the ED and the CF/epoxy/PEI adherend (see Figure 3.5a), at the centre of the overlap, just before the welding process. For this specific temperature measurement, the samples were welded at a displacement equal to the total thickness of the ED and the coupling layer, in order to monitor the temperature evolution during all 5 stages of the vibration phase. The second type of measurement targeted the temperature evolution in the top ply of the CF/epoxy adherend. The main objective was to evaluate whether the thick coupling layer (250 μm) was able to better shield the CF/epoxy adherend from the high temperature in the welding interface, as opposed to the thin coupling layer (60 μm). The thermocouple was placed in between the coupling layer and CF/epoxy laminate prior to the co-curing process (see Figure 3.5b). After the co-curing process, the samples seemed to remain flat, without waviness being introduced by the existence of the thermocouple. After curing, samples were cut from the laminate in such way that the tip of the thermocouple was in the middle of the overlap. For this second temperature measurement, the samples were welded until the target displacement that resulted in the highest LSS was reached, as it will be discussed in the following sections.

K-type thermocouples with a 100 μm diameter were used. The temperature during welding was measured with a sampling rate of 1000 Hz. An in-house built device was used to monitor the temperature. The temperature was measured in at least 5 samples per configuration.
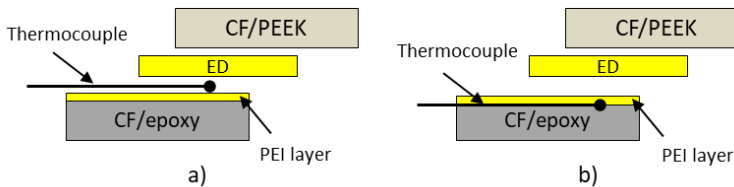
Figure 3.5: Schematic representation of the temperature measurements. a) thermocouple at the welding interface between the ED and the CF/epoxy/PEI adherend and b) thermocouple between the PEI coupling layer and the CF/epoxy adherend.

3.2.5 Microscopic analysis

Naked-eye observation and scanning electron microscopy (JEOL JSM-7500F Field Emission Scanning Electron Microscope, SEM) were used for fractographic analysis of tested joints. An optical microscope (Zeiss Axiovert 40) together with the SEM were used for cross-sectional analysis of as-welded specimens. Samples for cross-sectional microscopy were embedded in EpoFix resin and subsequently grinded and polished. To observe the epoxy-PEI interphase, polished samples were etched with 1 ml of N-Methyl-2-pyrrolidone

(NMP) and then immediately rinsed with ethanol and distilled water to provide contrast between the epoxy and PEI resins.

3.3 Results and Discussion

3.3.1 Material characterization

Figure 3.6 presents the viscosity of the PEI and PEEK resins as a function of temperature. Above around 250 °C the viscosity of the PEI resin drops linearly. The viscosity of the PEEK resin decreases rapidly once the temperature reaches around 310 °C and it becomes almost constant above 340 °C. At all considered temperatures, the viscosity of the PEI resin is lower than that of the PEEK resin. Note that the rheometer can only successfully measure the melt viscosity, thus results for the PEEK resin could only be obtained after around 290 °C.
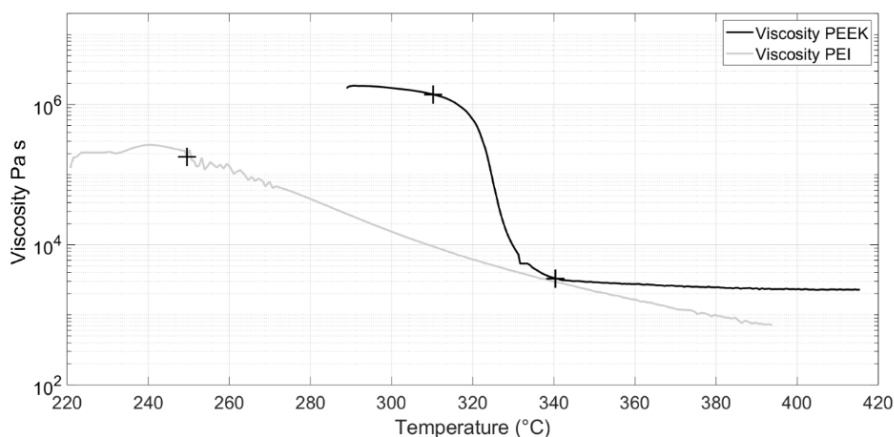
Figure 3.6: Viscosity of the PEEK and PEI resins versus temperature. The "+" signs indicate the changes in the viscosities.

The loss moduli of the PEI and PEEK resins can be seen in Figure 3.7. Four main stages can be identified:

i) 25-140 °C: The PEI resin generates heat faster than the PEEK one. Both resins generate heat at a constant rate.

ii) 140- 170 °C: The PEEK resin generates heat faster than the PEI resin. At 150 °C (i.e. close to the Tg of the PEEK resin) the loss modulus of the PEEK resin reaches a maximum and then starts decreasing again.

iii) 170- 230 °C: The PEI resin generates heat faster than the PEEK resin, with the highest rate being at the Tg of the PEI resin. After that, the loss modulus of the PEI resin drops again.

iv) 230- 350 °C: The two resins generate heat at a significantly lower rate than at lower temperatures. The PEEK resin generates heat somewhat faster than the PEI ED, until it reaches its melting point (343 °C).

Since the rate at which viscoelastic heat is generated is highly dependent on the loss modulus of the resins (see equation 1), it can be expected that the differences in the loss modulus mentioned above can potentially influence the temperatures reached at the weld interface when welding with either PEEK ED or PEI ED.
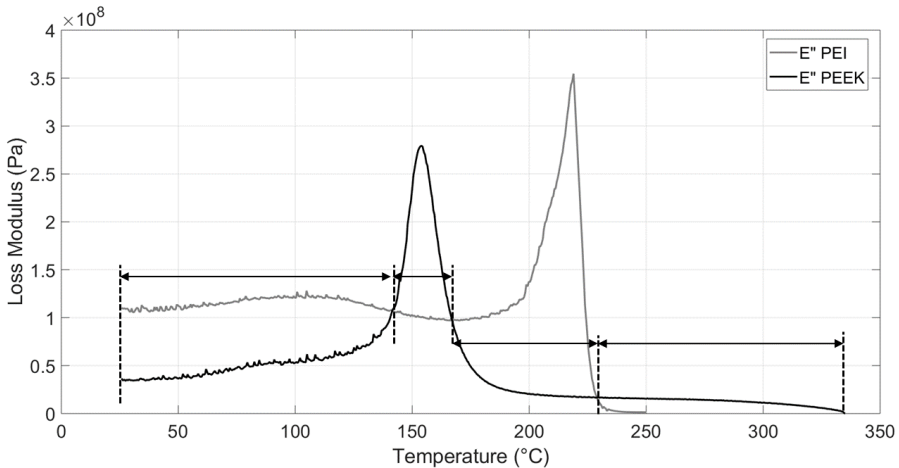
Figure 3.7: Loss modulus versus temperature of PEI and PEEK resins. The arrows indicate the intervals in which the PEI and PEEK loss moduli exhibited a certain behaviour with respect to each other.

3.3.2 Power and displacement curves

Figure 3.8 shows complete power and displacement curves of the hybrid-60, hybrid-250 and reference configurations. The term "complete curves" means that the samples were welded at a displacement value within the fifth stage of the vibration phase. The behaviour of the curves was similar to what was discussed in the introduction, following the typical 5 stages. The main difference in the displacement curves was that the displacement increased at a higher rate when a PEI ED was used rather than when a PEEK ED was used. Displacement of the sonotrode occurs as the ED flows, hence the PEI ED flowed faster than the PEEK ED, resulting in faster increase in the displacement. This can be attributed to the lower melt viscosity of the PEI resin when compared to the PEEK resin, as seen in Figure 3.6. No significant/consistent differences could be found between the power curves of different configurations. In most samples a change in the slope could be found at around 50 ms. This change in the slope could be possibly related to the change between the initial transient phase (duration 50ms) in which the amplitude is increased from 0 to 43.1 μm (which is the peak amplitude in this study) and the stable phase in which the amplitude is kept constant. This is further explained in the study by Villegas [7].
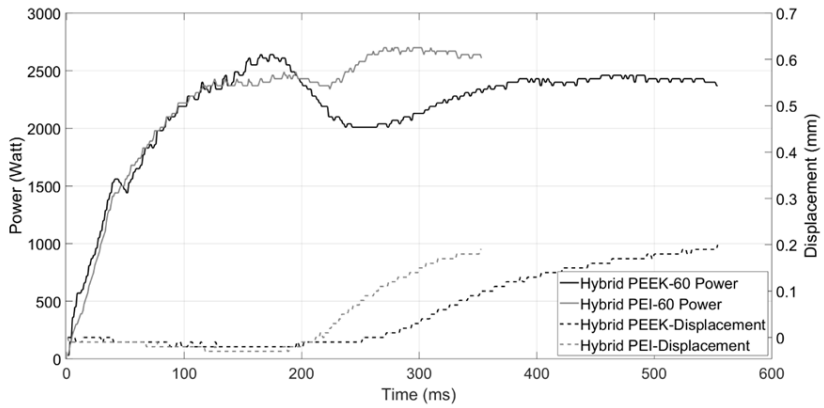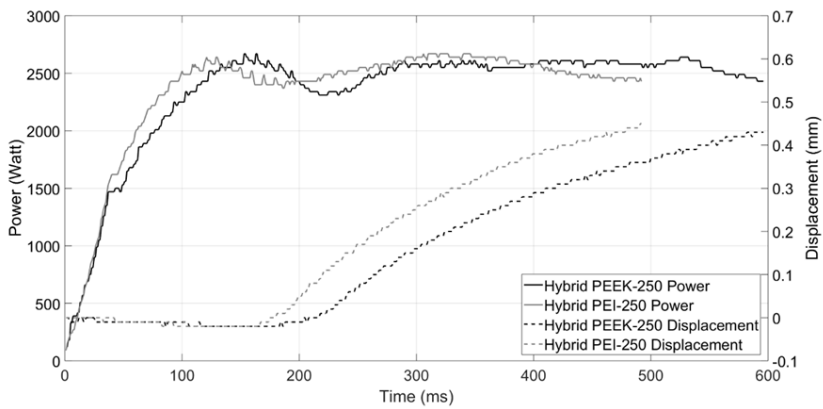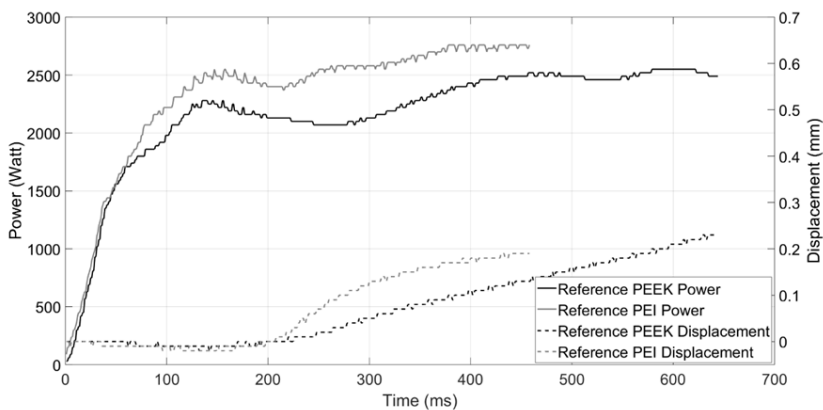
Figure 3.8: Power (solid line) and displacement (dotted line) curves of the a) hybrid-60 b) hybrid-250 and c) reference configurations.

3.3.3 Process characterization

Figure 3.9 shows temperature profiles taken at the welding interface (see Figure 3.5a) for different samples of each welding configuration. Figure 3.9a shows all the samples of the hybrid 60 configurations and Figure 3.9b shows all the samples of the hybrid 250 configuration (black lines indicate the usage of the PEEK ED and grey lines indicate the usage of the PEI ED). Note that out of the five samples tested in all configurations, only the ones in which the thermocouples remained intact after the welding process are presented, i.e., three samples of the hybrid PEEK-60, hybrid PEI-60 and hybrid PEI-250 configurations and four samples of the hybrid PEEK-250 configuration. The temperature in all configurations increased to an average maximum temperature of 750 ± 38 °C, 670 ± 38 °C, 702 ± 20 °C and 722 ± 35 °C (average temperature $\pm$ standard deviation) in the hybrid PEEK-60, hybrid PEI-60, hybrid PEEK-250 and hybrid PEI-250 configuration, respectively. The time frame within which the temperature increased to a maximum varied per sample. However, for most samples this increase happened within the first 200 ms of the vibration phase. After that, the temperature started fluctuating differently for each sample, possibly because of movement of the thermocouple along the weld interface and/or heating being generated at random locations in each sample. The vertical arrows indicate the completion of the vibration phase and initiation of the consolidation phase (i.e., the phase at which only a consolidation force was applied without the vibrations). Note that the maximum measured temperatures were higher than the degradation temperatures of the PEI and PEEK resins. However, no fumes were observed and also no degradation signs were found in the PEEK and PEI resins in the micrographs (as will be shown in the next sections). One explanation could be that the exceptionally short heating times allowed for such high temperatures without causing degradation of the resins. There is also the possibility that the peak temperature is not truly representative of the actual peak temperature at the interface but rather the response of the thermocouple, acting as an energy director. However, such potential interference should remain limited at the start of the vibration phase, since the thermocouple is expected to be embedded in the ED or coupling layer right after the resin surrounding it becomes soft. Regardless, since experimentally validating whether the measured peak temperature corresponded to the actual peak temperature was not possible, it was decided to only use the temperature measurements for comparison purposes and not to make conclusions regarding the highest temperatures reached. Considering the scatter in the measurements within the same configuration, it cannot be concluded whether the material of the ED or the thickness of the coupling layer played a significant role in how heat was generated during welding.

In addition to the temperature at the weld interface, the temperature between the coupling layer and the CF/epoxy adherend was measured as well. The main focus was to compare the maximum temperature reached underneath the coupling layer in each configuration, since the higher the temperature is, the higher the risk of thermal degradation of the epoxy resin. Representative measurements of each configuration are presented in Figure 3.10. The temperature kept increasing during the vibration phase, since i) more heat was being generated and transferred from the interface to the coupling layer and ii) the coupling layer most likely flowed during welding, hence it started losing its ability to act as a thermal barrier for the CF/epoxy adherend. Once the target displacement was reached, i.e., when the vibration phase was stopped (indicated by the vertical arrows), the temperature started dropping, since no further heat was generated. The two hybrid-250 configurations presented similar temperature curves, with some noise at the beginning of the welding process. The

hybrid PEEK-60 samples presented a change in the slope at around 155 °C, which might be because the PEEK ED generated viscoelastic heat with a much higher rate around that temperature (Figure 3.7). The maximum temperature reached was 461 ± 114 °C, 446 ± 156 °C, 176 ± 14 °C and 160 ± 18 °C in the hybrid PEEK-60, hybrid PEI-60, hybrid PEEK-250 and hybrid PEI-250 configuration, respectively. The particularly higher temperatures measured in the hybrid-60 configurations as compared to the hybrid-250 configurations could pose a greater risk of thermal degradation, especially since the duration of the vibration phase, thus the heating time, is similar in both cases. The exact temperature at which the epoxy resin is expected to degrade during ultrasonic welding is difficult to quantify, because the heating time is significantly shorter (less than 1 sec) than the capabilities of any thermal analysis apparatus. Moreover, as explained in the study by Abouhamzeh and Sinke [14], the material properties can start deteriorating even before the weight of the material decreases, which is how the degradation temperature is defined in Thermogravimetric Analysis (TGA).
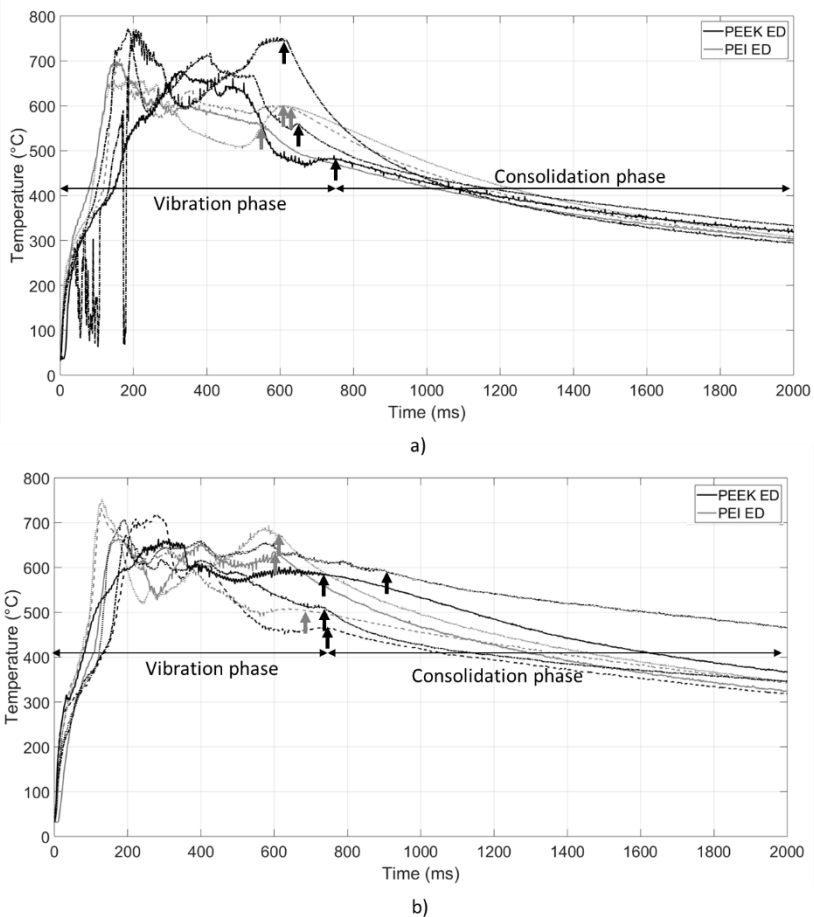
Figure 3.9: Temperature profile at the welding interface of the a) hybrid 60 and b) hybrid 250 configurations (see schematic in Figure 5a). Different line styles indicate different samples (welded with same parameters) within each configuration. The vertical arrows indicate when the vibration phase was stopped.
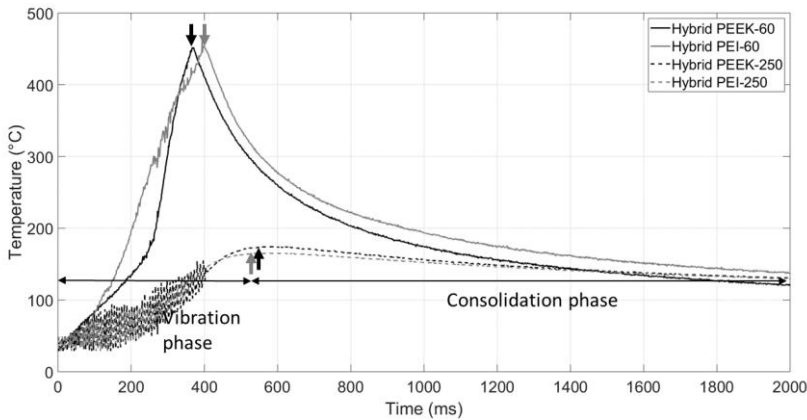
Figure 3.10: Temperature evolution between the coupling layer and the CF/epoxy adherend (see schematic in Figure 5b). The vertical arrows indicate when the vibration phase was stopped.

3.3.4 Cross-section analysis

Cross-section analysis was performed in order to evaluate the effect of the ED material and of the coupling layer thickness on the adherends and weld line. Figure 3.11 depicts the cross-section of a hybrid PEEK-60 sample (PEEK ED and 60 µm-thick coupling layer). The cross-section is representative of all other hybrid configurations. The final thickness of the weld line was similar in all hybrid cases and amounted to approximately 100 µm. Optical microscopy did not reveal any visible signs of thermal degradation of the resins, i.e., porosity caused by resin sublimation. A closer look on the cross-sections of the hybrid PEEK-60 and hybrid PEEK-250 samples is found in Figure 3.12. It can be seen in both figures a and b that the PEI resin is depicted as the dark grey area and the PEEK resin as the lighter grey area. The weld line of the hybrid PEEK-60 samples appears to consist mostly of PEEK resin, i.e., the light grey area. The PEI coupling layer seems to have flowed almost entirely in some locations. The reason for that is most likely the fact that PEI softens at a temperature much lower than the melting temperature of PEEK, hence the majority of the 60 µm-thick coupling layer probably flowed before the PEEK matrix in the adherend started melting. On the other hand, the weld line of the hybrid PEEK-250 sample consists of mostly PEI resin (implied by the ratio between the dark and light grey areas), since the coupling layer is much thicker. Using optical micrographs to determine whether the coupling layer flowed in the hybrid PEI-60 and hybrid PEI-250 samples was not possible, since both coupling layer and ED are made out of the same material, hence they could not provide any contrast in the images.
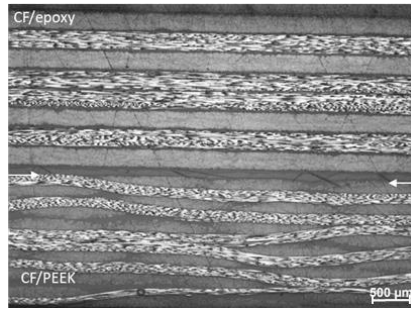
Figure 3.11: Cross-sectional micrograph of a hybrid PEEK-60 sample. White arrows indicate the weld line. Similar micrographs were obtained with all hybrid configurations.

a)   b)
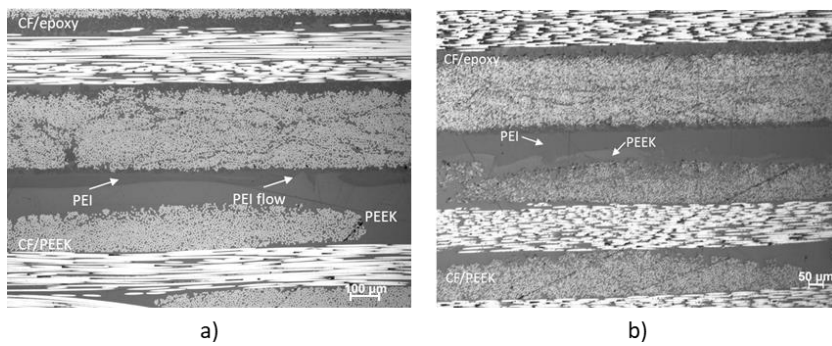
Figure 3.12: Higher magnification micrographs of a) a hybrid PEEK-60 sample and b) a hybrid PEEK-250 sample. The PEI coupling layer seems to flow entirely in some locations in the hybrid PEI-60 sample.

SEM analysis of the weld lines of the hybrid samples was performed in order to determine whether the welding process had an effect on the PEI-epoxy- interphase. Figure 3.13 and Figure 3.14 present SEM micrographs of the cross-section of representative hybrid-60 and hybrid-250 samples respectively. It is clearly seen that the interphase morphology in the hybrid-60 samples is altered during the welding process, as some of the epoxy spheres seem to flow along with the softened PEI coupling layer. The fact that the epoxy spheres flow in the hybrid PEI-60 samples is another indication that the coupling layer probably flowed almost entirely during the welding process. However, the interphase remains intact in the hybrid-250 samples. The 250 µm-thick coupling layer is probably thick enough in order to prevent flow of the PEI resin to occur close to the interphase.

Another observation made from the SEM micrographs is that there is a clear boundary between the PEI and PEEK resins. This means that the two resins do not blend very well at the weld line. This is probably because of the significantly short welding times provided by the ultrasonic welding process which prevent the two materials from diffusing into one another. Another hypothesis is that interdiffusion have happened locally at the boundary between the PEI and PEEK resins and that a complete blend was not obtained most likely since the two polymers were not mixed (i.e., following a typical polymer blending process in an extruder)

Figure 3.15 illustrates a representative cross-section of a reference PEI sample. A similar micrograph was obtained with the reference PEEK samples. Both reference configurations

produced samples with almost no distinguishable weld line, as expected from TPC samples welded under optimum conditions [7].

a)   b)
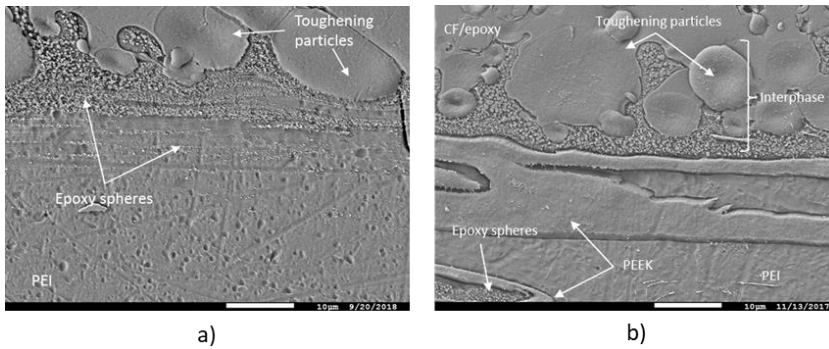
Figure 3.13: SEM micrographs of the cross-sections of a) a hybrid PEI 60 sample and b) a hybrid PEEK-60 sample. The interphase was affected by the welding process for both configurations

a)   b)
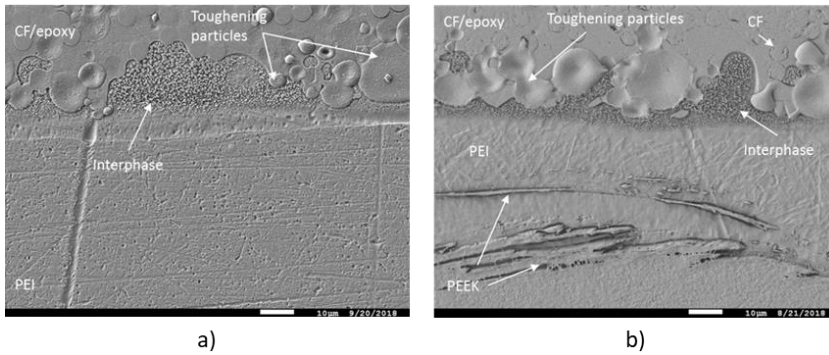
Figure 3.14: SEM micrographs of the cross-sections of a) a hybrid PEI 250 sample and b,c) a hybrid PEEK-250 sample. For both configurations, the interphase seems intact after the welding process.
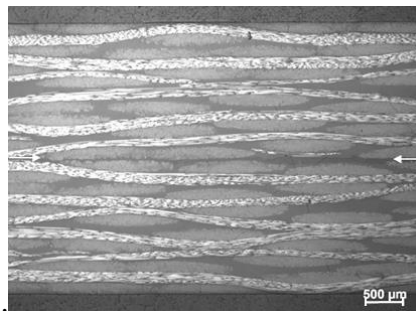
Figure 3.15: Cross-sectional micrograph a reference PEI sample. The weld line thickness is similar to that of the resin-rich areas in the composites. White arrows indicate the weld line. A similar micrograph was obtained with the reference PEEK samples.

3.3.5 Mechanical performance

Table 3.1 illustrates the results of the single-lap shear tests. The hybrid-250 configurations yielded higher average LSS as compared to the hybrid-60 configurations. However, the hybrid configurations yielded lower average LSS than their respective reference configurations. The results of the analysis of variance (ANOVA) presented in Table 3.2 show that whether the ED is PEEK or PEI does not have a significant effect on the apparent LSS of the hybrid-60 and reference welds. For the hybrid-250 samples, the F and F_{crit} values imply that the scatter within each configuration is too high to clearly determine whether they come from the same population. The hybrid PEI-250 samples yielded an average LSS of 37.5 ± 1.1 MPa (average ± standard deviation). The hybrid PEEK-250 samples yielded a somewhat higher average LSS of 40.8 ± 2.2 MPa. As seen in Figure 3.16, both configurations failed predominantly in the CF/PEEK adherend and the failure was characterized by broken fibre bundles, which were covered by a thin layer of fractured PEEK resin (see Figure 3.17). Some of the hybrid-250 samples also featured upon testing partial failure in the CF/epoxy adherend, characterized by exposed fibres and brittle matrix failure, as also seen in Figure 3.17. However, for the hybrid PEI-250 samples this type of failure can be neglected as it was very limited to areas close to an edge of the overlap, whereas for the hybrid PEEK-250 samples this failure type covered a larger area. Failure in the CF/epoxy in the hybrid PEEK-250 samples might indicate local thermal damage on the epoxy resin due to the high temperature of the molten PEEK ED.

As already mentioned, welding through a 60 µm -thick coupling layer resulted in a lower LSS than welding through a 250 µm-thick coupling layer. Figure 3.18a and b depict the fracture surfaces of representative hybrid PEI-60 and hybrid PEEK-60 samples respectively. For both configurations, failure occurred mostly in the CF/epoxy adherend which, as seen in Figure 3.19a, was characterized by exposed fibres and brittle matrix failure. This type of failure can be attributed to either the fact that the interphase was affected during welding, hence the bond between the epoxy and PEI resin might have been weakened, and/or the possibility that the epoxy resin was thermally damaged due to the high temperatures that were measured between the coupling layer and the CF/epoxy adherend in the hybrid-60 configurations (see Figure 3.10). Partial failure in the CF/PEEK adherend, towards the edges, can be seen as well, characterized by broken fibre bundles, covered by a thin layer of fractured PEEK matrix (see Figure 3.19 b,c).

Another feature of both hybrid-60 configurations was the unwelded areas that covered approximately 20% of the whole overlap. Evidence of the unwelded areas can be seen in Figure 3.19a, indicated by the intact PEI resin. The unwelded areas were an indication that a higher displacement (hence longer heating time) was needed in order to fully melt the surface of the CF/PEEK adherend. However, welding at a higher displacement (0.17 mm instead of 0.13 mm for the hybrid PEEK-60 samples and 0.19 mm instead of 0.17 mm for the hybrid PEI-60 samples) resulted in welds that failed entirely in the CF/epoxy adherend, with fracture surfaces that featured mostly exposed fibres as seen in Figure 3.20, and a noticeable decrease of LSS to around 20 MPa, when compared to samples welded at the lower displacement values. Such failure is an indication of thermal degradation of the epoxy resin. Therefore, achieving fully welded areas without a significant drop in the LSS was not possible when the 60 µm -thick coupling layer was used. This finding seems to support the hypothesis that the 60 microns coupling layer cannot shield the CF/epoxy adherend from the high temperature in the weld line long enough to prevent thermal degradation in the epoxy

resin, when welded to a CF/PEEK adherend. In previous work [11], in which a CF/PEI adherend was welded instead of the CF/PEEK adherend as in this study, the 60 µm -thick coupling layer was found to be sufficient for the production of high-strength welds, most likely because of the much lower temperature that is needed to soften the PEI matrix. Note that attempts to verify whether the epoxy was degraded via means of Fourier-transform infrared spectroscopy (FTIR) were not successful. Due to the roughness of the fracture surfaces useful results could not be obtained and be compared with untreated CF/epoxy specimens. Nevertheless, there are several reasons why thermal degradation of the epoxy resin is highly likely. First of all, the study by Villegas and Rubio [6] showed that visible thermal degradation occurred in CF/epoxy-CF/PEEK specimens welded with heating times of around 830 ms. In that study, the degradation was confirmed by both SEM analysis (dry fibres at the edges of the overlap) and FTIR analysis. Moreover, according to the study by Abouhamzeh and Sinke [14], deterioration of the mechanical properties (in that particular study the ILSS was measured) of the CF/epoxy adherend did not only happen when mass loss occurred (i.e., dry fibres), but even at lower temperatures. Finally, the observation in our previous study [11], that the PEI resin was degraded even when the heating time was kept short seems to further support the risk of thermal degradation of the more temperature-sensitive epoxy resin.

Table 3.1: Lap shear strength values with corresponding scatter

Configuration	Average LSS ± stdv (MPa)
Hybrid PEI-250	37.5 ± 1.1
Hybrid PEEK-250	40.8 ± 2.2
Hybrid PEI-60	32.4 ± 1.6
Hybrid PEEK-60	34.9 ± 1.4
Reference PEI	42.6 ± 0.5
Reference PEEK	44.8 ± 4.4

Table 3.2: ANOVA results

Comparison	F	F_{crit}	$(F < F_{crit})$?
Hybrid PEEK-60 and hybrid PEI-60	3.76	5.59	YES
Hybrid PEEK-250 and hybrid PEI-250	5.960315	5.317655	-
Reference PEEK and reference PEI	0.99408	5.317655	YES
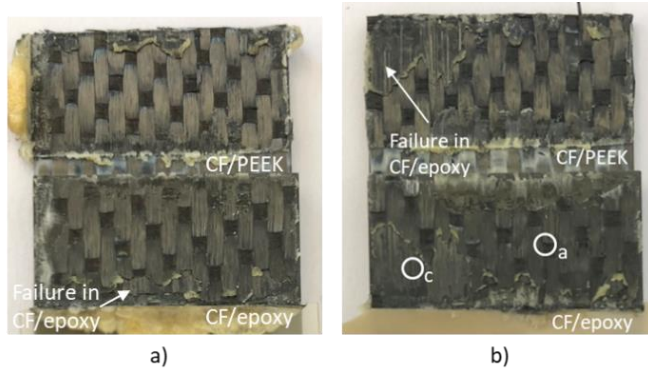
Figure 3.16: Fracture surfaces of a) a hybrid PEI-250 sample and b) a hybrid PEEK-250 sample.
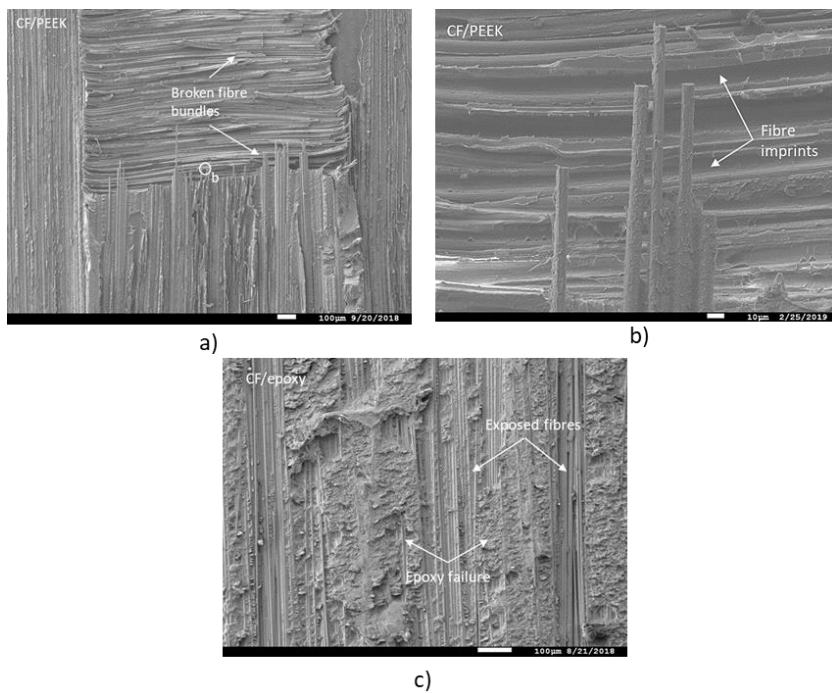
Figure 3.17: a) SEM detail of the circled area "a" in Figure 3.16b, showing broken fibre bundles of the CF/PEEK adherend attached on the CF/epoxy adherend, b) SEM detail of the circled area "b" in (a) showing fibres covered in PEEK resin and fibre imprints and c) SEM detail of the circled area "c" in Figure 3.16b showing failure in the CF/epoxy characterized by epoxy resin failure and exposed fibres. Note that the above-mentioned SEM micrographs also apply to the hybrid PEI-250 configuration.
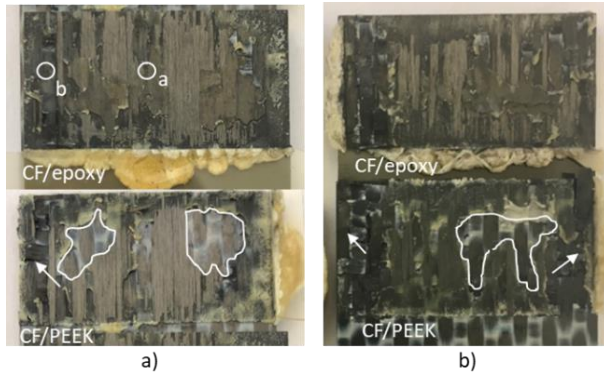
Figure 3.18: Fracture surfaces of a) a hybrid PEI-60 sample and b) a hybrid PEEK-60 sample. The unwelded areas are highlighted by the white lines. The locations where failure in the CF/PEEK adherend occurred is indicated by the white arrows.
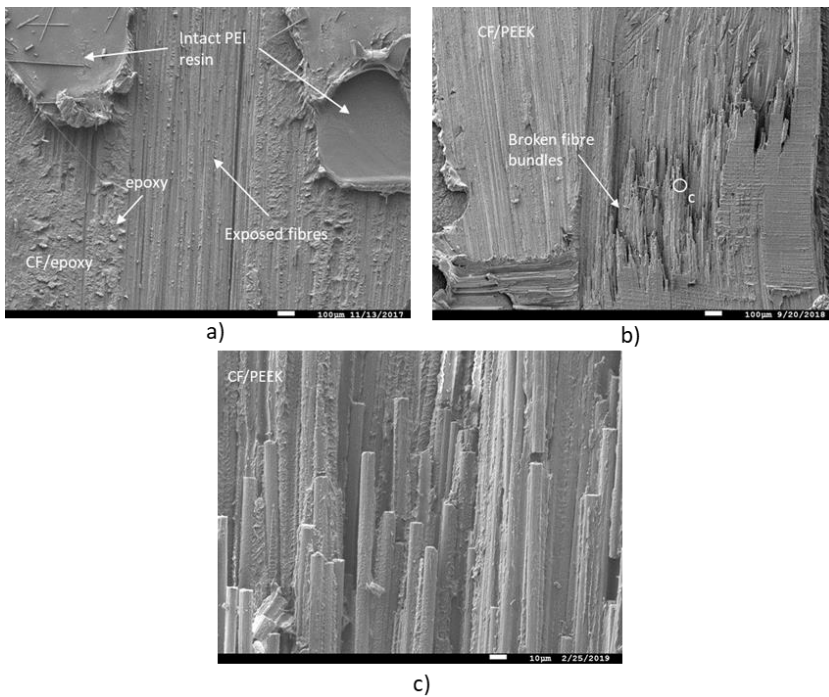
Figure 3.19: a) SEM detail of the corresponding circled area in Figure 3.18a, showing failure in the CF/epoxy characterized by epoxy resin failure exposed fibres and intact PEI resin, b) SEM detail of the corresponding circled area in Figure 3.18a showing broken fibre bundles of the CF/PEEK adherend attached on the CF/epoxy adherend and c) SEM detail of the corresponding circled area in (b) showing broken fibres covered in PEEK resin. Note that the SEM micrographs of the fracture surfaces were similar for both configurations, hence the micrographs apply to both hybrid-60 configurations.
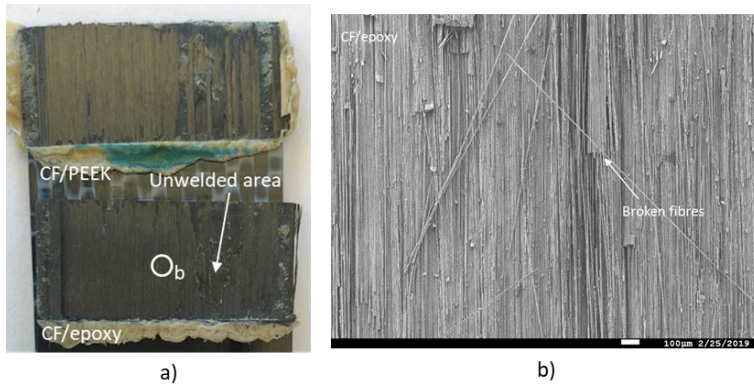
Figure 3.20: a) Fracture surfaces of a hybrid PEEK-60 sample welded at 0.17 mm displacement and b) SEM detail of the corresponding circled area in (a), showing failure in the CF/epoxy adherend characterized by exposed and broken fibres.

Table 3.1 also presents the LSS values of the reference samples. The reference PEEK samples yielded the highest average strength of all listed configurations. Both reference configurations presented fully welded areas as seen in Figure 3.21. Figure 3.22 shows that the main difference in the failure locus of the two configurations was that failure in the reference PEI samples occurred within the first ply of the adherends, whereas the reference PEEK samples also featured failure within the second ply.

The hybrid PEI-250 samples and the hybrid PEEK-250 samples exhibited only 12% and 9% lower LSS as compared to the corresponding reference samples, respectively. However, comparison between the LSS of the hybrid-250 and the corresponding reference samples is not straightforward because of the different adherends in each configuration.

In this study and in our previous one [11] several practices have been suggested in order to successfully weld epoxy- and thermoplastic-based composites by means of ultrasonic welding. In [11] it was shown that welding CF/epoxy and CF/PEI composites through a 250 µm-thick PEI ED on top of a 60 µm-thick PEI coupling layer resulted in welds with a similar mechanical performance as reference co-cured samples of the same adherends. In the current study, for welding of CF/epoxy and CF/PEEK adherends a 60 µm-thick coupling layer was not sufficient to produce welds with an acceptable LSS, possibly due to the higher melting temperature of the PEEK matrix as compared to the PEI matrix of our previous study. Increasing the coupling layer thickness to 250 µm and using either a PEEK or a PEI ED allowed for welds with a comparable LSS to reference CF/PEEK welds. Remaining open gaps in the knowledge of ultrasonic welding of such dissimilar composites include the determination of the robustness of this ultrasonic welding process with respect to the duration of the vibration phase and its sensitivity to the process parameters (i.e., welding force and amplitude of vibrations).
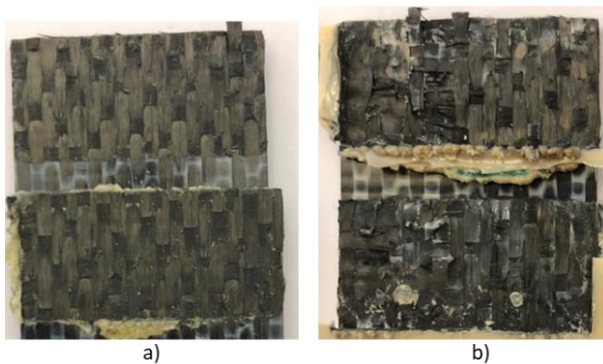
Figure 3.21: Fracture surfaces of a a) reference PEI sample and b) reference PEEK sample. Both samples featured fully welded overlaps.
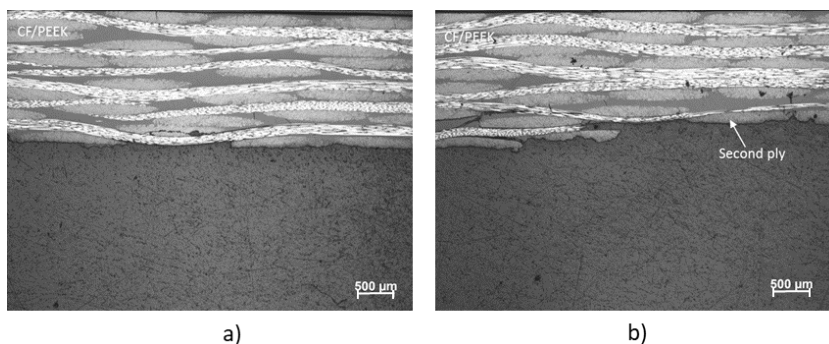
Figure 3.22: Cross-sections of one adherend after mechanical testing of a) the reference PEI configuration, showing failure within the first ply and b) the reference PEEK configuration, showing failure within the first and second plies.

3.4   Conclusions

This paper presents an experimental study on the effect of i) the ED material and ii) the thickness of the coupling layer on the ultrasonic welding process of CF/epoxy and CF/PEEK welds. Four welding cases were considered, welding with a) a 60 μm-thick PEI coupling layer and a PEI ED (hybrid PEI-60 configuration), b) a 60 μm-thick PEI coupling layer and a PEEK ED (hybrid PEEK-60 configuration), c) a 250 μm-thick PEI coupling layer and a PEI ED (hybrid PEI-250 configuration), and d) a 250 PEI μm-thick coupling layer and a PEEK ED (hybrid PEEK-250 configuration). These welding configurations were then compared to two reference cases, namely CF/PEEK welds with either a PEI ED (reference PEI configuration) or a PEEK ED (reference PEEK configuration). The main conclusions are the following:

- The nature of the material of the ED did not have a significant effect on the apparent LSS of the hybrid and reference configurations.

- In the hybrid-60 configurations, the morphology of the PEI-epoxy interphase was altered after welding, most likely because the coupling layer flowed almost entirely before the matrix of the CF/PEEK adherend melted. The interphase remained intact in the hybrid-250 configurations, since the coupling layer was much thicker.
- The hybrid-60 samples exhibited unwelded areas that covered approximately 20% of the overlap. Attempting to achieve fully welded areas in the hybrid-60 samples resulted in apparent thermal damage in the CF/epoxy adherend. Hence, it is believed that the thin coupling layer could not act as a sufficient thermal barrier for the CF/epoxy adherend.
- The hybrid-250 samples featured fully welded overlaps and failed predominantly in the CF/PEEK adherend, demonstrating non or limited thermal damage in the CF/epoxy adherend. The LSS were comparable to the reference configurations, demonstrating the promising potential of ultrasonic welding of dissimilar composites.

3.5 References

[1]   Villegas IF, van Moorleghem R. Ultrasonic welding of carbon/epoxy and carbon/PEEK composites through a PEI thermoplastic coupling layer. Compos Part A Appl Sci Manuf 2018;109:75–83.

[2]   Ageorges C, Ye L, Hou M. Advances in fusion boding techniques for joining thermoplastics materials composites: a review. Compos Part A Appl Sci Manuf 2001;32:839–57.

[3]   Lestriez B, Chapel J-P, Gérard J-F. Gradient interphase between reactive epoxy and glassy thermoplastic from dissolution process, reaction kinetics, and phase separation thermodynamics. Macromolecules 2001;34:1204–13.

[4]   Deng S, Djukic L, Paton R, Ye L. Thermoplastic-epoxy interactions and their potential applications in joining composite structures - A review. Compos Part A Appl Sci Manuf 2015;68:121–32.

[5]   Grewell DA, Benatar A, Park JB. Plastics and Composites Welding Handbook. Munich: Hanser Gardner Publications; 2003.

[6]   Villegas IF, Rubio PV. On avoiding thermal degradation during welding of high-performance thermoplastic composites to thermoset composites. Compos Part A Appl Sci Manuf 2015;77:172–80.

[7]   Villegas IF. In situ monitoring of ultrasonic welding of thermoplastic composites through power and displacement data. J Thermoplast Compos Mater 2015;28:66–85.

[8]   Zhang Z, Wang X, Luo Y, Zhang Z, Wang L. Study on heating process of ultrasonic welding for thermoplastics. J Thermoplast Compos Mater 2010;23:647–64.

[9]   Villegas IF. Strength development versus process data in ultrasonic welding of thermoplastic composites with flat energy directors and its application to the definition of optimum processing parameters. Compos Part A Appl Sci Manuf 2014;65:27–37.

[10]   Lionetto F, Morillas MN, Pappadà S, Buccoliero G, Villegas IF, Maffezzoli A. A Hybrid welding of carbon-fiber reinforced epoxy based composites. Compos Part A 2018;104:32–

40.

[11]   *Tsiangou E, Teixeira de Freitas S, Villegas IF, Benedictus R. Investigation on energy director-less ultrasonic welding of polyetherimide (PEI)- to epoxy-based composites. Compos Part B Eng 2019;173.*

[12]   *Schieler O, Beier U. Induction welding of hybrid thermoplastic-thermoset composite parts. Int J Appl Sci Technol 2016;9:27–36.*

[13]   *Benatar A, Gutowski TG. Ultrasonic welding of PEEK graphite APC-2 composites. Polym Eng Sci 1989;29:1705–21. doi:10.1002/pen.760292313.*

[14]   *Abouhamzeh M, Sinke J. Effects of fusion bonding on the thermoset composite. Compos Part A Appl Sci Manuf 2019;118:142–9. doi:10.1016/j.compositesa.2018.12.031.*

4 On the sensitivity of the ultrasonic welding of epoxy- to polyetheretherketone (PEEK)-based composites to the heating time during the welding process[3]

This chapter aims at assessing the robustness of the ultrasonic welding process for joining epoxy- to thermoplastic-based composites by determining its sensitivity to the heating time. For that, carbon fibre (CF)/epoxy adherends with a co-cured PEI coupling layer were ultrasonically welded to CF/polyetheretherketone (PEEK) adherends at different heating times. It was found that a processing interval, i.e., a range of heating times resulting in less than 10% decrease of weld strength could be obtained provided that the coupling layer had a sufficient thickness. The welding process of the dissimilar adherends was more sensitive to the heating time as compared to the welding process of CF/PEEK to CF/PEEK adherends, due to the sensitivity of the CF/epoxy adherend to the high welding temperatures.

4.1   Introduction

Owing to the fact that welding of composite materials is a very attractive alternative to mechanical fastening (drilling holes) and adhesive bonding (excessive surface pre-treatment, long curing cycles) [1], research on welding of composites is not only limited to thermoplastic but also thermoset composites. One of the most efficient ways to make thermoset composites (TSC) weldable is by attaching a compatible thermoplastic film, hereafter referred to as coupling layer, on top of the un-cured TSC laminate and curing them together [2]. The TSC can be afterwards fusion bonded or welded through this thermoplastic film. Fusion bonding techniques to join TSC parts have been successfully applied by different research groups and include co-consolidation in an oven [3–5], resistance welding [6–8], induction welding [9,10], vibration welding [11] and ultrasonic welding [2,10,12–14]. Out of these fusion bonding techniques, ultrasonic welding might be the most promising one, since the risk of thermal degradation of the thermoset resin can be rather limited by its exceptionally short heating times of less than 500 ms [12]. Moreover, ultrasonic welding is an excellent technique for joining composites, as it can provide strong joints in a rather fast and cost-effective way [15].

Villegas and Rubio in [12] investigated the effect of the heating time on the quality of (CF)/epoxy to CF/polyetheretherketone (PEEK) joints ultrasonically welded either directly or through a PEEK coupling layer by changing the welding force and amplitude of the vibrations. They showed that a combination of high force and amplitude results in very short heating times which in turn helps to prevent thermal degradation of the epoxy resin. Villegas and van Moorleghem investigated in [2] the ultrasonic welding of CF/epoxy to CF/PEEK composites through a polyetherimide (PEI) coupling layer. Their study focussed on the analysis of the morphology of the interphase formed between the PEI and epoxy resins, on the effect of the ultrasonic welding process on this interphase and they also showed promising results of single-lap shear testing. In a side study, they also demonstrated that lack of compatibility between a PEEK coupling layer and the epoxy resin resulted in a clear boundary after the co-curing process. Ultrasonic welding was used to weld two CF/epoxy adherends through poly-vynil-butyral (PVB) films in a study by Lionetto et al [10], in which comparison with samples welded by means of induction welding showed that ultrasonic welding can produce welds with higher strength. In our previous work, we investigated the possibility of welding CF/epoxy to CF/PEI samples solely through the coupling layer, and concluded that an energy director (ED) is required at the interface to help promote heat locally, without risking excessive bulk heating[13]. Bulk heating refers to overheating of the adherend (i.e., thermal degradation) and also melting beyond the ply adjacent to the interface, through the thickness of the thermoplastic composite laminate which can cause excessive resin squeeze out and fibre distortion. In that particular study a flat, 250 µm-thick PEI ED was used. The lap shear strength (LSS) of CF/epoxy and CF/PEI samples welded through a PEI ED and a 60 µm-thick PEI coupling layer was similar to that of reference co-cured CF/epoxy to CF/PEI samples. Finally, the results in [14] showed that for welding of CF/epoxy to CF/PEEK adherends a 250 µm-thick coupling layer results in better mechanical performance as compared to a 60 µm-thick one. In particular, samples provided with a 250 µm-thick coupling layer resulted in a LSS comparable to that of reference CF/PEEK to CF/PEEK welded samples. Compared to the study mentioned before [13], in which a 60 µm-thick coupling layer together with a 250 µm-thick PEI ED were found sufficient for the production of high-strength welds, the PEEK matrix has a higher melting temperature than the softening temperature of PEI, which increases the risk of thermal degradation of the

epoxy resin. Therefore, the 60 µm-thick coupling layer was not sufficient for the production of high-strength CF/epoxy to CF/PEEK welds. Nevertheless, the results obtained in all the mentioned studies show how promising ultrasonic welding is for dissimilar composite joints. To further assess the applicability of ultrasonic welding to dissimilar composites joints, it however is important to ascertain how sensitive the weld quality is to variations in the process parameters (welding force, vibrations amplitude and/or heating time), especially taking into account how critical it seems to be to keeping the heating time short [12].

As a first step to fill the abovementioned knowledge gap, this study focuses on investigating the sensitivity of ultrasonic welding of CF/epoxy to CF/PEEK through a PEI coupling layer to the time during which vibration is applied to create the joint, i.e., the heating time. The specimens were welded using a flat, 250 µm-thick PEEK ED, in order to generate preferential frictional heating in it and prevent overheating in the adherends. Firstly, a processing interval was defined for the CF/epoxy to CF/PEEK, i.e., dissimilar composite, welded joints. In this study the duration of the vibration phase of the welding process was indirectly controlled by the downward displacement of the sonotrode during the welding process (displacement-controlled welding). Hence, the processing interval was defined with respect to the lowest and the highest displacement values that resulted in a certain mechanical performance. The processing interval of the dissimilar composite joints was compared to that of reference CF/PEEK to CF/PEEK welded joints expecting the former to be narrower owing to higher sensitivity of the CF/epoxy adherend to the welding temperatures. Secondly, the major physical phenomena that limit the width of the processing interval were determined. Thirdly, the effect of the thickness of the coupling layer on the processing interval of the dissimilar composite joints was assessed. This is a mostly experimental study in which the processing intervals were determined through single-lap shear testing of the welded joints. Furthermore, fractographic analysis of the tested joints, cross-sectional analysis of the as-welded joints and analysis of the stress along the welded overlap using finite element analysis were used to investigate major physical phenomena limiting the width of the processing interval.

4.2 Experimental Procedure

4.2.1 Materials and manufacturing

In this study, Cetex® CF/PEEK (carbon fibre/polyetheretherketone) prepreg with a 5-harness satin fabric reinforcement, manufactured by TenCate Advanced Composites (the Netherlands) was used as the TPC adherend. CF/PEEK prepreg plies arranged in a $[0/90]_{3s}$ stacking sequence were consolidated in a hot-platen press at 385 °C and 1 MPa for 30 min. The thickness of the consolidated laminates was approximately 2 mm.

A T800S/3911 unidirectional CF/epoxy prepreg provided by TORAY (Japan) was used as the TSC adherend in a $[0/90]_{2s}$ configuration. PEI films with thicknesses of 60 µm (SABIC, the Netherlands), 175 µm and 250 µm (LITE, Germany) were used as the different coupling layers used in this study and were co-cured to the surfaces of the CF/epoxy laminates. The maximum thickness of 250 µm was chosen based on the high-strength welds that were obtained in [14]. Note that the 175 and 250 µm-thick films were co-cured on both sides of the laminates, since otherwise the laminates were warped, possibly because of different

thermal expansion coefficient of the CF/epoxy and PEI materials. The PEI coupling layers were degreased with isopropanol prior to their application on top of the pre-preg stack. The CF/epoxy laminates with the coupling layers were cured in an autoclave at 180°C and 7 bars for 120 min, according to the specifications of the manufacturer. To ensure smooth surfaces on both sides of the laminate, an aluminium caul plate on the side of the vacuum bag was used. The final thickness of the CF/epoxy/PEI laminates was approximately 2.15 mm, 2.45 mm and 2.6 mm with the 60, 175 and 250 µm-thick coupling layers, respectively. In our previous study [13] we found that an approximately 25 µm-thick gradient epoxy/PEI interphase was formed between these epoxy and PEI materials during the curing process. The gradient interphase consisted of epoxy spheres dispersed in the PEI resin. The diameter of these spheres was smaller closer to the PEI film than in the region with high epoxy resin content. More information on how the interphase was developed and looked like can be found in the authors' previous work [13].

A water-cooled circular diamond saw was used to cut the CF/PEEK and CF/epoxy/PEI adherends in 25.4 mm x 106 mm dimensions with the longitudinal direction of the former parallel to the main apparent orientation of the fibres and of the latter parallel to the 0° fibres on the outer surfaces of the laminate.

4.2.2 Welding process

Samples were welded with a HiQ DIALOG SpeedControl ultrasonic welder (Herrmann Ultraschal, Germany), using the custom-made jig that was used in [14]. The samples were welded in a single-lap configuration with a 12.7 mm long and 25.4 mm wide overlap, using a 250 µm-thick PEEK film (provided by Victrex, the Netherlands) as energy director (ED). A rectangular sonotrode with dimensions 30 x 16 mm was utilized. The welding force and peak-to-peak amplitude of vibrations used in this study were 1200 N and 86 µm, respectively. The solidification force and time were kept constant at 1200 N and 4 s, respectively. Displacement-controlled welding was used, i.e. the vibration time was indirectly controlled by the downward displacement of the sonotrode [16]. The process was stopped at different displacement values, in order to assess the effect of the duration of the vibration phase on the quality of welded joints.

A total of four configurations were considered, which are shown in Table 4.1. A processing interval for welding CF/epoxy to CF/PEEK adherends was defined in the epoxy-PEEK 250 configuration. This processing interval was then compared to that of reference PEEK-PEEK welded joints. To assess the effect of the thickness of the coupling layer on the processing interval of the epoxy-PEEK welds, two extra welding configurations were considered, namely epoxy-PEEK 60 and epoxy-PEEK 175.

Table 4.1: The welding configurations that were considered in this study and respective displacement values at which the vibration phase was stopped. At least 5 samples were welded per condition.

Configuration nomenclature	Coupling layer thickness	Displacement values (mm)
Epoxy-PEEK 250[1]	250	0.2, 0,22, 0.24, 0.26,0.28, 0.3, 0.32, 0.34, 0.36, 0.38
Epoxy- PEEK 175[1]	175	0.16, 0.18, 0.2, 0,22, 0.24, 0.26, 0.28, 0.3, 0.32
Epoxy- PEEK 60[1]	60	0.11, 0.13, 0.15, 0.17
PEEK-PEEK[2]	-	0.1, 0.12, 0.14, 0.16, 0.18, 0.2, 0,22, 0.24

[1]CF/epoxy adherend welded to CF/PEEK adherend through a 250- µm-thick PEEK ED

[2]CF/ PEEK adherends welded through a 250- µm-thick PEEK ED

4.2.3 Mechanical testing and fractography

Single lap shear tests were performed according to the ASTM D 1002 standard in a Zwick 250 kN universal testing machine. The lap shear strength (LSS) of the joints was calculated as the maximum load divided by the overlap area. Five specimens were welded per welding case to determine the average LSS and standard deviation. Naked eye observation, and scanning electron microscopy (SEM, JEOL JSM-7500F scanning electron microscope) were used for the fractographic analysis of the welded joints after mechanical testing. An optical microscope (Zeiss Axiovert 40) together with the SEM were used for cross-sectional analysis of as-welded specimens.

A processing interval was defined for displacement values that resulted in welds with an average LSS higher than 90% of the maximum average LSS that was achieved within each configuration. A similar practice to determine a processing window for resistance welding of CF/PEI samples was followed by Hou et al in [17]. In that study, the LSS of the considered welded configurations was compared to that of compression moulded benchmark samples.

4.3   Results

4.3.1 Processing intervals

Figure 4.1 illustrates the average LSS values that were obtained for epoxy-PEEK 250 and reference PEEK-PEEK samples welded at the respective displacement values in Table 4.1. Table 4.2 summarizes the results pertaining the definition of the processing intervals for these two configurations. The processing interval was defined to include the displacement values that resulted in an average LSS higher than the LSS threshold.
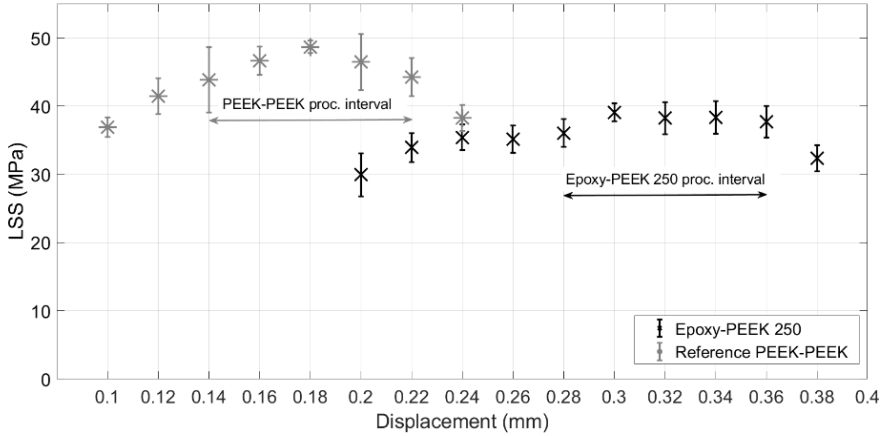
Figure 4.1: Average lap shear strength of the epoxy-PEEK 250 and reference PEEK-PEEK configurations versus the corresponding displacement. The processing intervals were defined for welds with an average LSS higher than 90% of the maximum achieved LSS within the configuration.

Table 4.2: Results regarding the processing intervals of the epoxy-PEEK 250 and PEEK-PEEK configurations. The threshold LSS was defined as 90% of the $LSS_{max.}$

	Epoxy-PEEK 250	PEEK-PEEK
LSS_{max} (average ± stdv, MPa)	39.1 ± 1.3	48.7 ± 0.9
d_{opt} (mm) (heating time, average ± stdv,ms)	0.30 (461 ± 38)	0.18 (609 ± 37)
Threshold LSS (MPa)	35.2	43.8
d_{low} (mm) (heating time average ± stdv, ms)	0.28 (441 ± 28)	0.14 (444 ± 32)
d_{high} (mm), (heating time average ± stdv, ms)	0.36 (607 ± 46)	0.22 (685 ± 45)
Width of processing interval (mm)	0.08	0.08

4.3.2 Fractographic analysis

The main physical phenomena that limit the width of the processing intervals can be determined when examining the fracture surfaces of samples welded at displacements below d_{low}, between d_{low} and d_{high} and right above d_{high}. Fracture surfaces of representative epoxy-PEEK 250 samples in all those stages can be seen in Figure 4.2. For specimens welded below d_{low}, the fracture surfaces featured un-welded areas which decreased in size with increasing target displacement. Epoxy-PEEK 250 specimens welded around the d_{opt} featured almost fully welded overlaps and first-ply failure in the CF/PEEK adherend. In a microscopic level, the main features were resin-rich CF bundles, exposed fibres and broken fibres, as seen in

Figure 4.3a. Epoxy-PEEK 250 specimens welded at displacement values equal or higher than d_{high} featured failure in both adherends, with failure in the CF/epoxy adherend being increasingly present for increasing displacement values. As seen in Figure 4.3b, the failure in the CF/epoxy adherend was characterized by exposed and broken fibres.

Figure 4.4 presents the fracture surfaces of reference PEEK-PEEK welded joints at different displacements. Below d_{opt}, the reference PEEK-PEEK specimens featured un-welded areas that decreased in size with increasing target displacement. Reference PEEK-PEEK specimens welded at d_{low} still featured un-welded areas that covered approximately 20% of the total overlap. As seen in Figure 4.5, specimens welded at d_{opt} featured mostly fully welded overlaps and first-ply failure which was characterized by ruptured resin, resin-rich CF bundles and broken fibres. Finally, in specimens welded at or right above d_{high}, squeeze out of fibre bundles could be found towards the edges of the overlap. Instead of experiencing first-ply failure, the specimens failed between the first and second ply of one of the adherends, indicated by the different morphology of the fracture surfaces as compared to samples welded at lower displacement values, i.e., main apparent orientation of the fibres being perpendicular to the direction of the applied load instead of parallel. In a microscopic level, similar failure mechanisms as in reference PEEK-PEEK specimens welded below d_{high} were observed.
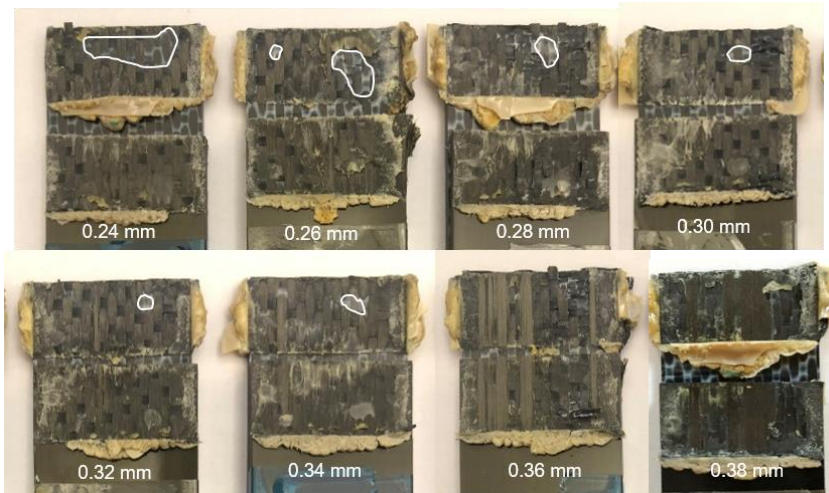
Figure 4.2: Fracture surfaces of representative epoxy-PEEK 250 samples welded at different displacement values. The 0.28 mm, 0.30 mm and 0.36 mm values correspond to the d_{low}, d_{opt} and d_{high}, respectively. The size of the un-welded areas (highlighted with white lines) decreased with an increasing target displacement. Welding at and above d_{high} resulted in failure in both adherends
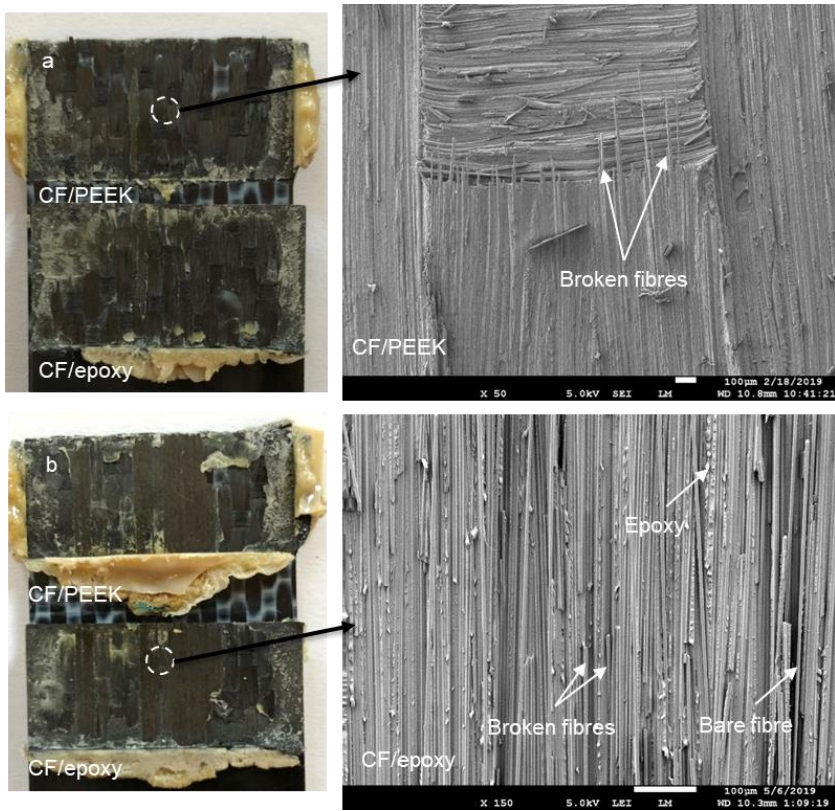
Figure 4.3: Closer inspection of the fracture surfaces of epoxy-PEEK 250 joints welded at a) $d_{opt.}$ showing failure in the CF/PEEK adherend, characterized by ruptured resin and broken fibres and b) at 0.38 mm, i.e. right above d_{high}, depicting failure in both adherends with failure in the CF/epoxy adherend characterized by exposed and broken fibres.

Figure 4.4*:* Representative fracture surfaces of reference PEEK-PEEK samples welded at different displacement values. The displacement values of 0.14 mm, 0.18 mm and 0.22 mm correspond to the d_{low}, d_{opt}, and d_{high}, respectively. The size of the un-welded areas decreased with an increased target displacement. The un-welded areas are highlighted with white lines. The vertical arrows point at locations where significant fibre squeeze out was observed. The parallel arrow indicates failure between the first and second ply.
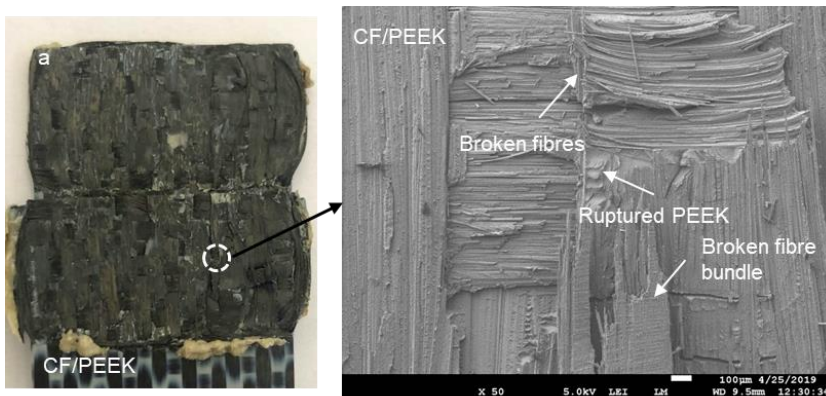
Figure 4.5: Closer inspection of the fracture surfaces of a reference PEEK-PEEK sample welded at d_{opt}, showing failure in the CF/PEEK adherend, characterized by ruptured resin and broken fibres and fibre.

4.3.3 Cross-sectional analysis

Cross-sectional analysis was performed in order to determine the weld line thickness of samples welded below, within and above the processing interval. Considering the known effect of the bond line thickness on the LSS of adhesively bonded joints [18], it was expected that the weld line thickness would play a role in the LSS of welded joints. Figure 4.6 shows cross-sectional micrographs in the middle of epoxy-PEEK 250 samples welded at a displacement below d_{low} (Figure 4.6a), at dopt (Figure 4.6b) and right above d_{high} (Figure

6c). The samples welded at 0.20 mm (below d_{low}) and at 0.38 mm (above d_{high}) were chosen since at those displacements the LSS was well below the 35.2 MPa threshold. Regarding the weld line thickness, the main observation is that it decreased from approximately 200 µm for samples welded before d_{low}, to 100 µm at dopt and finally to approximately 50 µm right above d_{high}. Given the different shades of grey shown by the PEI and the PEEK resins, it was possible to discern the contribution of the coupling layer and the energy director to those thickness values. In the sample welded well below dl_{ow} roughly two thirds of the total weldline (170 µm) were coupling layer while one third (70 µm) was energy director (Figure 4.6a). However, in samples welded at and above dopt (Figure 4.6b and Figure 4.6c) the energy director seemed to have been completely squeezed out, resulting in a mostly PEI weld line. In some cases, such as clearly shown in Figure 4.6b, the coupling layer was found to even flow in between the fibre bundles of the first layer of the CF/PEEK adherend.

Figure 4.7 presents cross-sectional micrographs of reference PEEK-PEEK welded joints at a displacement right below d_{low} (Figure 4.7a), at d_{opt} (Figure 4.7b) and right after d_{high} (Figure 4.7c). The weld line thickness decreased from approximately 90µm for samples welded before d_{low}, to 70 µm at d_{opt} and finally to approximately 0 µm right above d_{high}.
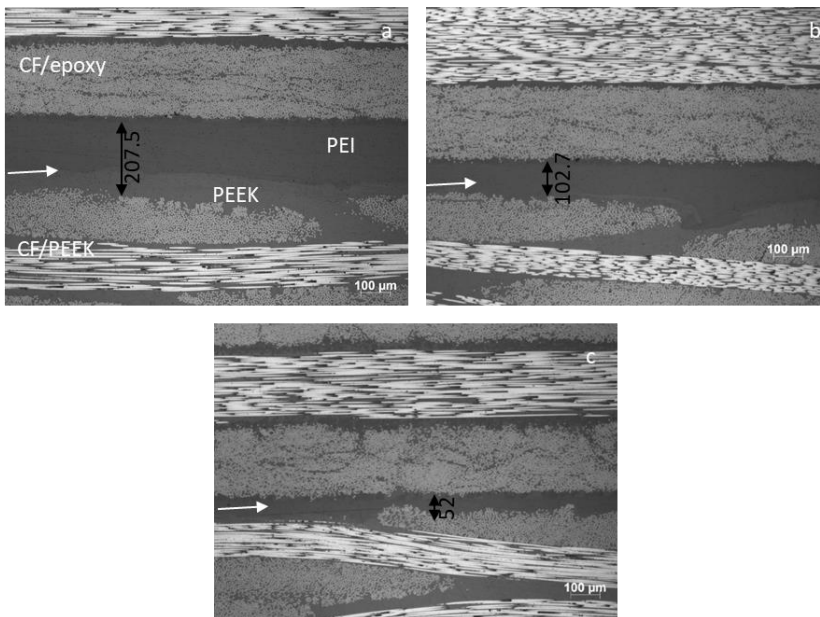
Figure 4.6: Cross sections of epoxy-PEEK 250 samples welded at t a) 0.20 mm, b) 0.30 mm and c) 0.38 mm. The thickness of the weld line decreases with an increasing travel. White arrows indicate the weld line.

With respect to the microstructure of the epoxy-PEEK 250 welds, increasing the displacement of the sonotrode above a certain threshold affected the condition of the gradient epoxy-PEI interphase originally formed during curing of the CF/epoxy adherends [13]. As seen in Figure 4.8a, at 0.38mm displacement the morphology of the interphase was affected by the welding process and featured bands of epoxy spheres interspersed with PEI-rich bands. This disruption of the interphase did however not happen at lower displacement values (0.30mm and below), as seen in Figure 4.8b.
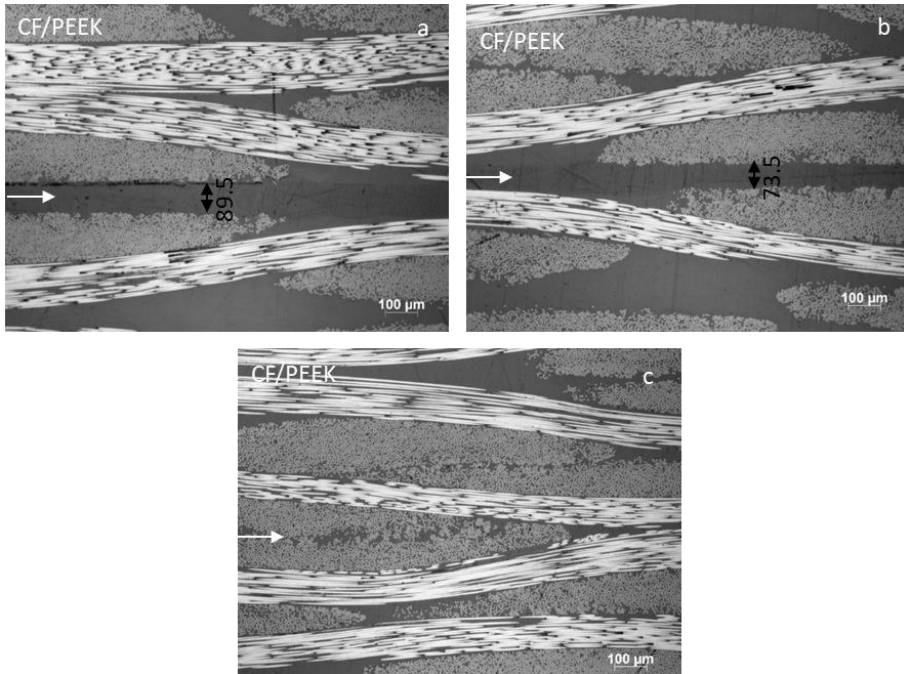
Figure 4.7: Cross sections of reference PEEK-PEEK CF/PEEK samples welded at a displacement a) right before d_{low} (at 0.12 mm), b) at d_{opt} (0.18 mm) and c) right above d_{high} (at 0.24 mm). The thickness of the weld line decreases with increasing displacement. White arrows indicate the weld line.
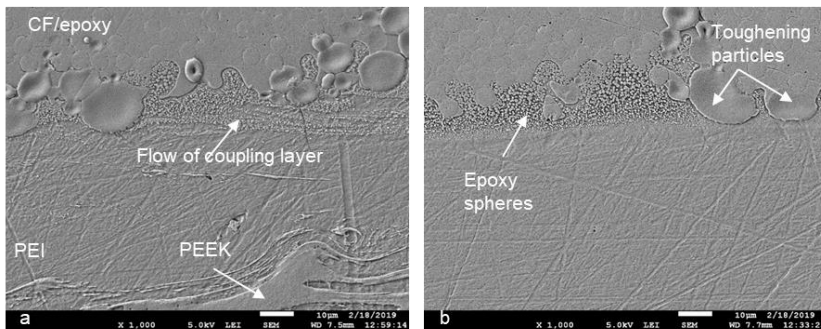
Figure 4.8: Representative SEM cross-sectional micrographs of epoxy-PEEK 250 samples welded at a) 0.38 mm and b) 0.30 mm. The interphase seems intact when samples are welded at dopt whereas flow of the epoxy spheres along with the PEI resin is observed when the samples are welded above d_{high}.

4.3.4 FE-model

In order to assess the effect of the weld line thickness on the shear and peel stresses in the epoxy-PEEK 250 welds, a FE-model was built. The specifications of the model can be found in Appendix A. Figure 4.9 shows the stress distributions obtained from the FE-model at a

load of 3.3 kN. The value of 3.3 kN was defined in order to remain within the region before damage initiation occurred in the welded joints. This load corresponded to approximately 40% of the lowest failure load that was reached during mechanical testing of the epoxy-PEEK 250 welded samples. Figure 4.9a and Figure 4.9b present the shear and peel stresses along the middle of the weld line for the measured weld line thicknesses of 50 µm, 100 µm and 200 µm (see section 4.3.3). As seen in Figure 4.9a, the shear stresses were not affected by the thickness of the weld line for the thickness values considered. However, the peak peel stresses at the edges of the overlap increased with decreasing weld line thickness. Hence the 100 µm-thick weld line resulted in peak peel stresses that were 18% higher than the ones in the 200 µm-thick weld line. Moreover, in the 50 µm-thick weld line the peak peel stresses were around 93% higher than those in the 200 µm-thick weld line. This increasing trend is also seen in Figure 9c, in which the peel stresses across the weld line are shown.
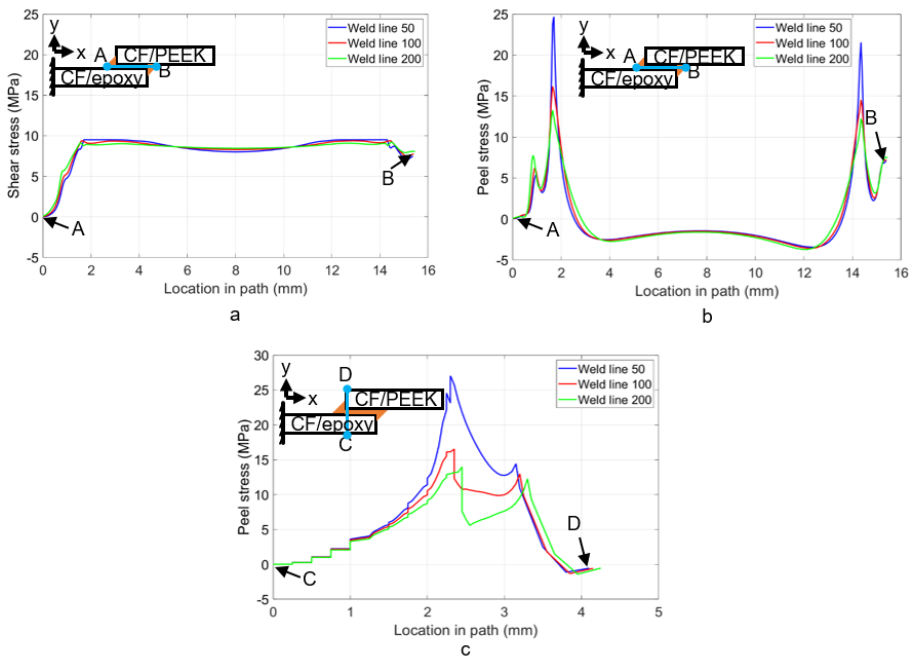
Figure 4.9: Stresses obtained from the FE-model. a) Shear stresses along the AB path, b) peel stresses along the AB path and c) peel stresses along the CD path.

4.3.5 Coupling layer thickness

Decreasing the thickness of the coupling layer was expected to decrease the width of the processing interval, as a result of higher risk of thermal degradation of the CF/epoxy material. Figure 4.10 presents the average LSS of the three considered epoxy-PEEK configurations plotted versus the respective displacement values found in Table 4.1. A similar trend was observed in all configurations, i.e., the LSS initially increases until it reaches a maximum value, and then decreases again. In the epoxy-PEEK 60 configuration the LSS decrease after the maximum occurs more abruptly than the other two configurations.

Moreover, the values at which these changes happen are shifted to lower displacement values with increasing coupling layer thickness. Table 4.3 summarizes the results pertaining the definition of the processing interval for the epoxy-PEEK 175 configuration. In the epoxy-PEEK 60 configuration, none of the considered displacement values resulted in an average LSS value well above the established threshold.
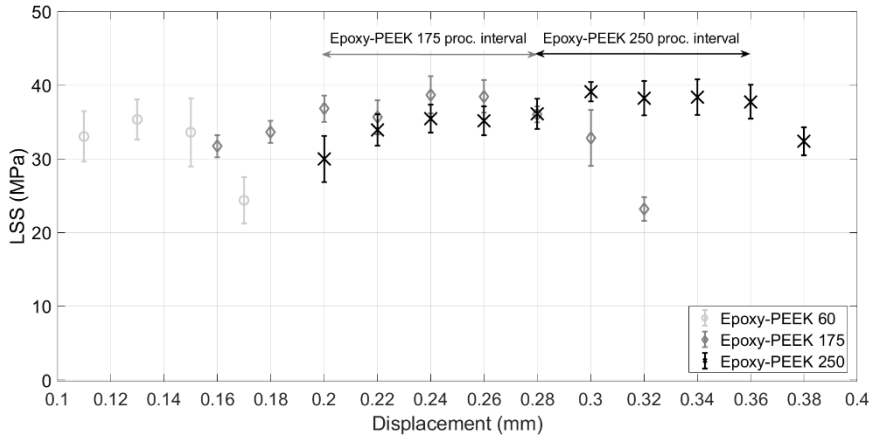
Figure 4.10: Average lap shear strength of the epoxy-PEEK, epoxy-PEEK 175 and epoxy-PEEK 60 configurations versus the corresponding displacement.

Table 4.3: Results regarding the processing interval of the epoxy-PEEK 175 configuration.

LSS_{max} (average ± stdv, MPa)	38.7 ± 2.5
d_{opt} (mm) (heating time, average ± stdv,ms)	0.24 (462 ± 67)
Threshold LSS (MPa)	35.2
d_{low} (mm) (heating time average ± stdv, ms)	0.20 (449 ± 22)
d_{high} (mm), (heating time average ± stdv, ms)	0.28 (547 ± 34)
Width of processing interval (mm)	0.08

Figure 4.11 presents fracture surfaces of epoxy-PEEK 175 samples welded at different displacement values. It is clearly seen that a similar trend as in the epoxy-PEEK 250 configuration occurred. Closer inspection of the fracture surfaces of these samples also showed failure mechanisms that were the same as in the epoxy-PEEK 250 configuration.
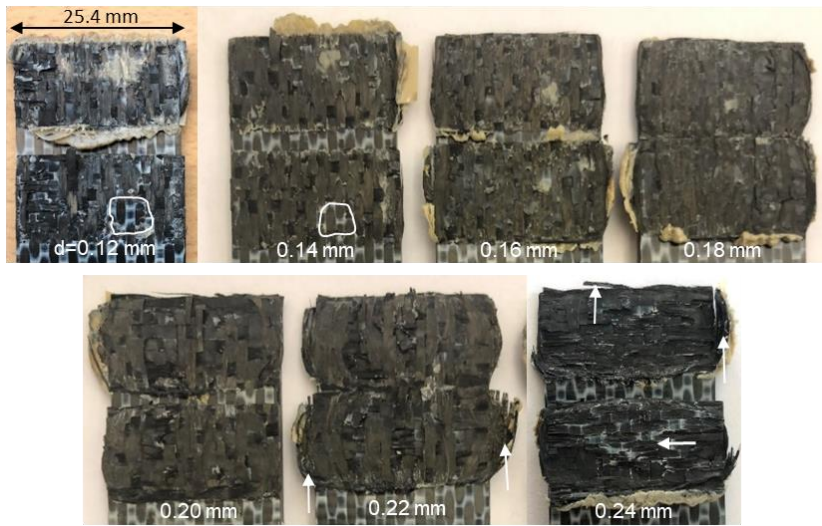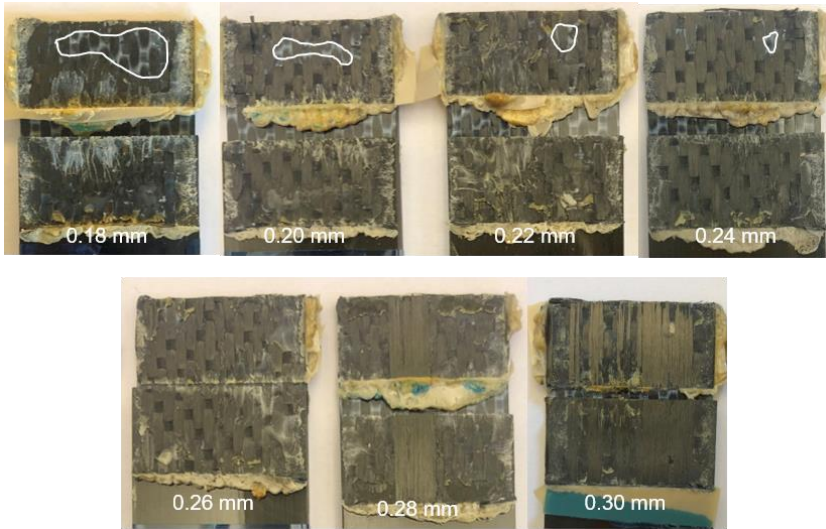
Figure 4.11: Fracture surfaces of representative epoxy-PEEK 175 samples welded at different displacement values. The displacement values of 0.20 mm, 0.24 mm and 0.28 mm correspond to the d_{low}, d_{opt}, and d_{high}, respectively.

4.4 Discussion

The results presented in the previous section were analysed in order to i) define a processing interval for the epoxy-PEEK 250 welded joints, i.e. CF/epoxy to CF/PEEK adherends welded through a 250 µm-thick PEI coupling layer and compare it to that of reference CF/PEEK-CF/PEEK welded joints (or reference PEEK-PEEK), ii) determine the major physical phenomena that limit the width of the processing interval and iii) assess the potential effect of the thickness of the coupling layer on the processing interval of the epoxy-PEEK welded joints.

To start with, the processing interval defined as the displacement values that resulted in welds with average LSS higher than 90% of the optimum LSS, had the same width in the epoxy-PEEK 250 welded joints as in the reference PEEK-PEEK welded joints, i.e., 0.08 mm (see Table 4.2). Therefore, the sensitivity of both processes to variations in the value of the controlling parameter, in this case the displacement of the sonotrode, could be considered to be similar. However, there were two main differences between these configurations. Firstly, the processing interval of the epoxy-PEEK 250 joints was shifted towards higher displacement values than that of the reference PEEK-PEEK joints. This behaviour is consistent with higher initial thickness of the neat resin layers between the composite material in the adherends prior to the welding process but rather similar final thicknesses of the weld line (see Figures 4.6b and 4.7b). Note that a direct correlation between the initial thickness of the resin-rich layers, the displacement of the sonotrode during the vibration phase and the thickness of the weld line is not possible since the sonotrode continues to travel downwards during the consolidation phase. Secondly, when translating the limits of the processing interval into average heating times (see Table 4.2), the lower limit was similar in both configurations. The higher time limit was however around 13% lower for the epoxy-PEEK 250 joints, a difference which was statistically significant (($F(1,9)=7.99$, $p=0.02$). The

shorter time-wise processing interval of the epoxy-PEEK 250 configuration is consistent with higher squeeze-out rates, i.e., faster vertical displacement of the sonotrode after the initial plateau, observed in the welding processes (see Figure 4.12). These higher squeeze-out rates can be explained by a potentially faster temperature rise in the ED owing to: (i) additional heat generated by the coupling layer (together with the ED, which was the same in both epoxy-PEEK and PEEK-PEEK configurations) and (ii) thermal insulation between ED and carbon fibres in the CF/epoxy adherend provided by the coupling layer. This might also explain why at d_{opt} most of the ED was squeezed out from the epoxy-PEEK 250 joints (see Figure 4.6b) whereas that was not the case in the reference PEEK-PEEK joints (see Figure 4.7b). Additionally, the time-wise upper limit of the processing interval of the epoxy-PEEK 250 welds correlates with the higher sensitivity of the CF/epoxy adherend to the high temperatures developed during the welding process, as compared to the CF/PEEK adherends, as it will be explained latter in this section.
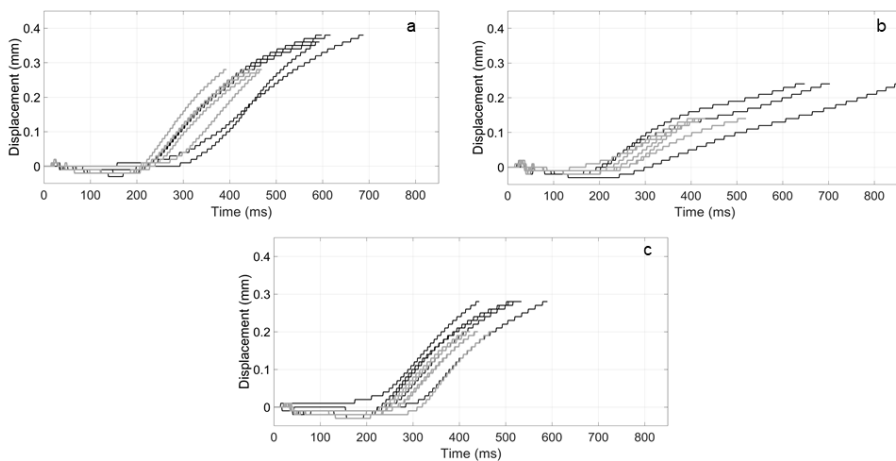
Figure 4.12: Displacement of the sonotrode during the welding process in the a) epoxy-PEEK 250, b) reference PEEK-PEEK and c) epoxy-PEEK 175 configurations. Note: grey curves correspond to specimens welded up to d_{low}; black curves correspond to specimens welded up to d_{high} (see Table 4.2 and Table 4.3).

Epoxy-PEEK 250 samples welded within the processing interval, i.e., between d_{low} and d_{high}, presented mostly fully welded overlaps and failure in the CF/PEEK adherend (see Figure 4.3a). On the one hand, the fully welded overlaps indicate successful overall inter-diffusion between the ED and the PEEK matrix on one side and between the ED and coupling layer on the other side. On the other hand, failure within the CF/PEEK adherend might imply that the epoxy resin was subjected to non or insignificant thermal degradation, since otherwise, for the type of adherends used in this study, the samples could have been expected to fail at least partially in the CF/epoxy adherend [14]. Welding at displacement values below d_{low} resulted in un-welded areas that decreased in size the closer the displacement was to the d_{low} (Figure 4.2). The samples in which the un-welded areas were found only in the middle of the overlap still yielded an average LSS close to 35.2 MPa. The reason for such strength was most likely the fact that the highest stresses during the lap shear test are developed at the edges of the joint [19]. Thus, un-welded areas limited at the centre of the overlap did not seem to have an effect on the LSS. Welding at displacement values above the d_{high} resulted in welded joints that failed predominantly in the CF/epoxy adherend (see Figure 4.3b). The change in failure locus might indicate some form of degradation in the CF/epoxy adherend

due to the high welding temperatures, despite the fact that no definitive visible signs of thermal degradation, such as porosity or dry fibres, were found. The altered interphase morphology that was observed in these samples (Figure 4.8), indicates that high temperatures were indeed reached close to the CF/epoxy adherend. Finally, according to the results of the FEM model, it seems that the weld line of 50 µm that was found in samples welded at a displacement above the d_{high} was more prone to inducing high peel stresses during the lap shear tests than the 100 and 200 µm-thick weld lines that were found in samples welded at d_{opt} and at much lower displacements than d_{low}, respectively (Figure 4.9). These high peel stresses might also contribute to the lower LSS of samples welded above d_{high} as compared to samples welded at and below d_{opt}.

Comparative analysis of the fracture surfaces of the epoxy-PEEK 250 and reference PEEK-PEEK samples welded at different displacement values showed that, whilst the lower limit of the processing interval was roughly defined by the same phenomenon in both cases, i.e., transition from partially to fully welded overlap, the upper limit had different causes. As it is, in the reference PEEK-PEEK configuration the LSS drop above d_{high} could be linked to the excessive squeeze out of the matrix resin and disruption of the fibre bundles (Figure 4.5b), however in the epoxy-PEEK 250 configuration the failure locus shifted to failure in the CF/epoxy adherend, before too much squeeze out of the PEEK matrix could occur.

Another interesting difference between the epoxy-PEEK 250 and the reference PEEK-PEEK configurations was that at d_{opt} the fracture surfaces corresponding to the epoxy-PEEK 250 configuration were less textured than those of the reference PEEK-PEEK configuration (e.g. see Figures 4.3a and 4.5a). Looking at the cross-section micrographs in Figure 6b and seeing that most of the weld line at d_{opt} was composed of PEI, it could be thought that the relatively flat fracture surface resulted from failure at the boundary between the PEI weldline and the CF/PEEK adherend. Likewise, occasional fibre breakage (Figure 4.3a) might have been the result of the flow of PEI within the first layer in the CF/PEEK adherend (see Figure 4.6b). Contrarily, in the reference PEEK-PEEK configuration the weld line was of the same material as the matrix in the adherends, hence they lacked a well-defined, relatively flat path for failure to occur. The more tortuous failure path, consistent with more textured fracture surfaces, might have been one contributing factor to the higher average LSS of the PEEK-PEEK. Another possible factor might have been a stiffness mismatch between the CF/PEEK and CF/epoxy adherends potentially inducing premature failure in the presumably less stiff CF fabric/PEEK material due to higher strains. Note that adding two 250 µm-thick PEI layers on the CF/epoxy adherend is expected to decrease the stiffness of the CF/epoxy adherend by around 18% (following the rule of mixtures as rough simplification). However, the stiffness of the CF/epoxy adherend is still expected to be higher than that of the CF/PEEK adherend (see Appendix, Table A.1).

Decreasing the thickness of the coupling layer from 250 to 175 µm neither affected the width of the processing interval nor the maximum average LSS (see Table 4.3). The processing interval of the epoxy-PEEK 175 configuration was however shifted towards lower displacement values. As in the comparison between the epoxy-PEEK 250 and the reference PEEK-PEEK configurations, this is consistent with a lower initial thickness of the neat resin layers between the composite adherends prior to the welding process but at the same time similar final thickness of the weld line (see Figures 4.3 and 4.13). Regarding the time-wise limits of the processing interval for the epoxy-PEEK 175 joints, according to analysis of variance both limits can be regarded similar to that of the epoxy-PEEK 250 configuration

($F(1,7)$=4.55, p=0.07). This is most likely attributed to the similar squeeze flow rates that were observed for displacements above the d_{low} in each configuration (see Figure 4.12). As seen in Figure 4.3 and Figure 4.15, the thickness of the coupling layer was similar in the epoxy-PEEK 175 and epoxy-PEEK 250 configurations at similar stages of the vibration phase. Hence, both coupling layers could shield the CF/epoxy adherend from the high temperatures with the same efficiency. However, further decreasing the thickness of the coupling layer to 60 µm, decreased its efficiency as a thermal barrier significantly. As a result, it was not possible to obtain fully welded overlaps without causing thermal degradation in the CF/epoxy adherend, as also discussed in [14].
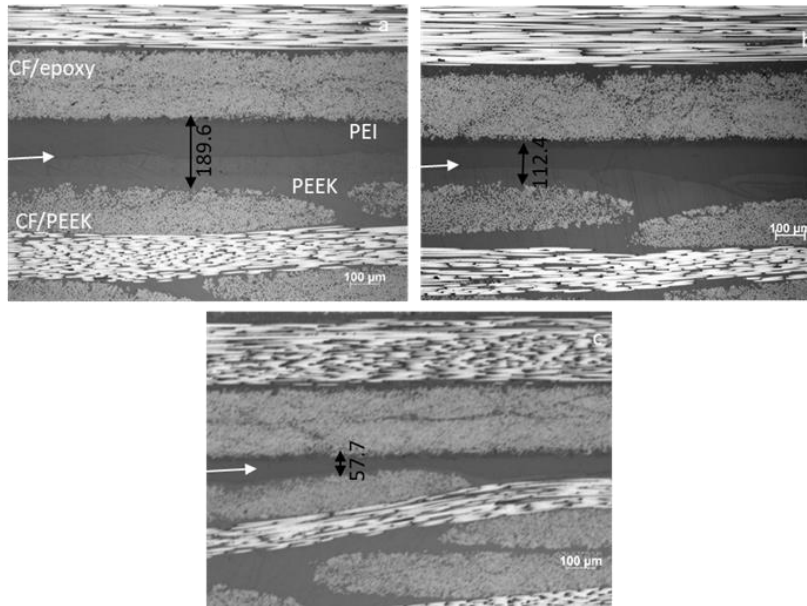
Figure 4.13: Cross sections of epoxy-PEEK 175 samples welded at a displacement a) before d_{low} (at 0.16 mm), b) at dopt (0.24 mm) and c) right above d_{high} (at 0.30 mm). White arrows indicate the weld line.

Lastly there were a couple of interesting similarities in the data obtained in this study despite the various differences among the epoxy-PEEK 250, epoxy-PEEK 175 and reference PEEK-PEEK configurations. Firstly, and as mentioned before, the displacement-wise width of the processing interval was the same for all three configurations. Secondly, the time to reach d_{low} was similar in all cases. The latter might suggest that exposure time of the CF/PEEK adherend to the molten PEEK ED plays a major role in achieving an almost fully welded overlap, i.e., the point at which d_{low} was reached. Likewise, the former might suggest that the decrease in the thickness of the weld line plays a major role in defining the point at which the welded joint degrades. However, these are only preliminary hypotheses that should be investigated in future research.

4.5 Conclusions

This paper presented a study on the sensitivity of the strength of CF/epoxy to CF/PEEK ultrasonic welded joints to the duration of the vibration phase of the welding process. The main objectives were: i) definition of a processing interval for CF/epoxy to CF/PEEK (epoxy-PEEK) welded joints and comparison with the processing interval for reference CF/PEEK to CF/PEEK (PEEK-PEEK) welded joints; ii) determination of major physical phenomena that limit the width of the processing interval; and iii) assessment of the effect of the coupling layer thickness on the processing interval of epoxy-PEEK welded joints. A 250 μm-thick coupling layer was used in the epoxy-PEEK welds used to address objectives i and ii. For objective iii, coupling layers with thicknesses of 175 and 60 μm were used. The main findings were:

- Despite the fact that the epoxy-PEEK welding process needs to be very fast to prevent thermal degradation of the CF/epoxy adherend, a relatively wide processing interval (defined by LSS > 0.9 optimum LSS_o) was found for the epoxy-PEEK welds provided with a 250 μm-thick coupling layer. When defined in terms of displacement of the sonotrode (used as the controlling parameter for the welding process), the processing interval of the epoxy-PEEK 250 joints was as wide as the processing interval of the reference PEEK-PEEK joints, both of them amounting to 0.08 mm. Hence the robustness of both processes, i.e., their sensitivity to variations in the value of the controlling parameter, could be considered similar. However, when translating the displacement values into average heating times, the reference PEEK-PEEK joints were able to withstand longer heating times than the epoxy-PEEK 250 ones consistent with the higher sensitivity of the former to thermal degradation.

- The lower limit in the processing interval of the epoxy-PEEK welded joints was determined by the amount of welded area in the overlap. Below this lower limit, significant un-welded areas lacking inter-diffusion between the ED and CF/PEEK adherend could be found within the overlap. Above the lower limit complete welded overlaps were obtained, which upon mechanical testing failed mostly in the CF/PEEK adherend. Beyond the upper limit of the processing interval the epoxy-PEEK welded samples featured i) a shift in the failure locus, i.e., failure in the CF/epoxy, ii) a thin weld line (thickness below 50 μm), which according to the FE-model could have caused higher peel stresses as compared to samples welded in optimum conditions; and iii) an altered morphology of the epoxy-PEI gradient interphase, which is a sign of high temperatures close to the CF/epoxy adherend. In the case of the reference PEEK-PEEK joints, the lower limit of the processing interval was also related to the amount of welded area whereas the upper limit was determined by disruption of the fibre bundles in the CF/PEEK adherends and potentially increased stresses due to decreased weld line thickness.

- Decreasing the thickness of the coupling layer from 250 μm to 175 μm did not decrease the achievable LSS values, the width of the processing interval defined in terms of the displacement of the sonotrode or the average heating times. Hence, decreasing the thickness of the coupling layer from 250 μm to 175 μm did not affect the outcome nor the robustness of the welding process. Further decreasing the thickness of the coupling layer to 60 μm resulted in a decrease of the achievable LSS and the appearance of thermal degradation signs even before fully welded overlaps could be obtained.

4.6 References

[1]   *Ageorges C, Ye L, Hou M. Advances in fusion boding techniques for joining thermoplastics materials composites: a review. Compos Part A Appl Sci Manuf 2001;32:839–57.*

[2]   *Villegas IF, van Moorleghem R. Ultrasonic welding of carbon/epoxy and carbon/PEEK composites through a PEI thermoplastic coupling layer. Compos Part A Appl Sci Manuf 2018;109:75–83.*

[3]   *Hou M. Thermoplastic adhesive for thermosetting composites. Mater Sci Forum 2012;706–709:2968–73.*

[4]   *Hou M. Fusion Bonding of Carbon Fiber Reinforced Epoxy Laminates. Adv Mater Res 2013;626.*

[5]   *Paton R, Hou M, Beehag A, Falzon P. A breakthrough in the assembly of aircraft composite structures. 25th Congr. Int. Counc. Aeronaut. Sci., 2006.*

[6]   *Don RC, McKnight H, Wetzel ED, Gillespie Jr. JW. Application of thermoplastic resistance welding techniques to thermoset composites. Annu Tech Conf Soc Plast 1994:1295–7.*

[7]   *Ageorges C, Ye L. Resistance welding of thermosetting composite / thermoplastic composite joints. Adv Mater 2006;32.*

[8]   *McKnight SH, Holmes ST, Gillespie JW, Lambing CLT, Marinelli JM. Scaling Issues in Resistance- Welded Thermoplastic Composite Joints. Adv Polym Technol 1997;16:279–95.*

[9]   *Schieler O, Beier U. Induction welding of hybrid thermoplastic-thermoset composite parts. Int J Appl Sci Technol 2016;9:27–36.*

[10]   *Lionetto F, Morillas MN, Pappadà S, Buccoliero G, Villegas IF, Maffezzoli A. A Hybrid welding of carbon-fiber reinforced epoxy based composites. Compos Part A 2018;104:32–40.*

[11]   *Beiss T, Menacher M, Feulner R, Huelder G, Osswald TA. Vibration joining of fiber-reinforced thermosets. Polym Compos 2010;31:1205–12.*

[12]   *Villegas IF, Rubio PV. On avoiding thermal degradation during welding of high-performance thermoplastic composites to thermoset composites. Compos Part A Appl Sci Manuf 2015;77:172–80.*

[13]   *Tsiangou E, Teixeira de Freitas S, Villegas IF, Benedictus R. Investigation on energy director-less ultrasonic welding of polyetherimide (PEI)- to epoxy-based composites. Compos Part B Eng 2019;173.*

[14]   *Tsiangou E, Teixeira de Freitas S, Villegas IF, Benedictus R. Ultrasonic welding of epoxy- to polyetheretherketone- based composites: Investigation on the material of the energy director and the thickness of the coupling layer. J Compos Mater 2020;54:22.*

[15]   *Villegas IF. Ultrasonic Welding of Thermoplastic Composites. Front Mater 2019;6:1–10. doi:10.3389/fmats.2019.00291.*

[16]   *Villegas IF. Strength development versus process data in ultrasonic welding of thermoplastic composites with flat energy directors and its application to the definition of optimum*

93

processing parameters. *Compos Part A Appl Sci Manuf 2014;65:27–37.*

[17]   Hou M, Ye L, Mai Y-W, Yuan Q. Manufacturing and joining of advanced thermoplastic composites. ICCM-13, Beijing, China: 2001.

[18]   Gleich DM, Tooren MJL Van, Beukers A. Analysis and evaluation of bondline thickness effects on failure load in adhesively bonded structures. J Adhes Sci Technol 2001;15:1091–101.

[19]   Her SC. Stress analysis of adhesively-bonded lap joints. Compos Struct 1999;47:673–8.

[20]   Palardy G, Villegas IF. On the effect of flat energy directors thickness on heat generation during ultrasonic welding of thermoplastic composites. Compos Interfaces 2016;24:203–14.

[21]   Camanho PP, Dávila CG, Pinho ST, Iannucci L, Robinson P. Prediction of in situ strengths and matrix cracking in composites under transverse tension and in-plane shear. Compos Part A Appl Sci Manuf 2006;37:165–76

5 On the sensitivity of the ultrasonic welding process of epoxy- to polyetheretherketone (PEEK)- based composites to the welding force and amplitude of vibrations[4]

This chapter addresses the sensitivity of the ultrasonic welding process for joining dissimilar composites to variations in either the welding force or amplitude of vibrations. For that, carbon fibre (CF)/ epoxy specimens were welded to CF/ polyetheretherketone (PEEK) specimens, through a polyetheretherimide, (PEI) coupling layer co-cured with the CF/epoxy material. It was found that reducing either the welding force or the amplitude of vibrations caused an increase in the heating time and maximum temperatures between the coupling layer and CF/epoxy adherend. In addition, local signs of thermal degradation were found in the CF/epoxy adherend even at that resulted in the highest strength. However, such alterations were not significant enough to have an apparent effect on the maximum lap shear strength of the welded joints.

5.1 Introduction

In the last decades the aerospace industry has been showing an increased interest in thermoplastic composites not only due to their appealing properties like fast processing, high damage tolerance, virtually infinite shelf life and chemical resistance but also because they can be welded. Welding can lead to much shorter assembly times as compared to adhesive bonding in which long curing cycles are normally required, and can eliminate the drilling of holes (which is not very composite friendly) as in mechanical fastening [1,2]. Even though welding is primary used for thermoplastic materials, it can also be applied to join thermoset to thermoplastic composites. Thus, it could, for instance, constitute a good alternative to the mechanical fastening process currently used to attach the thousands of carbon fibre (CF)/ polyetheretherketone (PEEK) clips and brackets to the CF/epoxy skin of the Airbus A350 and Boeing 787 aircraft [3].

Thermoset composites can be welded indirectly through a thermoplastic medium. As a common practice, a thermoplastic film, hereafter referred to as coupling layer, is attached on top of the surface of the thermoset composite that needs to be welded. There are several ways to achieve a bond between the coupling layer and the thermoset composite. One is to use a fiber fabric reinforcement partially impregnated with a thermoplastic resin. The rest of the fabric is impregnated with the thermoset resin during the curing process leading to mechanical interlocking as the primary bonding mechanism [4]. Another method is to treat the thermoplastic film with ultraviolet ozone in order to enhance its adhesion with the thermoset composite [5]. Finally, using a thermoplastic film that is partially miscible with the thermoset resin, as in the case of polyetherimide (PEI) and epoxy resins [3,6,7], results in the creation of a gradient interphase, i.e. a gradient transition from one material to the other, during the curing process. This last method is considered a reliable way to bond the thermoplastic coupling layer with the thermoset composite adherend [8].

One of the main challenges when welding advanced thermoset to thermoplastic composites is that in order to melt the thermoplastic matrix high temperatures need to be reached. This could pose a great risk for thermal degradation of the thermoset composite, since those temperatures are generally above its operational temperatures. One way to significantly limit this risk is by generating heat in a very fast manner, to prevent the degradation mechanisms from occurring [5]. Among the well-known thermoplastic composite welding techniques, ultrasonic welding offers the shortest heating times (even less than 500 ms when the adequate parameters are chosen) [9], thus it is an excellent candidate for joining the two dissimilar composites. Ultrasonic welding is a joining process based on the introduction of high-frequency and low-amplitude vibrations transverse to the interface to be welded [10,11]. In order to promote local heat generation an energy director (ED), either resin protrusions moulded on the adherends or a loose neat resin film, is commonly placed at the welding interface [12]. Ultrasonic heat generation is based on surface friction and viscoelastic heating [13,14], which are mainly driven by the static force and by the amplitude of the vibrations applied during the welding process [15]. A combination of high welding force and high amplitude of vibrations leads to short heating times, even below 500 ms, which, as indicated before, is regarded as beneficial when welding thermoset to thermoplastic composites.

The suitability of ultrasonic welding for welding thermoplastic and thermoset composites has been shown in a number of studies. A study by Villegas and van Moorleghem [3] on

ultrasonic welding of CF/epoxy and CF/PEEK adherends through a PEI coupling layer showed a promising average lap shear strength (LSS) of 28.6 ± 2.3 (average ± standard deviation) MPa. Lionetto et al [16] presented a comparison between ultrasonic and induction welding as potential solutions to join CF/epoxy specimens through poly-vynil-butyral coupling layers. That study revealed superior mechanical performance and overall weld quality of the ultrasonically welded specimens. The authors of the present study investigated in [8] the possibility of ultrasonically welding CF/epoxy to CF/ PEI specimens solely through the PEI coupling layer. The conclusion was that an ED is required at the interface to help generate heat locally, without risking excessive bulk heating and thermal degradation in any of the adherends. Moreover, the LSS of welded CF/epoxy to CF/PEI specimens through a PEI film acting as ED plus a 60 µm-thick PEI coupling layer was found to be similar to that of reference co-cured CF/epoxy and CF/PEI composites. In a later study [17], the authors of this study assessed the effects of the material of the ED and the thickness of the PEI coupling layer on ultrasonic welding of CF/epoxy to CF/PEEK adherends. It was shown that, for that specific material combination, a 250 µm-thick PEI coupling layer results in higher LSS than the 60 µm-thick coupling layer. In particular, the LSS of the specimens with a 250 µm-thick layer was comparable to the LSS of reference CF/PEEK welded specimens. Compared to the study in [8] in which a 60 µm-thick PEI coupling layer was sufficient to produce welds with acceptable mechanical performance, the PEEK matrix has a higher melting temperature than the softening temperature of PEI, which increases the risk of thermal degradation of the epoxy resin. Finally Rubio and Villegas showed in their study [5] that using a combination of high welding force and high amplitude of vibrations to join CF/epoxy to CF/PEEK adherends, resulted in short heating times and consequently in absence of thermal degradation in the CF/epoxy adherend. On the contrary, long heating times induced by selecting a low welding force and low amplitude of vibrations caused visible signs of thermal degradation in the CF/epoxy adherend.

All the above-mentioned studies on ultrasonic welding of thermoplastic to thermoset composites were carried out using the highest welding force and amplitude combinations allowed by the ultrasonic welder (i.e. those in which the maximum consumed power did not exceed the limits of the machine) combined with an optimum vibration time, defined as that which lead to maximum weld strength. Studies on the flexibility of the process with regards to variations on any of those three parameters are still scarce. They are however important in order to establish the robustness of the process, especially when considering future industrial applications. In a recent study [18], we investigated the sensitivity of ultrasonic welding of CF/epoxy to CF/PEEK composites to the heating time. It was shown that high-strength welds could be obtained for a relatively wide range of heating times, indicating that ultrasonic welding of dissimilar composites is not as sensitive to the heating time as originally suspected. It is however still unknown whether the process could also allow some flexibility regarding variations on the welding force and the vibrational amplitude.

Therefore, the main focus of the present study is to determine the sensitivity of the ultrasonic welding process of CF/epoxy to CF/PEEK composites to variations in the welding force and the amplitude of vibrations, in particular a decrease from the high values used for both parameters in previous studies. Firstly, the effect of a decrease in either the welding force or the vibration amplitude on the welding process was assessed through i) analyzing the welding output, i.e., dissipated power and displacement of the sonotrode, provided by the welder and ii) measuring the temperature in between the coupling layer and the CF/epoxy material, since the latter is the one at higher risk of thermal degradation. Secondly, the effects

97

of a decrease in the force or the amplitude on (i) the maximum achievable LSS and (ii) in the optimum heating time. The mechanical performance of the welds was assessed through single-lap shear tests and fractographic analysis.

5.2 Experimental procedure

5.2.1 Materials and manufacturing

In this study, Cetex® CF/PEEK (carbon fibre/polyetheretherketone) prepreg with a 5-harness satin fabric reinforcement, manufactured by TenCate Advanced Composites (the Netherlands) was used as the TPC adherend. CF/PEEK prepreg plies arranged in a $[0/90]_{3s}$ stacking sequence were consolidated in a hot-platen press at 385 °C and 1 MPa for 30 min. The thickness of the consolidated laminates was approximately 1.9 mm.

A T800S/3911 unidirectional CF/epoxy prepreg provided by TORAY (Japan) was used as the TSC adherend. Individual plies were manually laid up in a $[0/90]_{2s}$ configuration. A 175 µm-thick PEI film (LITE, Germany) was used as the coupling layer and was co-cured to both outer surfaces of the CF/epoxy laminates. It should be noted that co-curing the 175 µm-thick coupling layer on only one surface of the TSC laminate resulted in post-cure warpage, possibly because of the different thermal expansion coefficient of the CF/epoxy and PEI materials. Prior to its application on the pre-preg stack, the PEI coupling layer was degreased with isopropanol. The CF/epoxy laminate with the PEI films was cured in an autoclave at 180°C and 7 bars for 120 min, according to the specifications of the manufacturer. To ensure smooth surfaces on both sides of the laminate, an aluminium caul plate was used on the side of the vacuum bag. The final thickness of the CF/epoxy/PEI laminate was approximately 2.45 mm. In our previous study [8] we found that an approximately 25 µm-thick gradient epoxy/PEI interphase was formed between these epoxy and PEI materials during the curing process. The gradient interphase consisted of epoxy spheres dispersed in the PEI resin. The diameter of these spheres was smaller closer to the PEI film than in the region with high epoxy resin content. More information on how the interphase was developed and its main features can be found in [8].

CF/PEEK and CF/epoxy/PEI adherends with dimensions 25.4 mm x 106 mm were cut from the laminates using a water-cooled circular diamond saw. The CF/PEEK adherends were cut with their longitudinal direction parallel to the main apparent orientation of the fibres. The CF/epoxy/PEI adherends were cut with their longitudinal direction parallel to the 0° fibres on the outer surfaces of the laminate.

5.2.2 Welding process

Individual specimens were welded with a HiQ DIALOG SpeedControl ultrasonic welder (Herrmann Ultraschal, Germany) using the custom-made clamping jig shown in [17]. The jig comprised two separate clamping systems for the top and bottom adherend and was designed to minimize bending of the top adherend during the welding process. The specimens were welded in a single-lap configuration with a 12.7 mm long and 25.4 mm wide overlap and using a 250 µm-thick PEEK film (provided by Victrex, the Netherlands) as energy director (ED). A rectangular sonotrode with contact surface dimensions 30 x 16 mm

was utilized. Five welding combinations of welding force and peak-to-peak amplitude of vibrations were considered, namely 1200 N/86 µm, 1200 N/70 µm, 1200 N/ 60 µm, 800 N/ 86 µm and 400 N/86 µm. The consolidation force was the same as the welding force for each configuration and the consolidation time was fixed to 4s. Displacement-controlled welding was used, i.e., the vibration time was indirectly controlled by the downward displacement of the sonotrode.

5.2.3 Process characterization

Temperature measurements at the interface between the coupling layer and the CF/epoxy adherend were performed in order to evaluate whether changes in the process parameters affected the way heat was being transferred from the welding interface to the CF/epoxy adherend. For this purpose, K-type thermocouples with 100 µm diameter were placed between the coupling layer and CF/epoxy laminate prior to the co-curing process. After the co-curing process, specimens were cut from the laminate such that they had one thermocouple with its tip located in the middle of the overlap (see Figure 5.1). A data acquisition system built into the ultrasonic welder was used to monitor the temperature at a sampling rate of 1000 Hz. The temperature was measured in at least three specimens per combination of welding force and amplitude.
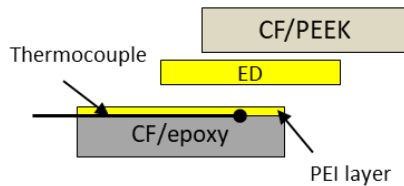
Figure 5.1: Schematic representation of thermocouple location in CF/epoxy adherends.

5.2.4 Mechanical testing and fractography

The mechanical performance of the welded specimens was assessed through single lap shear tests (ASTM D 1002 standard) performed in a Zwick 250 kN universal testing machine. The apparent lap shear strength (LSS) of the joints was calculated as the maximum load measured during testing divided by the overlap area. At least five specimens were welded per combination of welding force and amplitude to determine an average LSS value and its corresponding standard deviation. Naked-eye observation was used for the fractographic analysis of the welded joints after mechanical testing. An optical microscope (Zeiss Axiovert 40) was used for cross-sectional analysis of as-welded specimens.

5.3 Results

5.3.1 Process characterization

Changes in either the welding force or amplitude of the vibrations are expected to have an impact on the welding process and subsequently the welding output. As part of this output, Figure 5.2 shows representative power and displacement curves of specimens that were welded with different amplitude of vibrations and the same welding force (1200 N). As seen in this Figure, the time until the onset of the downward displacement of the sonotrode, i.e. the time until squeeze flow occurs at the welding interface [15], significantly increased with decreasing amplitude. In particular, the time until the displacement onset increased from an average of around 200 ms in the 1200/86 configuration to around 450 ms in the 1200/70 configuration and to around 700 ms in the 1200/60 configuration. Note that the notation F/A refers to a welding process in which the welding force amounted to "F" N and the peak-to-peak amplitude amounted to "A" µm. After its onset, the displacement increased at a slower pace for decreasing amplitude, i.e., lower squeeze-flow rate for decreasing amplitude. Regarding the evolution of the power consumed during the process, the main difference was that the level at which the power stabilized after a first pronounced power peak(s) was lower for decreasing amplitude of vibrations (Figure 5.2).

Figure 5.3 shows representative power and displacement curves of specimens welded with different welding forces and the same amplitude of vibrations (86 µm peak-to-peak). A first observation is that, the initial constant value of the displacement prior to the onset of the squeeze flow dropped below 0 mm when the welding force was lower than 1200 N. In particular, the initial displacement was around -0.08 mm in the 400/86 configuration; and between -0.02 mm and -0.04 mm in the 800/86 configuration. The time until the onset of the squeeze flow was similar in the 1200/86 and 800/86 configurations, whilst in the 400/86 configuration it was approximately 100 ms longer. After this onset, the displacement generally increased at a slower pace with decreasing force. Regarding the power consumed during the welding process, there was no clear trend on the effect of decreasing welding force on that particular output.

The evolution of the temperature at the interface between the PEI coupling layer and the CF/epoxy adherend in configurations welded with different amplitude of vibrations is shown in Figure 5.4. Generally, the temperature increased at a similar rate in the 1200/86 and 1200/70 configurations. In the 1200/60 configuration the temperature increased generally at a slower pace than the other two configurations. The maximum average temperatures reached when welding were 203 ± 4 °C, 274 ± 18 °C and 338 ± 24 °C in the 1200/86, 1200/70 and 1200/60 configurations, respectively. It should be noted that these measurements were obtained when welding up to 0.28 mm displacement, which as shown in the next subsection, is beyond the` displacement that resulted in the maximum LSS (i.e., LSS_{max}) for all configurations but it is nevertheless the displacement value that resulted in the most significant differences in LSS.

Figure 5.5 illustrates the temperature evolution at the interface between the PEI coupling layer and the CF/epoxy adherend in configurations welded with different welding forces. In the 1200/86 and 400/86 configurations the temperature increased at a similar pace. However, the temperature in the 800/86 configuration increased significantly faster. The maximum temperatures reached were 203 ± 4 °C, 339 ± 27 °C and 254 ± 19 °C for the 1200/86, 800/86

and 400/86 configurations, respectively. Please note that these maximum values were obtained when welding up to 0.28 mm displacement (1200/86 and 800/86 configurations) and 0.18 mm displacement (400/86 configuration), which as shown in the next subsection are the values beyond d_{max} that resulted in the most significant differences in LSS.
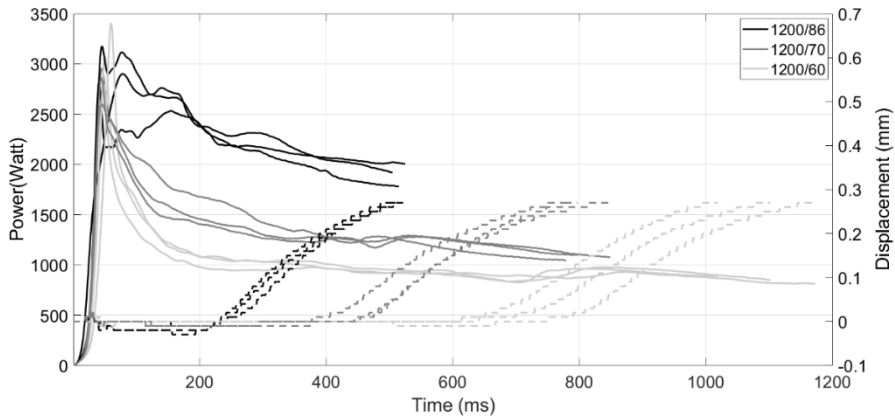
Figure 5.2: Representative power (solid lines) and displacement (dashed lines) curves of the 1200/86, 1200/70 and 1200/60 configurations (3 welded specimens per configuration). All specimens were welded up to 0.28 mm displacement, which coincides with the end of the processing interval defined in [18].
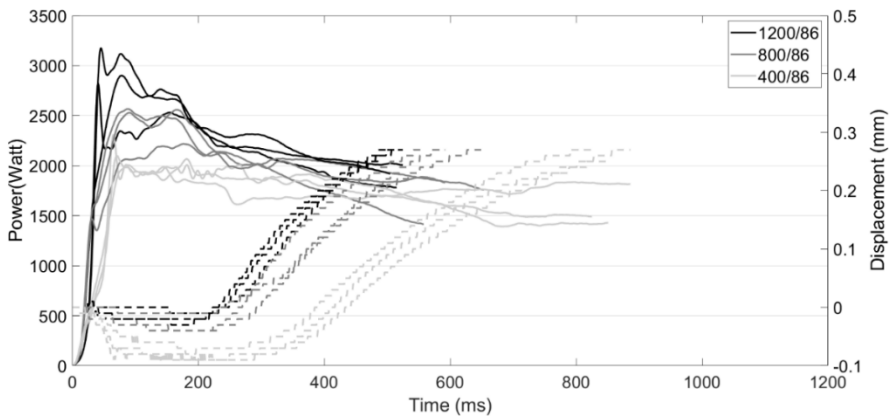
Figure 5.3: Representative power (solid lines) and displacement (dashed lines) curves of the 1200/86, 800/86 and 400/86 configurations (3 welded specimens per configuration). All specimens were welded up to 0.28 mm displacement, which coincides with the end of the processing interval defined in [18].
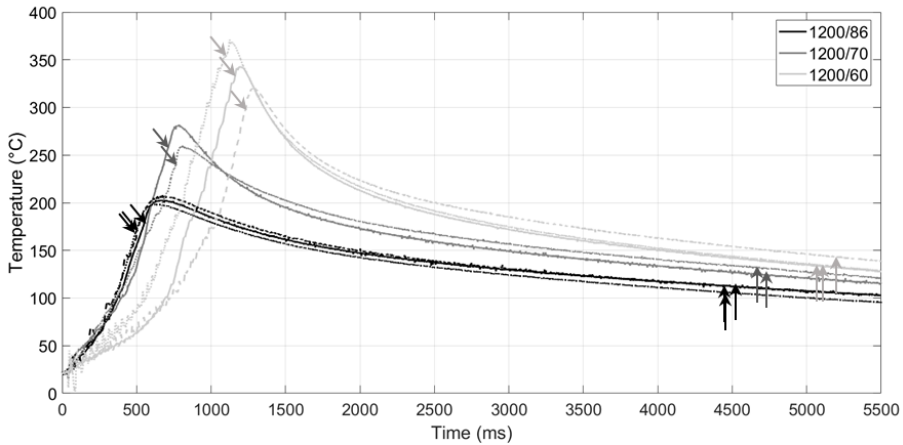
Figure 5.4: Effect of decreasing amplitude on temperature at the interface between PEI coupling layer and CF/epoxy adherend (three welding specimens per configuration, up to 0.28mm in all cases). Diagonal arrows indicate the end of the vibration. Vertical arrows indicate the end of the welding process (i.e., 4000 ms-long consolidation after the end of the vibration).
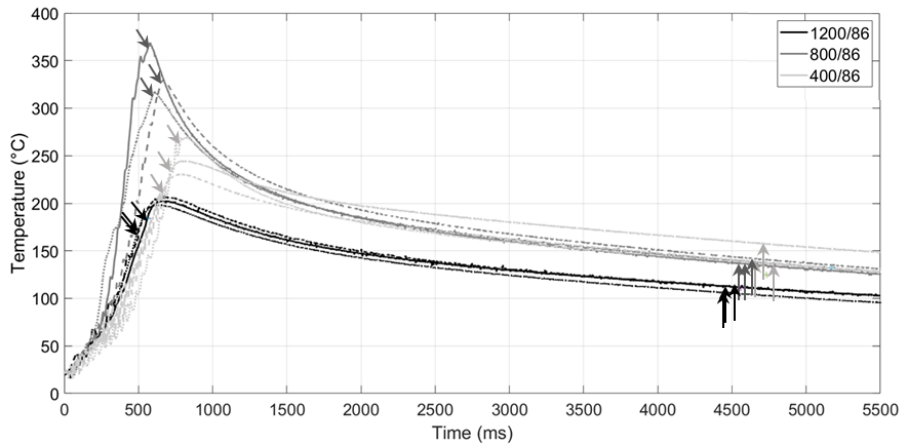
Figure 5.5: Effect of decreasing force on temperature evolution at the interface between the PEI coupling layer and CF/epoxy adherend (three welding specimens per configuration, up to 0.28mm displacement in the 1200/86 and 800/86 cases, up to 0.18 mm in the 400/86 case). Diagonal arrows indicate the end of the vibration. Vertical arrows indicate the end of the welding process (i.e., 4000 ms-long consolidation after the end of the vibration).

5.3.2 Mechanical performance

The effect of changing the amplitude of vibrations on the average LSS can be seen in Figure 5.6, which represents LSS data for different sonotrode displacement values in the 1200/86, 1200/70 and 1200/60 configurations. Note that in our previous study [18], these displacement values were considered to be within the processing window for welding same type of adherends as in the current study and according to the 1200/86 configuration. As shown in this Figure, the LSS values for all three configurations were practically overlapped for displacement values up to 0.26mm. The maximum average LSS values were achieved in all configurations at 0.24 mm and 0.26mm (referred to as d_{max}). The corresponding maximum average LSS values can be found in Table 5.1. After 0.26mm the LSS drop was much more pronounced for the 1200/70 and 1200/60 configurations than for the 1200N/86 configuration.

Figure 5.7 shows the LSS evolution versus the displacement of the sonotrode for configurations welded with different welding forces. As seen in this Figure, decreasing welding forces shifted the process towards lower displacement values. This shift was particularly significant in the 400/86 configuration. Consequently, the maximum LSS was obtained at 0.24mm and 0.26mm displacements in the 1200/86 configuration, at displacements between 0.22-0.26 mm in the 800/86 configuration and at 0.16mm in the 400/86 configuration. The corresponding maximum average LSS values can be found in Table 5.1. In both the 800/86 and the 400/86 configurations the LSS drop after the maximum (at 0.28 mm displacement for 800/86 and at 0.18 mm displacement for 400/86) was more pronounced than in the 1200/86 configuration.
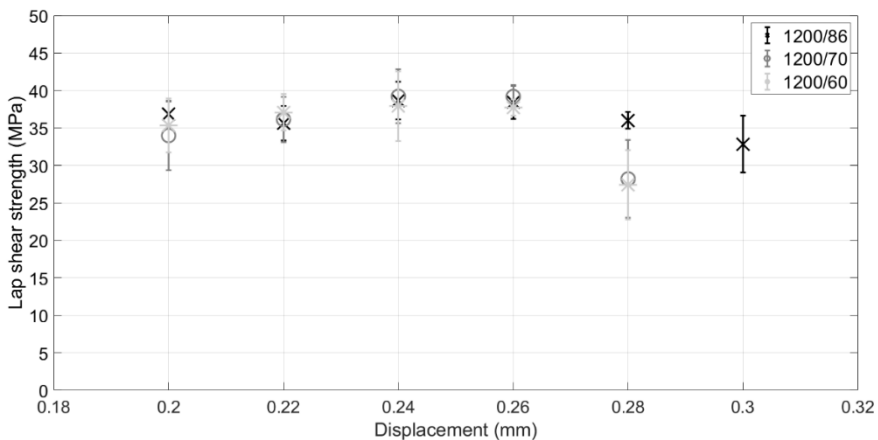
Figure 5.6: Evolution of the LSS versus displacement of the sonotrode in 1200/86, 1200/70 and 1200/60 configurations.
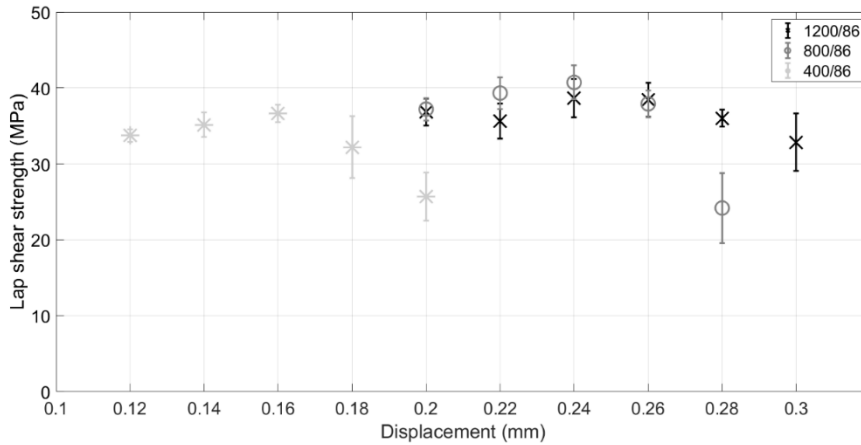
Figure 5.7: Evolution of the LSS versus displacement of the sonotrode in the 1200/86, 800/86 and 400/86 configurations.

Table 5.1 shows the heating times corresponding to the displacement values for maximum LSS (see Figures 5.6 and 5.7) as provided by the ultrasonic welder. Decreasing the amplitude while keeping the welding force constant significantly increased the vibration time needed to reach the maximum LSS, namely around 50% time increase by decreasing the amplitude from 86 to 70µm and a further 40-50% time increase by further decreasing the amplitude from 70 to 60µm. Decreasing the welding force while keeping the amplitude constant resulted in a moderate increase of the vibration time, namely less than 10% time increase by decreasing the welding force from 1200 to 800N and an additional 20% time increase by further decreasing the welding force from 800 to 400N.

Table 5.1: Displacement values resulting in maximum LSS, (d_{max}), maximum average LSS (LSS_{max}) and corresponding heating times (t_{max}) in each configuration.

Configuration	d_{max} (mm)	LSS_{max} (average $\pm$ stdv, MPa)	t_{max} (average $\pm$ stdv, ms)
1200/86	0.24, 0.26	38.7 ± 2.2	$467 \pm 57, 494 \pm 57$
1200/70	0.24, 0.26	39.2 ± 3.6	$717 \pm 37, 754 \pm 30$
1200/60	0.24, 0.26	37.9 ± 4.6	$1053 \pm 45, 1080 \pm 47$
800/86	0.24.	40.2 ± 2	507 ± 28
400/86	0.16	36.6 ± 1.2	604 ± 16

5.3.3 Fractography

Figure 5.8 presents fracture surfaces of 1200/86 specimens welded at different displacement values. For all the displacement values considered in this study, the predominant type of failure was first-ply failure in the CF/PEEK adherend. At 0.24mm the specimens presented unwelded areas covering around 6% of the overlap. Above 0.26 mm, failure also occurred in the CF/epoxy adherend as seen in Figure 5.8. Decreasing the amplitude while keeping the welding force at 1200 N (Figure 5.9) also resulted in unwelded areas at 0.24 mm (around 3% and 10% of the overlap in the 1200/70 and 1200/60 configurations, respectively). More importantly, decreasing the amplitude resulted in local failure in the CF/epoxy adherend even at the d_{max} values, i.e., 0.24 and 0.26 mm. Further increasing the displacement to 0.28 mm shifted the predominant failure locus to the CF/epoxy adherend.

When the welding force was decreased to 800 and 400 N (Figure 5.10) unwelded areas could not be found at the d_{max} value but porosity was visible at the edges of the overlap. This porosity seemed to increase with decreasing welding force. In the 800/86 configuration, specimens welded at the d_{max} (0.24 mm) featured a combination of first-ply failure in the CF/PEEK and in the CF/epoxy adherend. In the 400/86 configuration, specimens welded at the d_{max} (0.16 mm) featured first-ply failure in the CF/PEEK adherend as well as matrix failure (predominantly at the edges of the overlap). Increasing the displacement to 0.28 mm and to 0.18 mm in the 800/86 and 400/86 configurations, respectively, resulted in predominant failure in the CF/epoxy adherend.
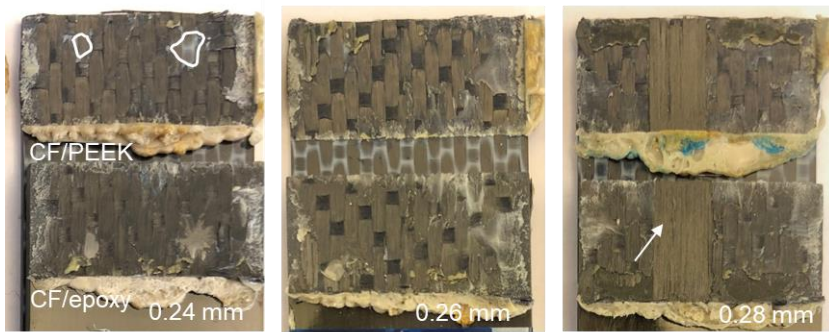
Figure 5.8: Representative matching fracture surfaces of 1200/86 specimens welded at different displacement values. The 0.24 mm and 0.26 mm displacements correspond to the maximum weld strength. The highlighted areas indicate unwelded areas. The arrows point at failure in the CF/epoxy adherend.
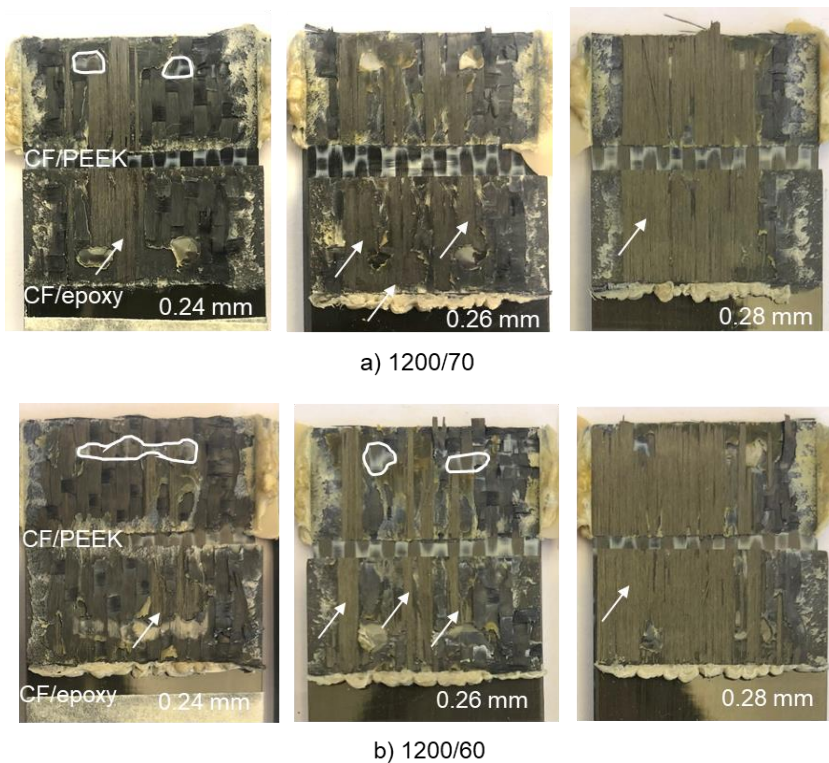
Figure 5.9: Representative matching fracture surfaces of a) 1200/70 specimens and b) 1200/ 60 specimens, welded at different displacement values. The 0.24 mm and 0.26 mm displacements correspond to the maximum weld strength. The highlighted areas indicate unwelded areas. The arrows point at failure in the CF/epoxy adherend.
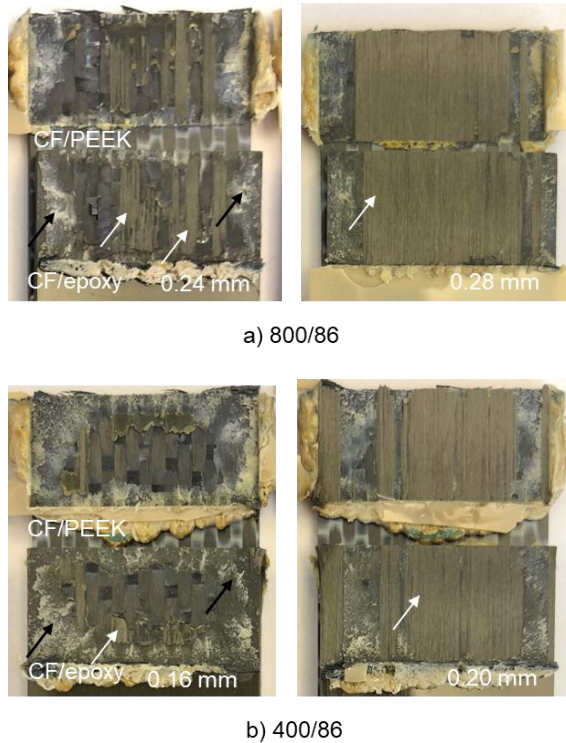
a) 800/86

b) 400/86

Figure 5.10: Representative matching fracture surfaces of a) 800/86 specimens and b) 400/86 specimens welded at different displacement values. The 0.24 mm in a) and 0.16 mm in b) correspond to the maximum weld strength. The white arrows point at failure in the CF/epoxy adherend. The black arrows point at the areas with porosity.

5.3.4 Cross-sectional analysis

Figure 5.11 shows cross-sectional micrographs from approximately the centre of the overlap of specimens corresponding to each force/amplitude configuration. In all cases the specimens were welded at a displacement value that resulted in maximum LSS. The thickness of the resin-rich weld line between the two composite adherends was approximately 100 µm in all cases, hence lower than the initial thickness of both the PEEK ED (250 µm) and of the PEI coupling layer (175 µm), individually. Moreover, in all cases, the weld line was composed of two distinct bands of roughly comparable thicknesses displaying different shades of grey. The dark grey band was identified as PEI whilst the light grey band was identified as PEEK.

a) 1200/86

b) 1200/70

c) 1200/60

d) 800/86

e) 400/86
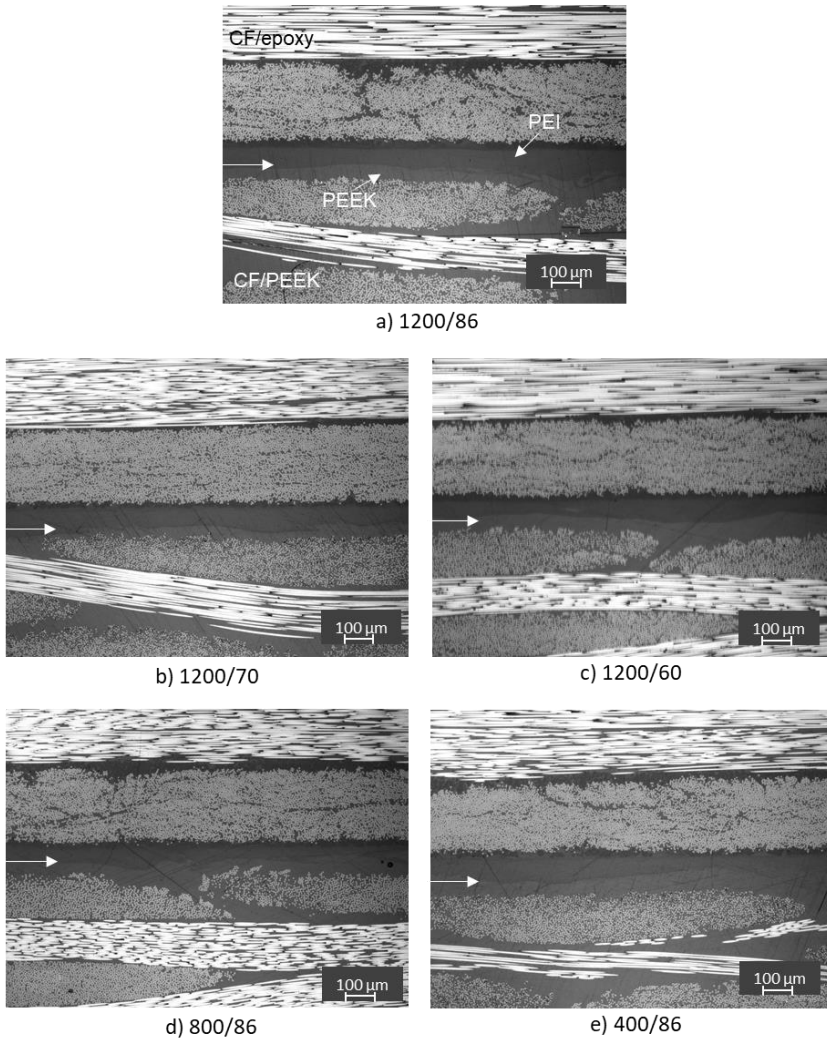
Figure 5.11: Cross-sectional micrographs of representative specimens welded in different force/amplitude configurations and at the displacement value that resulted in maximum LSS: a) 1200/86 (0.24 mm, b) 1200/70 (0.24 mm) c) 1200/60 (0.24 mm), d) 800/86 (0.24 mm) and e) 400/86 (0.16 mm). Arrows indicate the resin-rich weld line between the two composite materials.

5.4 Discussion

In previous works we looked into ultrasonic welding of CF/PEEK and CF/epoxy composites through a PEI coupling layer at high welding force and high amplitude values [3,5,8,18]. This procedure was based on the hypothesis that the welding process needs to be as fast as possible (accomplished by using high force and high amplitude) to prevent the occurrence of thermal degradation in the CF/epoxy adherend. This would occur through a twofold mechanism: i) short welding times can limit the amount of heat transferred to the CF/epoxy

adherend across the coupling layer; and ii) short welding times would not allow for thermal degradation reactions to occur even when the material is exposed to high temperatures. In our previous study [18] we showed that, for a combination of high force and high amplitude, the process offers some flexibility in terms of heating time, with a processing interval of around 170 ms width. The question posed in the present paper is whether the process also offers some flexibility in terms of variations (i.e., decrease) of either the welding force or the amplitude.

5.4.1 Welding force variations (welding at d_{max})

Decreasing the welding force from 1200N to 800N at a high vibration amplitude (86 µm) did not cause any significant change in the heating time corresponding to d_{max} (between 450 and 500 ms, see Table 5.1). It did not significantly affect the maximum achievable LSS (around 39 MPa) either (see ANOVA results in Table 5.2), but it did cause changes in the way the welds failed: from first-ply failure exclusively in the CF/PEEK adherend to also local first-ply failure in the CF/epoxy adherend (Figure 5.8). Firstly, the insensitivity of the heating time to the change in the welding force was surprising considering prior research [12] in which the effect of the welding force on the heating time was found to be very significant. That was mostly attributed to the effect of the welding force on the contact at microscopic level between ED and adherends and hence on friction between the two. In the particular configuration studied in the present paper, however, the higher compliance of the ED-coupling layer interface could result in a significantly lower effect of the force in the heating time. Secondly, local failure in the CF/epoxy adherend, which is considered as a sign of thermal degradation [18], is consistent with the higher temperatures registered at the interface between the coupling layer and the CF/epoxy adherend in the 800/86 configuration. Indeed, by superimposing the heating times corresponding to d_{max} (Table 5.1) to the temperature graphs in Figure 5.5, one can see that the temperature in the 800/86 configuration could be expected to reach around 280°C at the d_{max}, while it would be significantly lower, around 150°C, in the 1200/86 configuration. Nevertheless, the occurrence of thermal degradation in these specimens was apparently small enough to not have a measurable impact on the maximum achievable LSS.

Table 5.2: ANOVA of maximum LSS values relative to the 1200/86 configuration

Configuration	Results
1200/70	$F(1,12)= 0.11$, $p= 0.7$
1200/60	$F(1,15)= 0.21$, $p= 0.7$
800/86	$F(1,14)= 1.77$, $p= 0.2$
400/86	$F(1,12)= 3.64$, $p= 0.08$

A further decrease in the welding force to 400 N caused the heating time corresponding to d_{max} to increase from 450-500 ms to approximately 600 ms (see Table 5.1). It also caused

the maximum achievable LSS to decrease to values around 36.5 MPa. According to the results of our statistical analysis (see Table 5.2), this LSS value was however not significantly different from that obtained in the 1200/86 configuration. Fracture surfaces (Figure 5.10) showed that lowering the welding force to 400N increased the occurrence of matrix failure linked to porosity at the edges of the overlap, whilst first-ply failure in the CF/PEEK adherend, and occasionally in the CF/epoxy adherend, remained the main sources of failure in the centre of the overlap. Porosity at the edges of the overlap seemed to be linked to the combination of high temperature (higher than in the 1200/86 configuration, see Figure 5.5) and low pressure but its exact source is yet unknown to us.

It is interesting to note that decreasing the welding force did not show a consistent trend on the temperatures measured at the interface between the coupling layer and the CF/epoxy adhered (Figure 5.5). On one hand, decreasing the force from 1200 N to 800 N caused an increase in the maximum temperature (both at the d_{max} as well as the displacement used in Figure 5.5). On the other hand, further decreasing the force from 800 N to 400 N caused a decrease in the maximum temperature. Two could be the reasons for this apparently inconsistent behavior. Firstly, changing from 1200 N to 800 N welding force did not seem to affect the time until onset of squeeze flow at the welding interface but it did affect the squeeze flow rate (Figure 5.3). Note that in this particular study, both the energy director and the coupling layer experienced squeeze flow, as evidenced by the cross-section micrographs in Figure 5.11. We hence believe that heat generation rates were similar in both cases, as also evidenced by the fact that the temperature curves were overlapping until approximately 250 ms into the welding process (Figure 5.5), which roughly corresponds with the time at which onset of squeeze flow occurred (Figure 5.3). However, slower squeeze flow of the molten polymer at the welding interface led to higher temperature increase after the onset at 800 N welding force. Secondly, at 400N welding force a longer time was needed for squeeze flow to occur (Figure 5.3), which indicates slower heat generation. This might be related to increased hammering causing less efficient amplitude transmission to the welding interface(s) and hence less efficient heating during the initial stages of the welding process [19]. It should be noted that the hammering phenomenon is known to be more pronounced when the welding force is low [14], which would explain why it could have been more apparent at 400N than at 800N welding force. Less efficient heating could hence be the cause of the decrease in maximum temperatures observed when decreasing the welding force from 800 N to 400 N.

5.4.2 Amplitude variations (welding at d_{max})

Reducing the amplitude of vibration from 86 µm to 70 µm and further down to 60 µm while maintaining a high welding force (1200N) did cause a significant increase in the heating time corresponding to d_{max}: roughly a 50% increase in every step (see Table 5.1). It should be noted that the effect of decreasing the amplitude did have a much more pronounced effect on the heating time than decreasing the welding force. However, the maximum achievable LSS did not seem to be significantly affected by the changes in amplitude either (Table 5.2). As already observed when decreasing the welding force, decreasing the amplitude did cause increased local first-ply failure in the CF/epoxy composite. Similarly, the changes in failure were consistent with a gradual increase of the maximum temperature at the interface between the coupling layer and the CF/epoxy adherend: from 150°C to 200°C and then on to 300°C

at the d_{max} (Table 5.1 and Figure 5.4). The fact that, despite the significantly longer heating times, the effect of lowering the amplitude did not differ much from that of lowering the welding force could be attributed to the decrease in viscoelastic heating rate resulting from decreased amplitude. Indeed, viscoelastic heat generation is proportional to the cyclic strain, or in other words the amplitude, squared [15]. This slower heat generation was evident from the observation that reducing the amplitude mostly affected (increased) the time until the onset of squeeze flow (Figure 5.2).

5.4.3 LSS versus displacement

When looking at the sensitivity of the welding process to variations in the controlling parameter, i.e., displacement of the sonotrode, in the different force and amplitude combinations investigated in this study (Figure 5.6 and Figure 5.7), there are two main apparent effects. Firstly, decreasing the force or the amplitude caused a more severe drop of the LSS beyond the d_{max} values. This is linked to the prevalent occurrence of CF/epoxy failure in those instances (Figure 5.9 and Figure 5.10). Secondly, decreasing the welding force seemed to have a more pronounced effect on the LSS versus displacement curves, by shifting the curves to lower displacement values. However, that shift can be directly linked to the decrease in the initial constant value of the displacement caused by the lowering of the force (Figure 5.3). The fact that the weld line thickness was similar in all cases (see Figure 5.11) also supports the previous statement. The changes in the initial constant displacement values are likely related to a more notorious effect of thermal expansion of the welding stack when the welding force is low.

5.5 Conclusion

The present study focused on assessing the sensitivity of ultrasonic welding of CF/epoxy to CF/PEEK composites to decreasing either the welding force or the amplitude of vibrations. The reference case featured a high force and high amplitude combination, 1200 N and 86 µm, as used in previous research [18]. Within this study, the welding force was decreased to 800 N and to 400 N while keeping the amplitude at the reference high level, 86 µm. Likewise, the amplitude was decreased to 70 µm and 60 µm while keeping the force at the reference high level, 1200 N. The effect of those changes on the welding process as well as on the quality of the welded joints was evaluated experimentally.

As expected, decreasing the welding force or the amplitude generally caused an increase of the heating times required to obtain maximum weld strength, which was attributed to a decrease in the heat generation rates. Additionally, the temperature to which the CF/epoxy material was exposed during welding increased with decreasing force or amplitude. This temperature increase resulted in partial shift of the locus of failure from the CF/PEEK to the CF/epoxy adherend, interpreted as a sign of thermal degradation in the latter, even in welding conditions resulting in highest weld strength in each force/amplitude combination. The maximum achievable lap shear strength was however insensitive to the above-mentioned changes. Nevertheless, faster degradation of the weld strength for heating times beyond the

the ones corresponding to d_{max} was found in all the cases with lower force or amplitude than the reference case.

5.6   References

[1]   Ageorges C, Ye L, Hou M. Advances in fusion boding techniques for joining thermoplastics materials composites: a review. Compos Part A Appl Sci Manuf 2001;32:839–57.

[2]   da Costa AP, Botelho EC, Costa ML, Narita NE, Tarpani JR. A review of welding technologies for thermoplastic composites in aerospace applications. J Aerosp Technol Manag 2012;4:255–65.

[3]   Villegas IF, van Moorleghem R. Ultrasonic welding of carbon/epoxy and carbon/PEEK composites through a PEI thermoplastic coupling layer. Compos Part A Appl Sci Manuf 2018;109:75–83.

[4]   Jacaruso GJ, Davis GC, Mclntire AJ. Bonding of Thermoset Composite Structures, 1994.

[5]   Villegas IF, Rubio PV. On avoiding thermal degradation during welding of high-performance thermoplastic composites to thermoset composites. Compos Part A Appl Sci Manuf 2015;77:172–80.

[6]   Lestriez B, Chapel J-P, Gérard J-F. Gradient interphase between reactive epoxy and glassy thermoplastic from dissolution process, reaction kinetics, and phase separation thermodynamics. Macromolecules 2001;34:1204–13.

[7]   Deng S, Djukic L, Paton R, Ye L. Thermoplastic-epoxy interactions and their potential applications in joining composite structures - A review. Compos Part A Appl Sci Manuf 2015;68:121–32.

[8]   Tsiangou E, Teixeira de Freitas S, Villegas IF, Benedictus R. Investigation on energy director-less ultrasonic welding of polyetherimide (PEI)- to epoxy-based composites. Compos Part B Eng 2019;173.

[9]   Villegas IF, Moser L, Yousefpour A, Mitschang P, Bersee HEN. Process and performance evaluation of ultrasonic , induction and resistance welding of advanced thermoplastic composites. J Thermoplast Compos Mater 2012;26:1007–24. doi:10.1177/0892705712456031.

[10]   Benatar A, Eswaran R V, Nayar SK. Ultrasonic welding of thermoplastics in the near-field. Polym Eng Sci 1989;29:1689–98. doi:10.1002/pen.760292311.

[11]   Villegas IF. Ultrasonic Welding of Thermoplastic Composites. Front Mater 2019;6:1–10. doi:10.3389/fmats.2019.00291.

[12]   Villegas IF, Valle Grande B, Bersee HEN, Benedictus R. A comparative evaluation between flat and traditional energy directors for ultrasonic welding of CF/PPS thermoplastic composites. Compos Interfaces 2015;22:717–29. doi:10.1080/09276440.2015.1053753.

[13]   Zhang Z, Wang X, Luo Y, Zhang Z, Wang L. Study on heating process of ultrasonic welding for thermoplastics. J Thermoplast Compos Mater 2010;23:647–64.

[14]   Levy A, Le Corre S, Villegas IF. Modeling of the heating phenomena in ultrasonic welding of thermoplastic composites with flat energy directors. J Mater Process Technol 2014;214:1361–71. doi:10.1016/j.jmatprotec.2014.02.009.

[15]   Villegas IF. In situ monitoring of ultrasonic welding of thermoplastic composites through power and displacement data. J Thermoplast Compos Mater 2015;28:66–85.

[16]   Lionetto F, Morillas MN, Pappadà S, Buccoliero G, Villegas IF, Maffezzoli A. A Hybrid welding of carbon-fiber reinforced epoxy based composites. Compos Part A 2018;104:32–40.

[17]   Tsiangou E, Teixeira de Freitas S, Villegas IF, Benedictus R. Ultrasonic welding of epoxy- to polyetheretherketone- based composites: Investigation on the material of the energy director and the thickness of the coupling layer. J Compos Mater 2020;54:22.

[18]   Tsiangou E, Kupski J, Teixeira de Freitas S, Villegas IF, Benedictus R. On the sensitivity of ultrasonic welding of epoxy- to polyetheretherketone (PEEK)-based composites to the heating time. Compos Part A Appl Sci Manuf 2021;144.

[19]   Palardy G, Shi H, Levy A, Le Corre S, Fernandez Villegas I. A study on amplitude transmission in ultrasonic welding of thermoplastic composites. Compos Part A Appl Sci Manuf 2018;113:339–49. doi:10.1016/j.compositesa.2018.07.033.

6 Conclusions and recommendations

This chapter summarizes the main conclusions that were drawn on ultrasonic welding of epoxy- to thermoplastic based composites, which provided answers to the research questions throughout Chapters 2-5. Based upon these findings, recommendations for future studies are provided, in order to further understand such process and facilitate its industrial application.

6.1 Objective of this research

As indicated in Chapter 1, the objective of the current work was to gain further understanding on the ultrasonic welding of thermoset to thermoplastic composites and identify some of the potentialities and limitations of such process. Firstly, well-suited techniques for the production of ultrasonically welded thermoset- to thermoplastic based composites were defined. Secondly, the robustness of such process was assessed with respect to its sensitivity to process parameters. To achieve the abovementioned objectives the following research questions were proposed:

1. How are the ultrasonic welding process and weld mechanical performance affected when welding dissimilar composites solely through the coupling layer i.e., without an energy director?
2. How does the nature of the material of the energy director (i.e., PEI or PEEK) affect the ultrasonic welding process and mechanical performance of the dissimilar composite welds?
3. What are the limitations regarding the thickness of the coupling layer for the production of high-strength dissimilar composite welds?
4. How sensitive is the weld quality to changes in the duration of the vibration phase?
5. How sensitive is the ultrasonic welding process and mechanical performance of the welds to changes in the welding force and amplitude of vibrations?

A number of investigations were performed in order to address the abovementioned questions. The work in this thesis was mostly experimental, including ultrasonic welding, mechanical testing through single-lap shear testing and microscopic analysis via means of naked eye, optical microscopy and scanning electron microscopy. A finite element model was also developed and presented in Chapter 4. This model was used to assess the effect of the weld line thickness on the peak peel stresses developed during mechanical testing.

To conclude the present thesis, this chapter aims at addressing each of these research questions. The first three questions will be addressed in Section 6.2. The next two questions will be addressed in Section 6.3. The final conclusions of this thesis will be presented in Section 6.4. Finally, this chapter is concluded by addressing the current challenges of ultrasonic welding of dissimilar composite materials and recommending some solutions and topics for further research.

6.2 Manufacturing of dissimilar composite welded joints

Welding approaches were defined in order to weld T800S/3911 CF/epoxy to CF/polyetherimide (PEI) (Chapter 2) or CF/ polyetheretherketone (PEEK) (Chapter 3) adherends and achieve welded joints with comparable lap shear strength to co-cured dissimilar composites (CF/epoxy- CF/PEI) or reference welded thermoplastic composites (CF/ PEEK-CF/PEEK). An attempt to weld through solely the PEI coupling layer was presented in **Chapter 2**. It was found that welding through solely the coupling layer, (either a 60 µm- or 250 µm-thick one), resulted in high scatter in the achieved LSS and inconsistent fracture surfaces as well as overheating of the CF/PEI adherend and/or the PEI coupling layer. The high scatter is probably caused by a less compliant coupling layer as compared to

an ED, thus high variations in the immediate contact areas, i.e., initial hot areas. Overheating was probably caused by lower effectiveness of heat generation by the coupling layer (especially frictional heating owing to only one free surface). Ultimately, overheating had a negative effect on the lap shear strength (LSS) of the welded joints, since samples welded through solely the coupling layer yielded lower LSS than samples welded through an additional loose PEI ED (together with a 60 μm-thick coupling layer). In particular, welding through an additional loose ED resulted in a LSS similar to reference co-cured joints, thus this approach was adopted for the remaining of this thesis.

From **Chapter 3** onwards, the material of the thermoplastic composite adherend was changed to CF/ polyetheretherketone (PEEK) due to its usage in current applications in the aerospace industries. However, a PEEK film was not a preferable choice as the coupling layer material, due to its lack of compatibility with the epoxy resin, as demonstrated in [1]. Thus, PEI films were still used as the coupling layer, since they are also compatible with the PEEK resin. The first part of Chapter 3 comprised an investigation on the most suitable material for the ED; PEI as in the coupling layer or PEEK as in the matrix of the thermoplastic composite. The nature of the material of the ED affected the welding process in such way that when a PEI ED was used, it flowed at a faster pace than a PEEK ED. Such behaviour was attributed to the lower viscosity of the PEI resin than the PEEK resin, according to the results of the rheological analysis. Measurements of the loss moduli of these two resins across temperatures between room temperature and beyond the softening point or melting temperature of the PEI and PEEK resin, respectively, revealed different trends, such as loss modulus peaks at different temperatures (which was expected due to the different T_g of the two resins) and relative differences in the loss moduli with increasing temperature. Differences in the loss moduli were expected to impact the way heat was generated in the EDs. However, temperature measurements in the weld interface could not verify if that was the case, due to high scatter, potentially due to the thermocouple moving along the welding interface. Despite these differences in the viscoelastic and rheological properties of the two resins, using either of these materials as an ED resulted in a similar average LSS and failure mechanisms. The factor that was actually found to have a more significant effect on the welded joints was the thickness of the coupling layer.

In **Chapter 2**, a 60 μm-thick coupling layer (when combined with the use of an ED) provided satisfactory results when welding CF/epoxy to CF/PEI samples. However, when attempting to weld the former to a CF/PEEK adherend through such relatively thin coupling layer, apparent thermal damage was found in the CF/epoxy adherend (i.e., a shift in the failure locus from failure in the CF/PEEK adherend to failure also in the CF/epoxy adherend) before fully welded overlaps could be obtained. This is attributed to the higher melting temperature of PEEK, as compared to the softening point of PEI, welding of CF/epoxy to CF/PEEK adherends increased the sensitivity of the process to the thickness of the coupling layer. By increasing the coupling layer thickness to 250 μm, fully welded overlaps could be obtained, with the welded joints failing predominantly in the CF/PEEK adherend, i.e., with virtually no damage in the CF/epoxy material. As a result, such increase in the thickness of the coupling layer resulted in a 17% higher average LSS than the highest average LSS that could be obtained with a 60 μm-thick coupling layer. Comparison of these dissimilar composite welded joints (i.e., welded through a 250 μm-thick coupling layer) with CF/PEEK to CF/PEEK welded joints revealed comparable LSS to the reference configurations, demonstrating the promising potential of ultrasonic welding of dissimilar composites.

6.3 Robustness of the ultrasonic welding of dissimilar composites

Once suitable methods to successfully join dissimilar composites via ultrasonic welding were defined, it was important to investigate the robustness of such process. As a first step, the sensitivity of the process to the heating time (or duration of the vibration phase) was assessed in **Chapter 4**. The hypothesis was that, due to the sensitivity of the thermoset composite adherend to the high welding temperatures, the ultrasonic welding process would be demanding of the shortest heating times possible. Note that the heating time was indirectly controlled by the vertical displacement of the sonotrode. Based on the findings in **Chapter 3**, CF/epoxy samples were welded to CF/PEEK samples through a 250 µm-thick PEI coupling layer and a PEEK ED. A combination of high welding force and high amplitude of vibrations was selected in order to ensure very fast heat generation. Processing intervals were defined to include those displacement values that resulted in an average LSS higher than 90% of the maximum achieved LSS. Then, the processing interval of the dissimilar welded joints was compared to that of reference, CF/PEEK to CF/PEEK welded joints.

It was found that a relatively wide processing interval could actually be obtained for dissimilar welds provided with a 250 µm-thick coupling layer. When defined in terms of displacement of the sonotrode, i.e., the controlling parameter, the processing interval of the dissimilar joints was as wide as the processing interval of the reference CF/PEEK to CF/PEEK joints. However, translating the displacement values into average heating times revealed that longer heating times could be withstood by the CF/PEEK joints, as expected from the higher sensitivity of the epoxy resin to thermal degradation.

The major physical phenomena that were identified as the factors that influenced the mechanical performance of the joints welded at different heating times were as following; below the lower limit in the processing interval of the dissimilar welded joints, significant unwelded areas could be found within the welding overlap. Within the processing interval, fully-welded overlaps were obtained which upon mechanical testing failed mostly in the CF/PEEK adherend. Beyond the upper limit of the processing overlap: (i) failure shifted to the CF/epoxy adherend, signifying occurrence of thermal degradation; (ii) the joints featured very thin weld lines (thickness below 50 µm) which could have caused increased peel stresses; (iii) the morphology of the epoxy-PEI gradient interphase was significantly altered which indicates softening of the entire PEI layer, thus an increased risk of thermal degradation of the CF/epoxy adherend.

Since a relatively wide processing interval could be obtained when the dissimilar composite welds were provided with a 250 µm-thick coupling layer, it was interesting to assess the sensitivity of the width of the processing interval to decreasing the thickness of the coupling layer. Decreasing the thickness of the coupling layer from 250 µm to 175 µm did not affect the LSS values, nor the limits of the processing interval, both in terms of displacement of the sonotrode and average heating times. A further reduction in the coupling layer thickness to 60 µm resulted in a decrease of the maximum achievable LSS values as well as the occurrence of thermal degradation even before fully welded overlaps could be obtained, which was in line with the findings in Chapter 3. Nevertheless, provided that the coupling layer has a sufficient thickness (a minimum of 175 µm out of the considered thicknesses in

this thesis), it can be concluded that ultrasonic welding of dissimilar materials does not seem to be as demanding of the shortest heating times as originally assumed.

Based on the findings in **Chapter 4**, the selection of a combination of high force and high amplitude of vibrations (to keep the heating time as short as possible) that was adopted in previous studies on ultrasonic welding of dissimilar composites might have been a conservative one. Thus, the next question posed was whether the process also offers some flexibility in terms of variations, in particular decrease, of either the welding force or the amplitude of vibrations, which would increase its robustness. To investigate this, five configurations were considered, namely the reference 1200/86 (welding force in N/ peak-to-peak amplitude of vibrations in µm), i.e., the combination that was used in **Chapter 5**, 1200/70, 1200/60, 800/86 and 400/86.

Decreasing the welding force to 800 N while keeping the amplitude of vibrations constant (86 µm) did not have a significant effect on the maximum LSS or corresponding heating time. However, it did cause overall higher temperatures at the interface between the coupling layer and CF/epoxy adherend, probably as a result of slower resin squeeze flow. This led to the occurrence of failure in the CF/epoxy adherend (which is presumed to be related to thermal degradation) even in the welding conditions that resulted in maximum LSS. However, the thermal degradation was not severe enough to cause a drop in the maximum LSS relative to the high force and high amplitude case. Further decreasing the welding force to 400 N increased the heating time by approximately 30% and resulted in a moderately lower LSS. The former was attributed to inefficient heating due to the hammering effect, particularly significant at low welding forces. The latter was attributed to increased porosity and matrix-related failure found on the fracture surfaces of the 400/86 samples.

Decreasing the amplitude of vibrations while keeping a constant, high welding force of 1200 N significantly increased the heating time that resulted in maximum LSS, consistent with slower viscoelastic heat generation. The longer heating times were assumed to have caused the higher temperatures at the interface between the coupling layer and CF/epoxy adherend. Subsequently, such temperatures most likely caused thermal degradation in the CF/epoxy adherend even in samples with the maximum LSS. However, similarly to the 800/86 case, the degradation signs were not severe enough to affect the maximum LSS, even for heating times double the heating times that were achieved with the highest amplitude, i.e., 86 µm. Based on **Chapter 4**, such heating times should have caused severe degradation in the CF/epoxy adherend and a significantly lower LSS. However, decreasing the amplitude of vibrations decreased the heat generation rate, meaning that it took a longer time for the interface to reach the melting temperature. Consequently, it took a longer time for the CF/epoxy adherend to experience high temperatures.

Making conclusive remarks on the robustness of the process with respect to its sensitivity to variations in the welding force or amplitude of vibrations is not straightforward. The strength of the dissimilar welded joints did show a certain degree of flexibility with respect to variations in the welding force or amplitude of variations. However, the apparent thermal degradation signs that were found even in samples that exhibited the highest LSS might imply a lower joint quality, especially under different loading and environmental conditions.

6.4   Final conclusions

Prior to this thesis there was very limited knowledge on welding of dissimilar composites, as seen in the Introduction chapter. Thus, in this thesis the main focus was to generate the knowledge deemed necessary to assess whether ultrasonic welding is a viable option for joining high-performance, dissimilar composites, and if so, how flexible this process can be. As shown in this study and in particular in Chapters 3 and 4, the knowledge gained from ultrasonic welding of solely thermoplastic composites could not be directly applied to welding of dissimilar composites (see upper limit of processing interval and effect of decreasing the amplitude of vibrations and welding force on the welding process). Moreover, the existence of the different materials in the welding stack raised questions regarding their impact on the welding process (existence of ED and its material, coupling layer thickness) as well as their sensitivity to the welding temperatures and heating time, which had yet to be addressed. By answering these primary questions, progress was made in further understanding ultrasonic welding and by showing that the applications of this process can be expanded to joining thermoset composites.

The findings in this thesis showed comparable strengths of the welded, dissimilar composite joints to both co-cured, dissimilar composite joints and to welded, thermoplastic composite joints, which demonstrated that ultrasonic welding is a very promising joining technique. Moreover, this process was proven to be robust (with respect to the variations in the heating time), since despite the sensitivity of the thermoset composite adherend to the high welding temperatures, a relatively wide processing interval, i.e., range of heating times that result in a certain mechanical performance, could be obtained. Additionally, the weld strength presented a certain degree of insensitivity to changes in the process parameters, i.e., welding force and amplitude of vibrations. It should be noted however that the results obtained in this thesis are dependent on the specific CF/epoxy system (T800S/3911) used in this study. This means that changing this system could influence the sensitivity of the CF/epoxy to the heating time and/or maximum temperature, as well as the morphology of the interphase. Regarding the latter, a different epoxy-PEI interphase morphology was observed than the one described in this thesis, when a Hexply M18-1 (by Hexcel) CF/epoxy laminate was used in [1]. Nevertheless, the findings in this thesis not only provided answers to the knowledge gaps identified in the state of the art, but also showed how promising ultrasonic welding is as an alternative solution to the current joining practices through mechanical fastening.

6.5   Recommendations

This thesis further the knowledge on ultrasonic welding of dissimilar composite materials, particularly with respect to suitable manufacturing approaches and the robustness of such process. However, further research is necessary in order for this process to be deemed mature enough in order to be applied in industrial applications. Thus, in this section recommendations for future studies are proposed.

6.5.1   Weldability of thermoset composites

In this thesis the practice that was followed to make the thermoset composite "weldable" was the utilization of a (partially) soluble thermoplastic coupling layer and thermoset matrix

system. In this way it was assumed that a reliable bond through the development of a gradient thermoplastic-thermoset interphase was obtained. However, relying on miscible systems will limit the number of possible thermoplastic layer-thermoset matrix combinations.

A comparative study on different techniques to achieve a connection between the thermoplastic coupling layer and the thermoset composite might reveal different techniques that can produce a reliable bond without the need of compatible systems. The methods described in the Introduction (i.e. the utilization of a fabric reinforcement embedded partially in the coupling layer and the other part in the thermoset composite adherend or treatment of the coupling layer to enhance its adhesion properties) and the durability of the formed connection should be further investigated. In this way, not relying on compatibility between the thermoplastic and thermoset polymers could introduce practically endless combinations.

6.5.2 Modification of energy director geometry

The study presented in Chapter 4 showed that in order to decrease the sensitivity of the thermoset composite adherend to the heating time, a relatively thick coupling layer has to be used, in order to efficiently shield it from the high welding temperatures. Another way to decrease such sensitivity could entail the usage of a modified energy director geometry that could generate heat at the interface with an increased efficiency. An example could be an ED in the form of a mesh, which was found in a recent study [2] to generate heat rather uniformly across the overlap due to better initial contact with the adherends than a flat ED.

6.5.3 Mechanical performance of dissimilar composite welds

The strength of the dissimilar welded joints was found to be comparable to that of thermoplastic composite joints. However, this response is dependent on the type of loading during mechanical testing. Thus, mechanical testing under different static or dynamic loading should be performed to gather more information regarding the mechanical performance and damage tolerance of dissimilar composite welded joints.

The results of the FE-model that were presented in Chapter 4 indicated higher peel stresses with decreasing weld line thickness, for thicknesses up to $200\,\mu m$. The assumption was that such high peel stresses could have impacted the maximum (failure) load. To determine whether this was indeed the case, the FE-model that is presented in Appendix A should be modified to predict final failure as well. In this way, it can be determined to what extent the lower LSS after certain displacement values is caused by a very thin weld line or by significant thermal damage in the thermoset composite adherend.

6.5.4 Thermal degradation of the thermoset composite

In this study, it was assumed that thermal degradation of the CF/epoxy adherend is the cause of the shift in the failure locus from failure predominantly in the thermoplastic composite adherend (at optimum welding conditions) to failure predominantly in the thermoset composite adherend. Attempts to verify that the thermoset adherend was indeed degraded via Fourier transform infrared (FTIR) analysis were unsuccessful due to roughness on the fracture surfaces, thus inability to obtain useful data. However, for different material combinations or configurations that might not favour failure in the thermoplastic composite adherend at optimum welding conditions, such analysis is deemed important in order to

ascertain whether the thermoset composite adherend has been affected. Other characterization methods should take into account the particularities of the temperature profile during the welding process, i.e., very fast heating and cooling rates.

6.6 References

[1]   *Villegas IF, van Moorleghem R. Ultrasonic welding of carbon/epoxy and carbon/PEEK composites through a PEI thermoplastic coupling layer. Compos Part A Appl Sci Manuf 2018;109:75–83.*

[2]   *Jongbloed B, Teuwen J, Palardy G, Fernandez Villegas I, Benedictus R. Continuous ultrasonic welding of thermoplastic composites: Enhancing the weld uniformity by changing the energy director. J Compos Mater 2020;54:2023–35. doi:10.1177/0021998319890405.*

Appendix

Figure A.1 illustrates the 3D FE-model built in Abaqus software, including the dimensions and boundary conditions. The model was representative of the lap shear test, with one end having nodes fixed in 3 degrees of freedom, while on the other side, solely longitudinal displacement was allowed. Figure A.2 shows the mesh of the overlap of the single-lap joints. A spew fillet was also included in the model as a representation of the resin squeeze out that was observed in all epoxy-PEEK 250 samples. The spew fillet was designed with a 45° slope and a height reaching half the adherend's thickness, as an approximation of what was observed on most samples. In case of the CF/PEEK woven fabric adherend, with 6 layers and a total height of 1.8 mm, the fillet reached up 3 layers (3x 0.3 = 0.9 mm). In case of the UD-laminate adherend, with 8 layers and a total height of 2.0 mm, the fillet reached up 4 layers (4x 0.25 = 1.0 mm). The weld line was modelled with three thicknesses, 200, 100 and 50 µm. These thicknesses were based on the cross-sectional micrographs of epoxy-PEEK 250 samples welded at displacements below d_{low}, at d_{opt} and above d_{high} (see Figure 4.6). The weld line was modelled with a consistent element height of 50 µm for all topology configurations, which results in 4 elements through the thickness for 200 µm, 2 elements for 100 µm, and 1 element for 50 µm-thick weld line. The element thickness inside the adherends was decreased towards the weld line. The outside half of the adherends was modelled with one element per single layer through the thickness, resulting in 0.3 mm for a single layer of CF/PEEK woven fabric and in 0.25 mm for a single UD layer of CF/epoxy prepreg. The inside half of the adherends, alongside the fillet, was modelled with the element height used in the weld line, 50 µm.
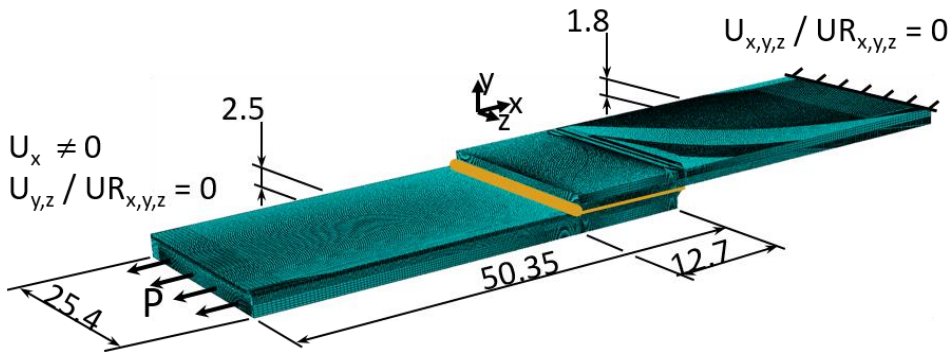

Figure A.1: 3D FE-model of the epoxy-PEEK 250 sample in a single-lap configuration, with boundary conditions. Dimensions are in [mm].
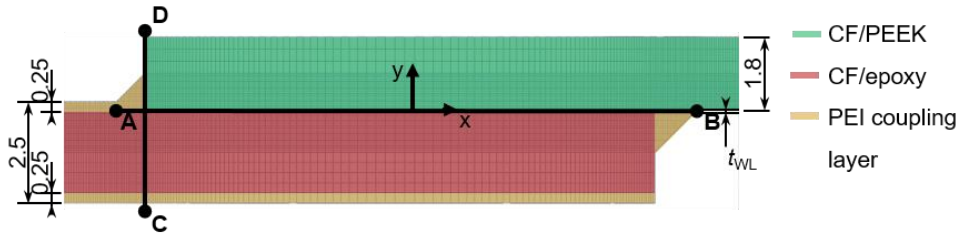
Figure A.2: 3D FE-model, central joint region for a single-lap design. The AB and CD paths correspond to the paths at which the peel and shear stresses were obtained. Dimensions are in [mm].

In order to guarantee that the results were mesh independent, a mesh convergence study was performed by comparison of different element types C3D8R, C3D8 and C3D20R, with constant number of elements. A sufficient convergence could be established with element type C3D8R. The length of one element in the overlap tip region was set to 50 µm and the width to 100 µm, gradually increasing towards the outer regions of the joint. These mesh designs resulted in a total mesh size of 1,082,633 elements for the 200 µm-thick weld line, 1,055,956 elements for the 100 µm-thick weld line and 1,040,300 elements for the 50 µm-thick weld line.

The adherends were modelled as linear elastic, based on the properties listed in Table A.1. The PEI coupling layer and the ED were modelled as linear-elastic/plastic, using the values in Table A.2. Note that even though the ED used in the experiments was made out of PEEK material, it was decided to model it as a PEI ED for simplicity. This decision was based on the fact that both ED materials resulted in similar LSS and failure locus in our previous research [1]. The load was applied in a single step taking into account non-linear geometry effects.

Table A. 1: Material properties of TENCATE CETEX TC1200 PEEK 5HS and TORAY T800S/3911 prepreg systems.

Property	Specification	CF/PEEK	CF/epoxy
Longitudinal tensile modulus (MPa)	E_{11}	56100[a]	172000[c]
Transverse tensile modulus (MPa)	E_{22}	55600[a]	8000[c]
Out-of-plane tensile modulus (MPa)	E_{33}	1000 [b]	8000[c]
In-plane shear modulus (MPa)	$G_{12} = G_{13}$	4500[a]	5000[b]
Transverse shear modulus (MPa)	$G_{23} = E_{33} / (2(1+ \nu_{23}))$	3846	3077
In-plane Poisson ratio	$\nu_{12} = \nu_{13}$	0.27[b]	0.27[b]
Transverse Poisson ratio	ν_{23}	0.30[b]	0.30[b]

[a] TDS TENCATE CETEX TC1200 PEEK 5HS laminate

[b] assumption, based on similar material Hexply 8552, Camanho et al. [2]

[c] provided by manufacturer TORAY (Japan)

Table A.2: Material properties of ULTEM 1000 PEI resin

Tensile modulus (MPa)	E_{neat}	3280[a]
Poisson ratio	ν_{neat}	0.36

[a] TDS ULTEM 1000

References

[1]   *Tsiangou E, Teixeira de Freitas S, Villegas IF, Benedictus R. Ultrasonic welding of epoxy- to polyetheretherketone- based composites: Investigation on the material of the energy director and the thickness of the coupling layer. J Compos Mater 2020.*

[2]   *Camanho PP, Dávila CG, Pinho ST, Iannucci L, Robinson P. Prediction of in situ strengths and matrix cracking in composites under transverse tension and in-plane shear. Compos Part A Appl Sci Manuf 2006;37:165–76*

Acknowledgments

The last four years would not have been the same if it wasn't for all the people who helped me throughout these years and those who made my journey so much more fun and interesting.

So, first and foremost, thank you so much Irene for believing in me and helping me stay on track. You taught me how to be critical, how to work independently and be more structured. Thank you for being so patient during the never-ending writing process, I hope you finally find the magic recipe for writing scientific papers. But mainly thank you for being there for me when I personally needed it and for sharing your passion for health and sustainability. I hope I get to work with more people like you in the future. I really could not have done it without you!

To my second supervisor, Sofia, I am very grateful that you saw potential in me after our interview in the fall of 2015. I'm really glad we did end up working together and I really value all the talks we had, both on a professional and personal level.

To my co-promotor, Rinze, thank you for giving me the opportunity to pursue a PhD within your group. I really appreciate the support you showed me when I needed it.

Of course, this journey would have been much more difficult if it wasn't for you, Gemma. As a management assistant (I know how much you love these titles) you made my life so much easier, I really appreciate it. And on a personal level, you know how much I admire your attitude towards life and how much I value all the time we spent talking. No one will ever understand my shoe addiction better than you. I will really miss having you around.

Thank you also Marianne for the brief time we worked together. I'm very thankful for your eagerness to help whenever there was an issue.

As I spent more than four years mainly in some corner in the lab, I could not, not acknowledge the people who helped me in the lab, the head the lab Johan and our technicians Berthil, Fred, Kees, Johan, Marlies, Misja, Victor. Special thanks to Gertjan and Frans with whom I spent so much time and had some of the most bizarre discussions.

I am also so thankful for my colleagues and friends in the welding group. Bram, Camila, Genevieve, Tiago, Tian, Yannos, you were there for me when I needed help with my research but most importantly when I needed to vent. I really value the time we spent together and the memories we made. Truly the best group I could be a part of! Bram, you especially helped me so much in the last four years, from solving issues in the lab to translating my summary. Thank you so much! Gen, thank you for helping me getting started and with all the experiments and papers. Thank you also Regis for helping me understand welding of dissimilar composites during my first month.

Now, what can I say about my office mates. Leila, you are so fun to be around! I really admire your strength and perseverance. Lucas, I will never forget that you proposed to me on my first day at work haha. Thank you for making me feel as part of the group right from the start. Nick, my sushi-partner in crime, you are one of the coolest people I know. I'm so

glad for the time we spent together and I can't wait to see what the future holds for you. Nicolas, you ended up being one of my closest colleagues and friends. Talking with you for hours was such an easy and fun thing to do! I'm so glad that I get to call you all my friends now. To my "new" office mates, Chantal, Lubin, Luigi and Ozan, I really enjoyed the little time we spent together.

I'm also grateful for all the colleagues who made work a fun place to be. So big thanks to Abhas, Agnes, Calvin, Chizoba, Cornelis, Davide, Fabricio, Giacomo, Hongwei, Ilias, Ines, John-Alan, Jos, Javier, Julie, Li Xi, Maria, Maro, Marta, Megan, Nakash, Niels, Otto, Pedro, René, Romina, Timo, Wandong. To anyone who I might have neglected to mention, thank you for being a part of my journey. Special thanks to Dimitris for all the funny and serious discussions, I'm so thankful for all the advice you gave me; to Julian, thank you for the help with the FE analysis and for giving so much of your time. Thank you also Clemens for your help with material characterization.

One of my favorite experiences during the PhD has to be working for the EFFICOMP project. From trying to order from Japanese menus in Tokyo to spending hours talking in the hotel lobbies, Ali, Klaus, Manuel, Mathias and Philipp, it was so great to get to know you and travel with you.

To my colleagues-turned-good friends, Genevieve, Mari, Laxmi and Chelsey and my food buddy Chau, I'm so glad for all the trips and fun days we shared together. I'm so lucky to be surrounded by such awesome people like you! Special thanks to my best friend Chirag who has been there for me since the beginning of my PhD. Thank you for tolerating all my mood swings and for bringing such positive energy :)

To my friends back in my home country, Alexandra, Alexandros, Maria and Stavroula, you have no idea how lucky I feel to have you in my life, even if we are so many km away. You have supported me and continue to do so in so many ways. So huge thanks to you my friends.

Last but certainly not least I want to thank my family for always believing in me, even when I was lost. Your love and support are what keep me going every day. Ειδικά εσύ μαμά μου, είσαι δίπλα μου στις πιο χαρούμενες και πιο δύσκολες στιγμές. Δεν θα ήμουν εδώ αν δεν είχα την ανιδιοτελή αγάπη και στήριξή σου. And to my amazing partner, Johnny. I don't think a few lines will be enough to show you how grateful I am to have you in my life. You make my life brighter every day. Wǒ ài nǐ!

Curriculum Vitae

The author was born on the 28th February, 1992 at Giannitsa, Greece. Since then, she moved to different cities within Greece but spent most of her teenage years on the island of Lesbos.

In 2010 she moved to Patras, Greece in order to study at the department of Mechanical Engineering and Aeronautics at the University of Patras. It was during the last two years when she chose the track of Applied Mechanics, Technology of Materials and Biomechanics that she realized her interest in polymers and polymer-based composites. Her diploma thesis was on the effect of thermal shock cycling on the viscoelastic properties of GF/epoxy composites under the supervision of Professor Papanicolaou.

Shortly after she received her diploma degree, she moved to Delft, the Netherlands in April 2016, in order to start her PhD at the Aerospace faculty of TUDelft, in the Aerospace Structures and Materials department. There, she worked under the supervision of her promotors Dr.ir. Irene Fernandez Villegas and Professor Rinze Benedictus and second supervisor Dr.ir. Sofia Teixeira de Freitas on the topic of ultrasonic welding of dissimilar composites.

Since April 2021 she is working as a Project Engineer for KVE Composites Group.

List of publications

Journal Papers

1. Tsiangou E, Teixeira de Freitas S, Villegas IF, Benedictus R. *Investigation on energy director-less ultrasonic welding of polyetherimide (PEI)- to epoxy-based composites*. Composites Part B: Engineering, vol. 173, 2019
2. Tsiangou E, Teixeira de Freitas S, Villegas IF, Benedictus R. *Ultrasonic welding of epoxy- to polyetheretherketone- based composites: Investigation on the material of the energy director and the thickness of the coupling layer*. Journal of Composite Materials vol. 54, 2020.
3. Tsiangou E, Kupski J, Teixeira de Freitas S, Benedictus R, Villegas IF. *On the sensitivity of ultrasonic welding of epoxy- to polyetheretherketone (PEEK)-based composites to the heating time*. Composites Part A: Applied Science and Manufacturing, vol. 144, 2021.
4. Tsiangou E, Teixeira de Freitas S, Benedictus R, Villegas IF. *On the sensitivity of the ultrasonic welding process of epoxy- to polyetheretherketone (PEEK)- based composites to the welding force and amplitude of vibrations*. Composites Part C. [Under Revision].

Conference Proceedings

1. Tsiangou E, Teixeira de Freitas S, Villegas IF, Benedictus R.: *Investigation on energy director-less ultrasonic welding of thermoplastic to thermoset composites*. Proceedings of the 7th EASN international conference, Warsaw, Poland, 2017.
2. Tsiangou E, Teixeira de Freitas S, Villegas IF, Benedictus R.: *Ultrasonic welding of CF/epoxy to CF/PEEK composites: effect of the energy director material on the welding process*. Proceedings of the 18th European conference on composite materials, Athens, Greece, 2018.
3. Tsiangou E, Teixeira de Freitas S, Villegas IF, Benedictus R.: *Ultrasonic welding of thermoset- to thermoplastic based composites: effect of the process parameters on the weld strength.* Proceedings of the ASC 34th technical conference, Atlanta, USA, September 2019.
4. Tsiangou E, Teixeira de Freitas S, Villegas IF, Benedictus R.: *Recent developments in ultrasonic welding of epoxy- to thermoplastic-based composites*. Proceedings of the 5th international conference and exhibition on thermoplastic composites, October 2020